The Dissertation Committee for Penny Denise Riha certifies that this is the approved version of the following dissertation:

Metabolic Impairment of the Posterior Cingulate Cortex and Reversal by Methylene Blue: A Novel Model and Treatment of Early Stage Alzheimer's Disease

Committee:

Francisco Gonzalez-Lima, Supervisor

Theresa A. Jones

Michelle A. Lane

Timothy Schallert

David M. Tucker

Metabolic Impairment of the Posterior Cingulate Cortex and Reversal by Methylene Blue: A Novel Model and Treatment of Early Stage Alzheimer's Disease

by

Penny Denise Riha, B.A.

Dissertation

Presented to the Faculty of the Graduate School of

The University of Texas at Austin

in Partial Fulfillment

of the Requirements

for the Degree of

Doctor of Philosophy

The University of Texas at Austin
December 2007

Dedication

with thanks and love to my parents, Frank and Debbie Riha

and to Jonathan Buck, my wonderful partner and my biggest fan

Acknowledgements

Metabolic Impairment of the Posterior Cingulate Cortex and Reversal by Methylene Blue: A Novel Model and Treatment of Early Stage Alzheimer's Disease

Publication No._____

Penny Denise Riha, Ph.D.

The University of Texas at Austin, 2007

Supervisor: Francisco Gonzalez-Lima

Alzheimer's disease (AD) is associated with decreased brain energy metabolism. Hypometabolism in the posterior cingulate cortex (PCC) occurs before the onset of memory deficits in subjects at genetic risk for AD who are not yet cognitively impaired. There is a specific inhibition in cytochrome oxidase (C.O.) in the PCC, an area involved in spatial navigation. Creating an animal model that exhibits the early pathophysiology of AD is important for developing and testing drugs that could reverse memory problems associated with such deficits. Methylene blue (MB) is a compound that improves C.O. activity and memory retention in rats.

This dissertation had three specific aims: 1) to examine if isolated PCC hypometabolism causes spatial memory deficits in rats; 2) to find a dose of MB

that improves memory without nonspecific behavioral effects; and 3) to prevent memory deficits from PCC hypometabolism with low dose MB.

PCC hypometabolism was produced by focal administration of sodium azide, an inhibitor of C.O. activity. PCC hypometabolism resulted in impaired spatial memory in a hole board food-search task, increased oxidative damage, and neurotoxicity in the PCC. In addition, PCC hypometabolism resulted in reduced inter-regional correlations in brain activity.

Our second set of studies examined the dose-response effects of MB. Our findings demonstrated that a low dose of MB: 1) enhanced memory in open field habituation and object recognition tasks; 2) did not affect general locomotor activity, exploration, motivation, or anxiety; and 3) increased brain oxygen consumption 24 hr after *in vivo* administration.

Finally, our last study found that low dose MB prevented the deficits caused by PCC hypometabolism. MB did not prevent PCC inhibition or cell loss caused by sodium azide. Inter-regional correlations of brain metabolic activity suggested that rats treated with MB were using a different, but equally efficient, strategy for memory retrieval.

This animal model of C.O. hypometabolism in the PCC can provide information to understand the mechanisms that regulate early pathological degeneration and reveal new therapeutic strategies aimed at reducing or preventing cognitive decline. Studies of low dose MB in humans are needed to examine its effects in AD patients.

Table of Contents

List of Tables

List of Figures

Chapter 1: Modeling the Early Pathophysiology of Alzheimer's Disease

Alzheimer's disease (AD) is associated with decreased brain metabolism. Studies of Alzheimer's patients reveal a specific inhibition in mitochondrial cytochrome oxidase (C.O.) in the posterior cingulate cortex (PCC), an area involved in spatial navigation. Hypometabolism in the PCC occurs before the onset of memory deficits in (1) subjects at genetic risk for AD who are not yet cognitively impaired and (2) subjects with mild cognitive impairment who later develop AD.

There is a need to model the early pathophysiology of AD. In the United States alone, 4 million people are affected with an estimated annual cost of $100 billion (National Institute on Aging). It is important to accurately model the metabolic deficits in early-stage AD because the disease is irreversible, and most therapeutic drugs are effective only in the early to middle stages of AD (Silverman, 2004). Creating an animal model that exhibits the early pathophysiology of AD is important for developing and testing drugs that could reverse memory problems associated with such deficits.

1.1. Alzheimer's Disease

Alzheimer's disease is a progressive neurodegenerative disorder that is clinically manifested as dementia that affects memory, mood, and behavior. A diagnosis of probable AD requires fulfillment of the following criteria, which were developed by a joint task force of the National Institute of Neurological and

Communicative Disorders and Stroke and the Alzheimer's Disease and Related
Disorders Association (NINCDS-ADRDA) (McKhann et al., 1984):

(1) Dementia established by clinical examination and documented by the
Mini-Mental Test, Blessed Dementia Scale (or some similar
examination) and confirmed by neuropsychological tests;

(2) Deficits in two or more areas of cognition (for example, word
comprehension and task-completion ability);

(3) A progressive worsening of memory and other cognitive functions;

(4) A lack of disturbance of consciousness;

(5) An onset between ages 40 and 90, most often after age 65; and

(6) An absence of systemic disorders or other brain diseases that could
account for the progressive deficits in memory and cognition.

AD is confirmed postmortem by the existence of abnormal protein
deposits in the brain, namely insoluble amyloid plaques and neurofibrillary
tangles, but there is considerable debate on the relationship between cognitive
decline and the underlying neuropathology. The cause of AD is unknown. It has
been proposed that genetic mutations, especially those in mitochondrial DNA,
intensify other risk factors, including low education, head injury, vascular disease,
high cholesterol, and age (Blennow et al., 2006). Age is the most significant risk
factor among those proposed.

1.1.1 Impaired Energy Metabolism in Alzheimer's Disease *in vivo*

There is a growing consensus that impaired energy metabolism is a
critical component in AD. AD is associated with reduced neuronal metabolism
which correlates to the degree of dementia and the duration of symptoms (Chase
et al., 1984). Studies of cerebral blood flow consistently show a decrease in

blood perfusion in AD patients (for review, see Silverman, 2004). Positron

emission tomography (PET) imaging that reveals fewer correlations between

parietal and frontal lobe metabolism in AD patients than healthy controls

suggests that a breakdown of organized functional activity is also a hallmark of

AD (Horwitz et al., 1987). Thus, energy hypometabolism is a consistent feature

of AD.

Of all the regions of the brain, the PCC displays the greatest decrease of

glucose utilization in patients in the early stages of Alzheimer's disease

(Minoshima et al., 1997). This decrease cannot be explained by

histopathological markers such as plaques and tangles that are found in

relatively lower amounts in this region (Valla et al., 2001). Metabolic inhibition in

the PCC occurs before the onset of memory deficits in (1) subjects who are at

genetic risk for AD but are not yet cognitively impaired (Reiman et al., 1996) and

(2) subjects with mild cognitive impairment who later develop AD (Mosconi,

2005). In fact, metabolic reductions in the parieto-temporal cortex and the PCC

are considered to be the most reliable indicators of early AD (Chetelat et al.,

2001; Mosconi, 2005; Borroni et al., 2006).

1.1.2 Impaired Energy Metabolism in Alzheimer's Disease *in vitro*

The majority of neuronal energy is provided by mitochondrial oxidative

phosphorylation (OXPHOS; Figure 1), which constitutes the major cellular ATP-

producing mechanism under aerobic conditions. There are five enzymatic

protein complexes (complexes I–V) located in the mitochondrial inner membrane

that catalyze OXPHOS. Electrons are passed through these enzymes until they

reach the fourth complex, cytochrome c oxidase (C.O.), the terminal enzyme in

the mitochondrial electron transport chain. C.O. catalyzes the final transfer of

electrons from cytochrome c to molecular oxygen. Concomitantly, protons are pumped through the enzymes from the matrix into the inner membrane space, creating a proton gradient. This stored energy is used by complex V (ATPase) to convert ADP into ATP. In the brain, ATP is used to perform a variety of tasks including transport, neurotransmitter synthesis, and, importantly, repolarizing cellular membranes.

Figure 1.1   Schematic of the mitochondrial electron transport chain and OXPHOS. Adapted from: http://courses.cm.utexas.edu/emarcotte/ch339k/fall2005/Lecture-Ch19-2.html.
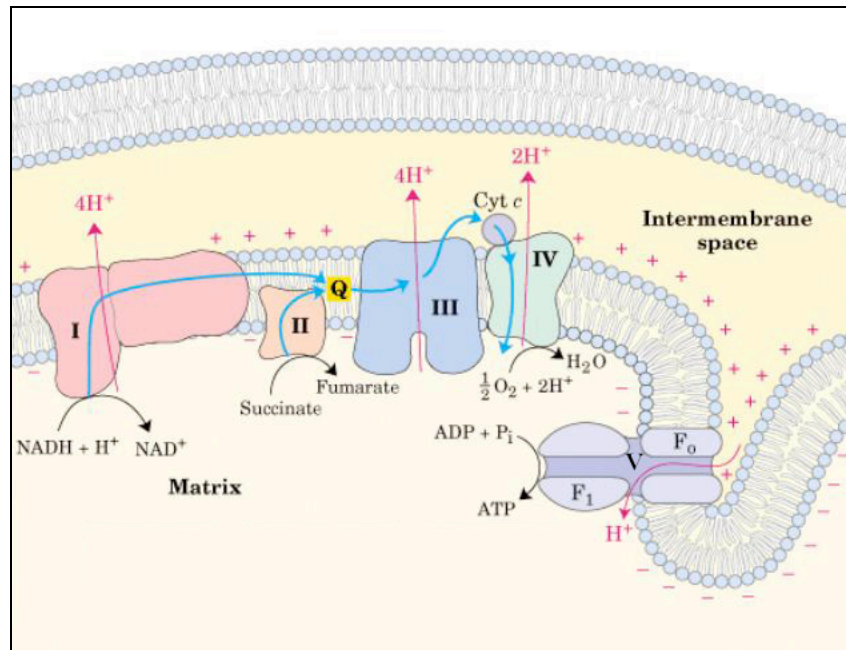
C.O. gene expression is upregulated in response to high energy demand (Wong-Riley et al., 1998). Therefore, neuronal demands regulate C.O. levels and distribution. Furthermore, the Na^+/K^+ pump that maintains the cellular electrical potential is co-localized with C.O. within neurons (Hevner et al., 1992); thus, C.O. activity can be used as a marker of neuronal activity. Levels of C.O. are higher in brain cells and areas of the brain that have excitatory input, which indicates that C.O. significantly contributes to the energy needed to repolarize the membrane potential after neural activity (Wong-Riley et al., 1998). C.O. is composed of 13 subunits and requires bigenomic regulation. The first three subunits (I–III) are encoded by mitochondrial DNA (mtDNA) and are responsible for catalytic activity. The remaining subunits (IV–XIII) are encoded by nuclear DNA (nDNA) and perform functions relating to structure, allosteric binding, and proton pumping. Coordinated expression between the subunits from mtDNA and nDNA is necessary for the proper function of C.O.

Approximately 95–98% of brain oxygen is consumed through C.O. and the remaining 2–5% forms free radical oxygen species (Floyd, 1999). A dysfunction in any part of OXPHOS increases the generation of free radicals and, consequently, increases the oxidation of lipid, protein, and genomic macromolecules (Wallace, 1999; Beal, 2005). Postmortem analysis of AD brain tissue reveals that the detrimental effects mentioned above are increased (for reviews, see Smith et al., 1995; Markesbery, 1997; Perry et al., 2000). For example, AD brain tissue shows increased mtDNA and nDNA damage as compared to control tissue (Mecocci et al., 1994). Furthermore, the damage to mtDNA is greater than damage to nDNA in tissue from AD patients, which suggests that mtDNA is more susceptible to oxidative stress (Mecocci et al.,

1994). RNA oxidative damage in AD tissue is increased in the hippocampal formation, subiculum, and entorhinal cortex, as well as in the frontal, temporal, and occipital neocortices (Nunomura et al., 1999). There is also evidence that tissue from AD patients exhibits increased oxidative damage to proteins (Smith et al., 1998) and cell membranes (Mecocci et al., 1996). The damage to DNA, proteins, and lipids may contribute to the neurodegenerative process in AD. These events can increase membrane permeability, leading to NMDA receptor-mediated excitotoxicity and cell death.

In postmortem brain tissue from AD patients, the respiratory enzymes of the electron transport chain are less active than those in control samples; of all the enzymes reduced, C.O. is the least active (Mutisya et al., 1994; Parker et al., 1994b). Certain areas of the brain are affected more than others. In comparison with control subjects, patients with AD show less C.O. activity in the frontal, temporal, and parietal association cortices than in the occipital cortex, putamen, or the hippocampus (Kish et al., 1992). The reduction of C.O. activity cannot be explained solely through the loss of brain cells, as there was a significant reduction in C.O. activity in the frontal cortex, which is an area not typically affected morphologically in AD. Likewise, there was no significant difference in C.O. activity between the control hippocampus and the AD hippocampus (Kish et al., 1992), which is an area with a large number of plaques, tangles, and cell loss (Thal et al., 2000).

In AD patients, C.O. activity is observed to be lower not only in brain tissue (Kish et al., 1992; Mutisya et al., 1994; Parker et al., 1994b), but also in peripheral tissue, such as blood platelets (Parker et al., 1994a; Valla et al., 2006b) and fibroblasts (Curti et al., 1997). Parker Jr. et al. (1994b) did not find a

change in the concentration of respiratory electron carriers or redox sites. In addition, they analyzed isolated C.O. protein and were able to detect the low-substrate binding site in control but not AD tissue (Parker and Parks, 1995). Therefore, C.O. inhibition in AD may be a result of abnormal catalytic activity of the enzyme rather than from a loss of the enzyme itself that might occur from a loss of cells or mitochondria.

Analysis of C.O. subunit profiles from AD patients suggests that the mitochondrial-encoded subunits may be affected more than nuclear-encoded subunits. In brains unaffected by AD, the mRNA levels of mitochondrial-encoded subunits I and III in the midtemporal association cortex and the primary motor cortex are the same; in brains affected by AD, however, this is not the case (Chandrasekaran et al., 1994). In AD brains, the mRNA levels of mitochondrial-encoded subunits I and III in the midtemporal association cortex are 50–65% lower compared to the primary motor cortex of AD brains and the midtemporal assocation cortex from control brains (Chandrasekaran et al., 1994). Within the hippocampus, Simonian and Hyman (1994) also found differences in a mitochondrial-encoded subunit (II) between AD and control brains but did not find a difference in nuclear-encoded subunit IV. Chandrasekaran et al. (1997), on the other hand, did find decreases in subunit IV in the hippocampus. Some authors suggest that AD is caused by a primary genetic defect in C.O., while others suggest that inhibition of C.O. is a secondary effect of decreased neuronal activity. However, decreased neuronal activity does not explain the systemic inhibition of C.O. activity observed in platelets and fibroblasts from AD patients.

A decrease in C.O. activity in brain and peripheral tissue supports the hypothesis that a primary defect in C.O. causes AD. Additional evidence

supporting a primary mitochondrial deficit comes from hybrid cells, which are cells whose mitochondria have been replaced with mitochondria from AD patients. Hybrid cells show decreased activity in C.O. but not in complex I (Sheehan et al., 1997). The decreased C.O. activity in these cells led to increased oxidative stress, reduced ATP, and changes in calcium homeostasis and membrane potential (Swerdlow et al., 1997; Cassarino et al., 1998; Ghosh et al., 1999; Cardoso et al., 2004b).

1.2 Posterior Cingulate Cortex

1.2.1 Metabolic Inhibition in Alzheimer's Disease

Postmortem analysis of the PCC of AD patients shows a significant decrease in C.O. activity in each of the six layers of the PCC when compared with the C.O. activity in control tissue (Valla et al., 2001). In AD brains, the decrease in the superficial PCC layers (I–II) was greater than the decrease in the deep layers (III–VI). In addition, the decrease in C.O. activity in layer I was directly associated with the duration of the disease. The superficial layers contain the synaptic neuropil which consumes a great amount of energy due to repolarization following action potentials (Valla et al., 2001). The adjacent motor cortex in AD patients showed a similar, but nonsignificant, pattern of C.O. inhibition as compared to control subjects. There were no differences in complex II activity between the AD and control groups, confirming a specific defect in C.O. in AD patients.

In healthy human subjects, the PCC shows high levels of baseline activity in PET imaging studies (Minoshima et al., 1997). The PCC contains many glutaminergic excitatory synapses that require a substantial amount of energy to repolarize the cellular membrane (Hevner et al., 1992). This high energy

demand renders the PCC vulnerable. For example, a systemic injection of an N-methyl-D-aspartic acid (NMDA) antagonist in rats produces region-specific neurotoxicity, with the PCC being the most affected area (Li et al., 2002). Likewise, the PCC may be one of the first areas affected by C.O. inhibition, which compromises energy generation and, eventually, cell survival.

Clinical deficits correspond to hypometabolism in specific regions of the brain. For example, poor performance in language tests is correlated with hypometabolism in the left temporal lobe (Chase et al., 1984). C.O. inhibition in the PCC may be related to spatial memory deficits that are common in AD (Hof and Morrison, 1990; de la Torre, 2000; Holroyd and Shepherd, 2001).

1.2.2 General Functions of the PCC

The PCC is a division of the medial limbic cortex and lies dorsal to the caudal aspect of the corpus callosum. Anatomical-connectivity studies show that the PCC is connected with motor, visual, and subicular cortices, as well as the anterior thalamus (Vogt and Miller, 1983; Sanderson et al., 1991; van Groen and Wyss, 1992a; Shibata, 1994, 1998, 2000; van Groen and Wyss, 2003; Shibata et al., 2004). The PCC is included in the Papez circuit. The pathway includes the following areas as seen in Figure 2 (Papez, 1937; Vertes et al., 2001).

Figure 1.2   Papez circuit

cingulum

cingulate
cortex

entorhinal
/perirhinal

perforant pathway

PAPEZ
CIRCUIT

hippocampus
proper

atr

anterior
thalamic
nuclei

alveus

mtt

subiculum

mammillary
bodies

fornix
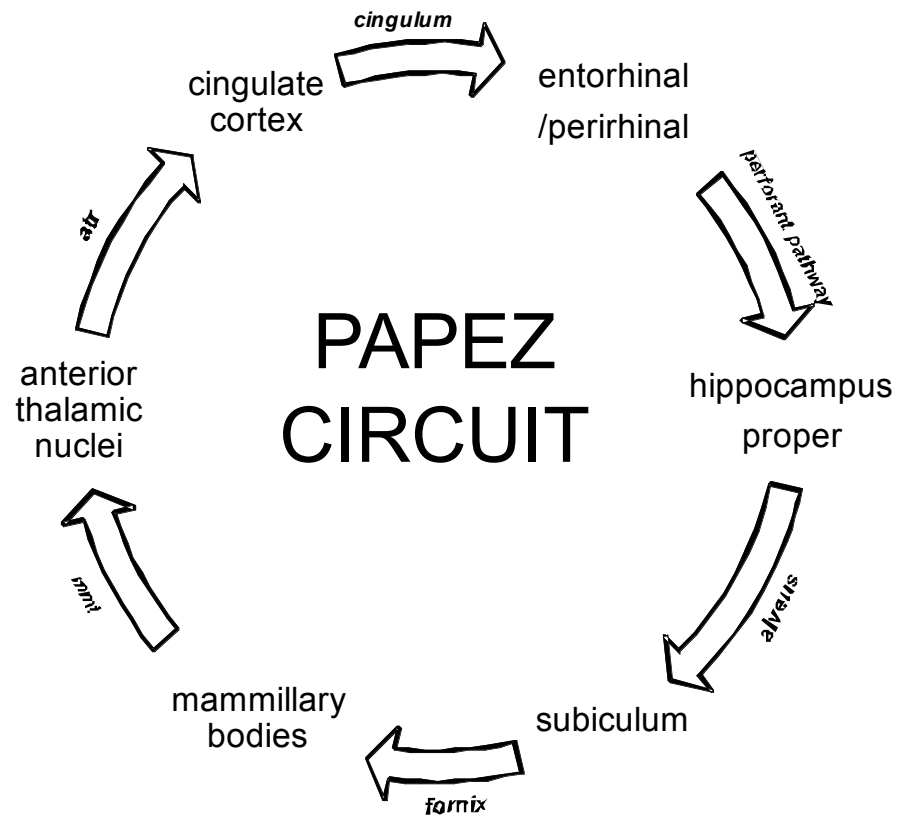
The PCC is in a strategic position to mediate signals between the hippocampal formation, thalamus, and cortex. Papez (1937) originally proposed that the functional anatomy of this circuit may underlie emotion, but its function has recently been reformulated to include processes of learning and memory (Harker and Whishaw, 2002; van Groen et al., 2004). The two propositions are not mutually exclusive. In fact, emotional states facilitate learning and memory (for review, see Packard and Cahill, 2001).

The PCC contributes to several processes. The human PCC participates in tasks of emotional processing (Aleman, 2005; Malhi et al., 2007), which may explain its involvement in bipolar disorder (Nugent et al., 2006; Roth et al., 2006) and schizophrenia (Franck et al., 2002; Haznedar et al., 2004; Shimizu et al., 2007). Functional imaging of healthy individuals reveal that the PCC is engaged while both encoding and retrieving episodic memories (Nyberg et al., 1996; Desgranges et al., 1998; Krause et al., 2006). The PCC is activated during route recall and landmark memory tasks (Maguire, 1997; Ohnishi et al., 2006). In rats, the PCC is involved in functions that include fear-based learning (Mello e Souza et al., 1999; Souza et al., 2002) and conditioned discrimination (Gabriel, 1993; Bussey et al., 1996). It also plays a significant role in spatial navigation and memory.

1.2.3 Studies Supporting a Role of the PCC in Spatial Memory

The PCC receives information from thalamic nuclei and the subiculum to allow for learning of specific sensory stimuli and changing a behavioral response according to previous experiences (Gabriel, 1993). Reciprocal connections with the entorhinal cortex suggest that the PCC analyzes objects spatially and sends this information to the hippocampal formation for further processing (Warburton

12

et al., 1998). Substantiating this theory, one study revealed a significant increase in gene expression in the PCC in rats performing a radial arm maze task (Vann et al., 2000).

1.2.3.1 Animal Studies

Head-direction cells are located in several areas of the Papez circuit including anterior thalamic nuclei, the subiculum, and the PCC (Chen et al., 1994; Taube, 1998). These cells respond when the animal faces a specific direction, regardless of the animal's location in the environment. Interestingly, head-direction cells are also found in the striatum (Taube, 1998), which is not included in the Papez circuit, but is connected to the PCC (McGeorge and Faull, 1989; van Groen and Wyss, 1992b; van Groen and Wyss, 2003). Cho and Sharp (2001) elaborated on the firing characteristics of PCC cells with spatial correlates: they not only verified the existence of head-direction cells in the PCC, but they also identified cells that fired to certain combinations of place, head direction, and running speed. Their findings, along with the fact that the PCC is connected to the motor cortex, confirm that the PCC has a role in path integration and/or landmark navigation.

Complete removal of the PCC generally produces spatial impairment in rats. The removal of the PCC impairs learning and memory in both the single-place and the place-alternation versions of the Morris water maze, which is a behavioral test commonly used to assess spatial memory (Sutherland et al., 1988). In the typical procedure for the single-place navigation (reference memory) test, a rat is placed randomly in different start positions in a pool of water containing a hidden escape platform in a fixed location. The rat learns to find the platform by using the visual cues placed around the pool. After a few

trials, rats become very proficient in finding the hidden platform. A probe test is often performed the day after the acquisition phase. In the probe test, the rat is placed in the same pool of water but the platform is removed; the percentage of time it spends in each pool quadrant is analyzed. Nonimpaired rats spend more time swimming in the quadrant where the platform was located during acquisition. The place-alternation (working-memory) version of this task differs in that the platform location changes daily. Whishaw et al. (2001) removed the PCC in Long-Evans rats and tested allocentric and egocentric navigation using the Morris water maze, a food-search task, and matching-to-place tasks. They observed impairment in all navigation tasks.

Vann & Aggleton (2002) administered an excitotoxic lesion from the level of the fornix to almost the caudal limit of the cerebral cortex and examined the effects in several tests of allocentric and egocentric learning. Agouti rats were impaired in two tasks of allocentric learning: the radial arm maze and the water maze. However, there were no group differences in T-maze alternation, a task of egocentric discrimination. Interestingly, there was a group difference in an object-in-place spatial task. In this task, rats explored four different objects that are placed in the chamber. After a delay of 15 minutes, two objects were switched in location. When the rats were reintroduced to the chamber, the PCC-lesioned rats did not explore the newly-located objects as long as control rats.

But results from other studies in which the PCC was inflicted with excitotoxic lesions rather than complete removal are less consistent. Riekkinen et al. (1995) tested three groups of Wistar rats in the water maze. One group was injected with an anticholinergic drug in the PCC before training, one group was injected after training, and the last group was injected before testing. Only

14

the rats injected before training were impaired. However, when Agouti rats were injected with an excitotoxin in the PCC before training in the water maze, no impairments were observed in single-place or place-alternation training, or in probe trials (Warburton et al., 1998). The results from the Warburton study (1998) agree with an earlier study that did not find impairment in Agouti rats in three tests of spatial memory when the PCC was lesioned with an excitotoxin (delayed nonmatching-to-position and spatial reversal learning in a spatial discrimination task, and forced alternation in a T-maze) (Neave et al., 1994). Conversely, a later study examining PCC-lesioned Sprague-Dawley rats found significant impairment in the place-alternation version of the water maze (van Groen et al., 2004).

These inconsistent results from PCC lesion studies led Harker & Whishaw to test two strains of rats (2002). They used Long-Evans, which showed impairments from PCC lesions, and Agouti rats, which did not. This study revealed that control Long-Evans rats performed better than control Agouti rats in the water maze. Removal of the PCC in Long-Evans rats impaired their behavior in the single-place and the place-alternation water maze tasks compared to control Long-Evans rats. Control Agouti and PCC-lesioned Agouti rats were not different from each other in the single-place task, but both performed worse than control Long-Evans rats. Furthermore, PCC-lesioned Agouti rats performed poorly on the more demanding place-alternation task relative to control Agouti rats. The performance of the strains in a visual acuity test was not different. Thus, the PCC was shown to be important in spatial behavior in both strains, but an innate nonspatial deficit in the Agouti rat may disguise the role of the PCC in the water maze task.

Single-cell recordings of neurons in the PCC during discrimination learning suggest that cingulate neurons may be important in long-term retention of memory. In a discriminative avoidance procedure, an animal learns to respond to a tone that predicts a foot shock (positive conditioned stimulus) and they learn to ignore a different tone that is not followed by foot shock (negative conditioned stimulus).   In the PCC, discriminative neuronal activity occurs during the positive conditioned stimulus relatively late in learning (Gabriel, 1993). Consistent with this, rats with neurotoxic PCC lesions are impaired during the late, but not early, stages of acquisition in a conditioned visual discrimination task (Bussey et al., 1996).

While there is disagreement as to the exact contribution of the PCC to spatial learning, it is evident that the PCC is involved in spatial processes. Lesion studies, along with PCC connections to visual, motor and subicular cortices, suggest that the PCC has a role in navigation, perhaps with a bigger contribution during the late stages of learning. Although there is debate as to whether the PCC is involved more in navigation using allocentric cues (ones that are both external and independent of the animal's body position) or navigation using egocentric cues (those generated from self-movement), the fact that there is a spatial function within the PCC is undeniable. The human literature confirms and extends these findings.

1.2.3.2 Human Studies

One interesting case study described a patient with topographical amnesia, a condition that refers to the inability to navigate because of the failure to use landmarks for route finding (Cammalleri et al., 1996). The patient was unable to find his way in familiar or unfamiliar environments. MRI revealed a

tumor between the anterior and posterior cingulate cortices. Another study discussed a patient with a lesion in the PCC and who also had topographical disorientation. This patient also got lost in new environments, but unlike the aforementioned patient, she was able to navigate in familiar surroundings (Katayama et al., 1999).

In healthy human subjects, PCC activation is strongly correlated with the speed of target detection during a spatial attention task (Mesulam et al., 2001). The PCC also responds when subjects are visualizing a previously learned route, including the landmarks and their movements along this route (Berthoz, 1997). This work is consistent with the animal research that showed the presence of head-direction cells (Cho and Sharp, 2001). Furthermore, the PCC was also involved in tasks in which subjects remembered environments recently learned and environments very familiar (Maguire, 1997). Taken together, both animal and human studies support the hypothesis that the posterior cingulate is involved in spatial memory.

1.3 Sodium Azide: An Inhibitor of Cytochrome Oxidase as Model of AD

Sodium azide is a toxin that specifically inhibits C.O. activity, and therefore oxygen metabolism, which results in a form of chemical hypoxia. Based on the findings of reduced C.O. activity in blood platelets from AD patients, Bennett et al. (1992) developed a rat model of chronic C.O. inhibition by implanting subcutaneous pumps that delivered a constant rate of sodium azide. Rats receiving 24 mg/kg/day showed a significant decrease (35%) in C.O. activity and a decrease in long-term potentiation, which is a proposed cellular correlate of memory formation. This treatment also decreases protein kinase C, a regulator of many cellular processes (Bennett et al., 1995). Behaviorally, rats were

impaired in spatial learning in a radial arm maze and Pavlovian conditioning in a shuttle box task (Bennett et al., 1992). Another study found impairments in sodium azide-treated rats in the Morris water maze (Bennett and Rose, 1992). These impairments were not due to sensorimotor deficits, as measured by open field activity and flinch-jump testing (Bennett et al., 1992). The spatial memory deficits produced by the chronic subcutaneous infusion of sodium azide were later verified in our laboratory using a baited holeboard task (Callaway et al., 2002).

Regional C.O. activity in the brain was measured after chronic sodium azide administration (Cada et al., 1995). After two weeks of subcutaneous treatment, all 22 regions sampled showed a significant reduction in C.O. activity when compared with that of saline-treated animals. The enzymatic reduction ranged from 26% to 37%. There were also different correlations of C.O. activity between brain regions in control versus azide-treated brains. Therefore, systemic inhibition of C.O. activity can cause regional vulnerability, perhaps due to regional differences in energy demand or C.O. gene expression (Chandrasekaran et al., 1992). Luques et al. (2007) recently demonstrated that systemic treatment resulted in signficant C.O. inhibition in the PCC after four weeks of administration.

Another study used sodium azide to locally impair metabolism in the rat striatum (Brouillet et al., 1994). Intrastriatal administration of 1.5 M, 2 M, and 3 M sodium azide reduced levels of several neurochemicals, including dopamine, GABA, substance P, somatostatin, and neuropeptide Y. These decreases were age and dose dependent. At the highest dose, there were decreases in ATP and increases in lactate, neuronal loss, and gliosis. However, Brouillet et al. (1994)

did not measure behavior changes associated with focal administration of sodium azide.

In vitro, inhibition of C.O. activity by 3 mM sodium azide increases the accumulation of insoluble amyloid fragments (Gabuzda et al., 1994), while 500 µM–1 mM sodium azide decreases the amount of soluble fragments but does not result in a loss in cell viability (Gasparini et al., 1997). Accumulation of insoluble amyloid deposits is one of the pathological features in the brains of AD patients. Sodium azide induces heat shock protein activity and increases lipid peroxidation in vitro, which is similar to hypoxic conditions (Kositprapa et al., 2000). Sodium azide-inhibited cells increased the production of superoxide and hydrogen peroxide, which may lead to oxidative damage (Partridge et al., 1994). An increase in hydroxyl radical production was found in vivo in sodium azide-treated rats (Smith and Bennett, 1997). Furthermore, sodium azide treatment in vivo changes the cellular distribution of kynurenine aminotransferase, an endogenous NMDA antagonist (Knyihar-Csillik et al., 1999). Thus, sodium azide administration in rats may be useful for modeling the impaired physiological and behavioral features of AD.

Studies in this and other laboratories have shown that chronic sodium azide administration produces memory retention deficits in rats (Bennett et al., 1992; Bennett and Rose, 1992; Callaway et al., 2002). We propose that C.O. inhibition in the PCC will result in deficits in a spatial holeboard task in rats. If a positive correlation is found between the inhibition of mitochondrial metabolism in the PCC and spatial memory impairment, then the development of this animal model can provide a tool for studying the pathophysiology of AD and assessing drugs for treating AD.

1.4 Methylene blue: A Therapeutic Candidate for Alzheimer's Disease

Methylene blue (MB) is a phenothiazine drug approved by the U.S. Food and Drug Administration for the treatment of methemoglobinemia (Wright et al., 1999). It is colored in its oxidized state and colorless after a two-electron reduction. It was first used as a biological dye by Paul Ehrlich to differentiate live cells from dead cells. In 1886, Ehrlich injected MB into living rats and described it as a selective vital stain for nerve cells and their processes (Foot, 1954). Since then, MB has been widely used in biology and chemistry as a redox indicator and dye. MB has been safely used for a number of pharmacological applications such as treating manic-depressive psychosis (Narsapur and Naylor, 1983; Naylor et al., 1986) and severe depression (Naylor et al., 1987). MB has also been used for the preventive treatment of drug-induced encephalopathy (Kupfer et al., 1996; Wainwright and Crossley, 2002).

1.4.1 Biochemical Effects of Methylene Blue

MB is a lipid-soluble compound that has a low molecular weight and can penetrate cellular membranes. MB has cationic and lipophilic properties that attract it to the mitochondrial membrane (Visarius et al., 1999). After *in vivo* administration, MB passes through the blood-brain barrier and accumulates in the human brain within hours (Peter et al., 2000). Thiazine reductase reduces MB to leucomethylene blue (LMB) on the cell surface (Merker et al., 1997). After LMB diffuses inside, it is reoxidized and sequestered inside organelles such as mitochondria and/or lysosomes (Merker et al., 1997; Gabrielli et al., 2004).

Although microscopy has not revealed a specific site (Buehring and Jensen, 1983), numerous studies support the theory that MB acts within mitochondria. Scott et al. (1966) systematically used different mitochondrial

inhibitors and concluded that MB accepts electrons near complex I and complex III, forming LMB. Afterwards, LMB donates electrons near cytochrome c, which is the electron carrier between complexes III and IV. Within mitochondria, low concentrations of MB stimulate cellular respiration in the rat liver (Visarius et al., 1997) and rat brain (Riha et al., 2005), and increase cytochrome c oxidation in the rat brain (Callaway et al., 2004).

One hypothesis that explains the myriad of uses for this compound is that MB has an affinity for proteins containing iron (May et al., 2003). MB is commonly used to treat drug-induced methemoglobinemia. This condition is characterized by the accumulation of methemoglobin, a form of hemoglobin that cannot bind oxygen. MB accepts electrons from NADPH-dependent methemoglobin reductase and donates the electrons to methemoglobin, thereby converting it back into oxygen-carrying hemoglobin. MB also prevents and reverses neurotoxicity caused by ifosfamide chemotherapy by inhibiting monoamine oxidase, which prevents the excitatory effects of ifosfamide (Kupfer et al., 1996; Lerch et al., 2006). Moreover, MB restores oxygen consumption in fish gills treated with rotenone, a complex I inhibitor, by transferring electrons downstream of complex I and allowing OXPHOS to continue (Lindahl and Oberg, 1961). Additional targets of MB include endothelial nitric oxide synthase, cytochrome c-dependent reductase (May et al., 2003), and glutathione (Kelner and Alexander, 1985).

In a model of ischemia-reperfusion using tissue slices, it was shown that MB treatment prevents the formation of free radicals such as superoxide (Salaris et al., 1991). During ischemia, there is a buildup of oxygen that is reduced to superoxide by xanthine oxidase upon reperfusion. MB prevents the reduction of

oxygen to superoxide by accepting two electrons at the iron-sulfur center of xanthine oxidase. LMB then transfers two electrons to oxygen, producing hydrogen peroxide rather than the more dangerous superoxide radical. MB also inhibits nitric oxide synthesis (Mayer et al., 1993) and prevents lipid peroxidation caused by complex I inhibition (Zhang et al., 2006). The antioxidant properties of MB would be beneficial to patients with AD, as an increase in free radical production and a decrease in antioxidants is associated with neurodegenerative diseases (Smith et al., 1995; Markesbery, 1997; Perry et al., 2000).

1.4.2 Memory-enhancing Effects of Methylene Blue

Martinez et al. wrote the first report of the ability of MB to improve memory (1978). They found that a low dose of MB (1 mg/kg) injected in rats post-training enhanced the memory of an inhibitory avoidance response when tested 24 h later. This effect did not occur when MB was injected 15 minutes before training, 6 hours after training, or 15 minutes before testing. Therefore, low dose MB does not facilitate memory by affecting retrieval or performance but rather through enhancing memory consolidation immediately after training. Conversely, a high dose of MB (50 mg/kg) administered to mice 15 minutes before training produced a retention deficit (Martinez et al., 1978).

Recent studies in our laboratory examined the effects of 1 mg/kg and 4 mg/kg doses in appetitive and aversive tasks. These studies provide evidence that MB improves memory retention without modifying anxiety (Callaway et al., 2002; Callaway et al., 2004; Gonzalez-Lima and Bruchey, 2004; Wrubel et al., 2007). When rats treated chronically with sodium azide are administered 1 mg/kg MB post-training, their reference memory in a baited holeboard task is restored to the level of control rats (Callaway et al., 2002). In this task, 1 mg/kg

MB given post-training to normal rats also enhanced memory retention when compared with saline-treated animals (Callaway et al., 2004).

Although low doses of MB improve memory in various tasks, MB has not been examined with regard to its effects on locomotor activity and feeding behavior, which may contribute to the modification of the behavior observed in previous avoidance and appetitive tasks. For example, MB could simply decrease locomotor activity, thereby increasing inhibitory avoidance responses.

In summary, low-dose MB administered post-training improves memory retention when tested 24 hours later in avoidance and appetitive tasks (Callaway et al., 2004; Gonzalez-Lima and Bruchey, 2004; Wrubel et al., 2007) and restores spatial memory impaired by sodium azide (Callaway et al., 2002). MB may improve memory retention by acting as an antioxidant and metabolic enhancer.

1.5 Specific Aims

This dissertation will address two general hypotheses. The first is that inhibition of C.O. activity in the PCC is sufficient to cause memory impairment in a spatial task. The second is that low-dose MB treatment can prevent these deficits. The following chapters will explore these topics. Specifically, the first study will test the hypothesis that isolated inhibition of C.O. activity in the PCC produces spatial memory deficits in a holeboard food-search task. Spatial memory deficits will be produced in rats by local administration of sodium azide. Study 2 will determine what dose of MB improves behavioral habituation and recognition memory without nonspecific effects on behavior. Different doses of MB will be evaluated in wheel running, feeding, open field habituation, and object recognition tests. In addition, we will examine the time and dose dependent

effects of MB on brain oxygen consumption. Oxygen consumption is an important indicator of neuronal activity (Wong-Riley et al., 1998; Kasischke et al., 2004). The measurement of brain oxygen consumption may provide insight into cellular mechanisms mediating the effects of MB on memory. After determining an effective MB dose, we will use it in rats treated with sodium azide in the PCC to prevent spatial memory impairment (study 3). Previous studies demonstrate that memory difficulties in AD are correlated with impaired mitochondrial oxidative metabolism and decreased brain oxygen utilization (de la Torre, 2004; Beal, 2005). MB increases brain mitochondrial metabolism and improves memory in rats. MB may be beneficial for humans with disorders characterized by metabolic energy deficiency, such as AD.

Chapter 2: Posterior Cingulate Cortex Hypometabolism Impairs Food-rewarded Spatial Memory

2.1 ABSTRACT

Evidence from human and animal studies supports a role of the posterior cingulate cortex (PCC) in spatial orientation and memory. Human functional brain imaging shows that this area is the earliest affected metabolically in patients with Alzheimer's disease (AD) and in patients with mild cognitive impairment who later develop AD. In particular, cytochrome oxidase (C.O.) activity is reduced within the PCC in AD. Inhibition of brain C.O. and resulting learning and memory impairments were experimentally induced in rats by injecting sodium azide directly into the PCC. Rats were trained in a baited holeboard task, received either sodium azide injections into the PCC or sham surgery, and then tested in an unbaited probe trial. Brains were extracted and analyzed for C.O. activity. In addition, the effect of C.O. inhibition on lipid peroxidation, a measure of oxidative stress, was studied *in vitro*. Rat brain homogenates were exposed to different concentrations of sodium azide and quantified using the thiobarbituric acid reactive substances assay. Although the groups did not differ in reference memory in the probe test, a significant within-subject difference was found. Only sodium azide-treated rats were impaired in their memory of the baited pattern in the probe trial as compared to their training scores before treatment. This was not due to a difference in general activity since the time to complete the task and the total number of nosepokes were not

different in sodium azide-treated rats than in control rats. C.O. histochemistry revealed a significant decrease in PCC activity in sodium azide-treated rats as compared to control animals. Other brain regions with purported anatomical connections to the PCC did not show group differences in average C.O. activity. However, interregional covariance analysis of C.O. activity revealed significant correlations between the PCC and several other brain regions in the control group that were absent in the sodium azide-treated group. Compared to control samples, a seven-fold increase in lipid peroxidation was produced by the concentration of sodium azide used in the *in vivo* experiment. Thus, C.O. inhibition in the PCC resulted in reduced interregional correlations in brain activity, an increase in oxidative stress, and memory impairment in a spatial holeboard task. An animal model presenting a metabolic inhibition similar to that in early stage AD will advance understanding of the disease by providing opportunities to characterize behavior impairments and test therapeutics that reverse impairments.

2.2 INTRODUCTION

The posterior cingulate cortex is the posterior division of the medial limbic cortex. It is located above the caudal aspect of the corpus callosum. The posterior cingulate includes Zilles' retrosplenial agranular (RSA) and retrosplenial granular (RSG) cortices, rostral to the splenium of the corpus callosum (Bussey et al., 1997; Paxinos and Watson, 1997). Because we did not investigate the area caudal to the splenium of the corpus callosum, the term "posterior cingulate" cortex (PCC) will be used to describe this cortical region rather than the name "retrosplenial" cortex. Dorsal PCC and ventral PCC will be used to refer to RSA and RSG, respectively. Anatomical connectivity studies show that the PCC is connected with motor, visual, and subicular cortices, and the anterior thalamus (Berthoz, 1997; Ohnishi et al., 2006).

The human PCC has a crucial role in spatial memory. Cammalleri et al. (1996) described a patient with a tumor in the PCC who was unable to navigate in familiar or unfamiliar surroundings due to the inability to use landmarks for route finding. Functional studies in healthy subjects also provide evidence for a role of the PCC in the processing of visually-guided behavior relating to aspects of attention, landmarks, and navigation. A spatial attention task showed fMRI activation in the PCC that was strongly correlated with the speed of target detection when spatial cues were present (Mesulam et al., 2001). The PCC was also active when subjects were asked to remember visual landmarks and their movements along a previously learned route (Berthoz, 1997). Similarly, Maguire et al. (1997) found that the PCC was involved during tasks that required learning a room that contained salient objects and empty rooms only distinguished by

27

their shape, as well as remembering environments recently learned and those very familiar.

Animal studies confirm a role of the PCC in spatial navigation and memory. Specific sensory stimuli can activate cingulate neurons, as examined with single-cell recordings. For example, the PCC contains head-direction cells that are sensitive to the direction the animal is facing (Chen et al., 1994). Furthermore, the PCC may specifically be involved during the late stages of learning. In an active avoidance task, discriminative neuronal activity (cells firing to a stimulus that predicts shock) occurs late in learning in the PCC (Gabriel, 1993). This is supported by studies showing that lesioning this area before acquisition impaired rats only during the late stages of task acquisition (Bussey et al., 1996, 1997).

Lesioning the PCC with N-methyl-D-aspartic acid (NMDA) impaired rats' performance in the radial arm maze, water maze, and an object-in-place task, whereby objects are switched in location in the second trial (Vann and Aggleton, 2002). Aspiration of the PCC produced deficits in the water maze and matching-to-place tasks (Sutherland et al., 1988; Whishaw et al., 2001; Harker and Whishaw, 2002).

The evidence from human and animal studies indicates that the PCC is involved in spatial navigation, perhaps with a bigger contribution during late stages of learning. This study tested this hypothesis by locally inhibiting PCC function after rats were trained in a spatial food-search task, and examining the effects on memory retention. Importantly, rather than using a neurotransmitter-specific lesion, PCC hypometabolism was produced by administration of sodium azide, a mitochondrial toxin that inhibits cytochrome oxidase (C.O.) activity by

blocking the transfer of electrons to oxygen. Cada et al. (1995) previously demonstrated that chronic and systemic sodium azide infusion in rats produces regional brain differences in C.O. inhibition. Comparing systemic sodium azide-treated rats to control rats revealed significant decreases in C.O. activity in all the brain regions sampled, including the PCC (Cada et al., 1995; Luques et al., 2007). This suggests that the PCC is part of a group of brain regions with distinct neurobiological features that renders them more vulnerable to metabolic insults.

We addressed the hypothesis that isolated PCC hypometabolism is sufficient to produce impairment in a spatial memory task. C.O. histochemistry-based metabolic mapping was used to analyze brain interregional effects due to PCC inhibition. The local neurotoxic effects of sodium azide administration *in vivo* was further confirmed by determining neuronal and glial densities in the PCC. Finally, we tested the hypothesis that the neurotoxicological effect of C.O. inhibition from sodium azide is mediated by an increase in oxidative stress by measuring lipid peroxidation in brain tissue after administration of sodium azide *in vitro*.

2.3 METHODS

2.3.1 Pilot Study

It was previously determined that a 3 M intrastriatal injection of sodium azide significantly increased lactate and decreased ATP concentrations after 3 hours (Brouillet et al., 1994). However, behavioral effects from this concentration were not assessed. Therefore, a pilot study was conducted to determine if behavioral impairment occurs 24 hours after sodium azide administration directly into the brain.

We injected rats in the sensorimotor cortex (SMC) and assessed their behavioral function during locomotion. This area was chosen based on the literature showing that lesioning the SMC decreases the use of the impaired forelimb in the Schallert cylinder and footfault tests (Schallert et al., 2000; Adkins et al., 2004). Two Sprague Dawley rats each received four injections of 0.5 μL sodium azide (3 M sodium azide dissolved in phosphate buffer, pH = 7.4) in the SMC using Paxinos coordinates (from Bregma, in mm): A/P -0.5 to +1.5; M/L ±3.0 to 4.5; D/V -1.2. (The details of the surgical procedures are described in a later section.) Measures of forelimb asymmetry were assessed before and 24 hours following the sodium azide injections, and scored using a slow-play videotape.

The footfault test measured coordinated forelimb placement during locomotion. Rats were placed on an elevated platform (47 cm X 30 cm) consisting of grid openings (3.25 cm^2 and 2.75 cm^2) and allowed to walk on the platform for 2 min. A footfault was defined as a slip of the forelimb through the grid openings. The number of contralateral (impaired) and ipsilateral (nonimpaired) forelimb footfaults were counted. Functional impairment was

expressed as the percentage of contralateral footfaults to total footfaults. Rats performed at 48% on the day before surgery and 67% one day following sodium azide administration in the SMC.

The Schallert cylinder test was conducted in a transparent Plexiglass cylinder (20 cm diameter X 30 cm height). Rats were placed in the cylinder before and 24 hours after injection and their behavior was videotaped for 2 min. We recorded the number of instances that the rat placed one limb on the cylinder wall while the animal was rearing and presented the data as a percentage of contralateral forelimb use. In addition, sequential paw placement was also assessed. This parameter was defined as the number of sequential placements of the same forelimb on the cylinder wall as the rat is rearing. Sequential paw placements were also presented as a percentage of contralateral use. In both measures, there was a decrease in the use of the impaired (contralateral) limb. Pre and post percentages in the asymmetry single use of the contralateral limb were 49% versus 33%, and 38% versus 23% in sequential paw placements of the impaired limb. Therefore, in all three measures of forelimb use, 3 M sodium azide administration directly into the SMC resulted in functional impairment one day following surgery. Therefore, we tested subjects one day following sodium azide injection in the PCC.

2.3.2 Subjects

Subjects were 25 male Sprague Dawley rats (Harlan, Houston, TX) weighing 225–250 grams upon arrival and single-housed on a 12 h light-dark cycle. After 1–2 days of acclimation, they were placed on a food restriction procedure and weighed daily to ensure that their weight did not drop below 85% of free-feeding rats of a similar age. They were fed at the end of each day.

Water was freely available. Rats were handled daily for 5 min on each of the 4–5 days before habituation began. On the two days preceding habituation, rats were given two sucrose pellets (45 mg, Noyes, Lancaster, NH) in their home cage. All animal procedures were approved by the Institutional Animal Care and Use Committee (IACUC) at the University of Texas at Austin, and conform to all NIH and USDA guidelines. All experiments were conducted in facilities approved by the Association for Assessment and Accreditation of Laboratory Animal Care (AAALAC) International.

2.3.3 Behavioral Procedures

2.3.3.1 Apparatus

The holeboard was a Med Associates open field chamber 43.2 cm^2 (St. Albans, VT) surrounded by clear plexiglass walls 30.5 cm high. Inside the chamber was a holeboard floor insert with sixteen equidistant-spaced holes (3.2 cm^2) in a 4 X 4 array and an underlying food tray. The holes were 4.5 cm apart and the outer holes were 8.6 cm from the chamber wall. The bottom insert consisted of a bottom tray, a screen and a top tray that were positioned underneath the holeboard floor. The bottom insert contained 16 holes with the same dimensions as the holeboard floor. The wire screen was positioned over the holes of the bottom tray which each contained five inaccessible sucrose pellets to mask potential odor cues emanating from the food in the baited holes. Thus, the rats could not use olfactory cues to discriminate between baited and unbaited holes. The task floor was placed 2 cm over the food tray. Infrared photobeams located just under the surface of the top floor detected entries into the holes. The testing room was dimly lit (33 lux) and contained large spatial cues. The chambers were wiped with a diluted solution of Bio-Clean (Stanbio

Laboratories, Boerne, TX) and the task floors were rotated between subjects to discourage the use of the previous animal's markings as a navigational strategy.

Med Associates computer software recorded the latency to complete each trial, novel hole entries, repeat entries and total entries, and organized the data by task and non-task. Reference memory was the index of spatial memory. Reference memory was defined as the ratio of the number of visits and revisits to the baited holes divided by the total number of visits to baited and nonbaited holes.

2.3.3.2 Habituation & Training

Rats were run in cohorts of 4–5 rats, resulting in a total number of five cohorts. During habituation, the animals were placed in the holeboard apparatus with all sixteen holes baited with one sucrose pellet. A habituation trial began with the first nosepoke and ended after all pellets were consumed or after 5 min elapsed. Trials continued until each rat consumed at least 15 pellets within a trial; this criteria was achieved in an average of four trials.

After 1–2 days of habituation, training began (Table 1). Four holes were baited in a consistent pattern throughout the training procedure (Figure 1). A trial began with the first nosepoke and ended after 5 min or after all 4 pellets were consumed. Each rat received 5 trials per day for a total of 8 days. Subjects remained in the behavioral room until all the rats in their cohort completed 5 trials. The average intertrial interval was 10 min.

Subjects were divided into two groups matched on their pretreatment acquisition performance which was calculated by averaging their reference memory scores for the 8-day training period. On the 9th day, surgery was performed. On the day following surgery, they received one unbaited probe trial

33

to test for memory retention. Thereafter, rats were tested daily for 4 days to determine how long the behavioral effects of C.O. inhibition lasted. Retraining was identical to training with the exception of the rats receiving 4 trials per day instead of 5 trials.

Table 2.1   Experimental design

SUBJECTS				TRAINING		
Sample Size	**Group**			**Day**	**Procedure**	**Configuration**
n = 12	control			1-2	habituation	all holes baited
n = 13	sodium azide			3-10	training	4 holes baited
				11	surgery	
				12	probe	no baited holes
				13-16	retraining	4 holes baited

Figure 2.1   Schematic drawing of the holeboard chamber. Solid circles correspond to baited holes and open circles to unbaited holes.
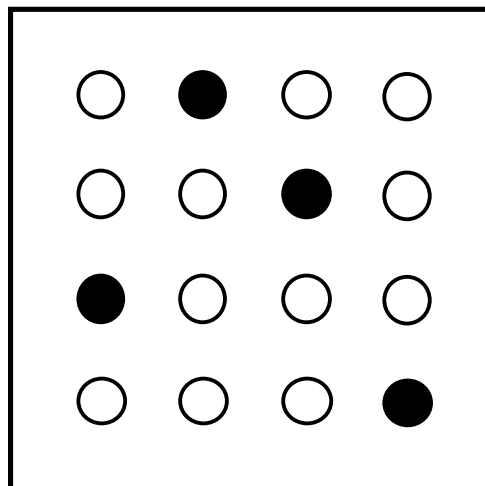
2.3.4 Surgery

Subjects were anesthetized using a vaporizing machine (E-Z Anesthesia, Euthanex Corp, Palmer, PA). Animals were induced in a host cage filled with 97% breathing air and 3% isoflurane (Aerrane, Baxter Pharmaceutical Products, Deerfield, IL). After the rat was fully anesthetized (~ 3 min), they were placed on a surgical bed maintained at 37°C with their nose in a cone connected to the anesthesia machine. During the surgical procedure, animals were monitored for breathing and anesthesia state, and the concentration of isoflurane was adjusted accordingly.

Rats were placed in the flat skull position in a Stoelting stereotaxic frame. The head was shaved, disinfected with Nolvasan (Wyeth, Madison, NJ), and Lacrilube (Allergan, Irvine, CA) was applied over the eyes to prevent drying. A 2 cm mid-sagittal incision was made over the scalp and a retractor was inserted into the skin to expose the area. The periosteum was removed by scraping with cotton swabs. Bone wax (Ethicon, Somerville, NJ) was used to stop bleeding, if necessary.

After drilling 0.8 mm bilateral holes over the PCC, a 30-G dental needle was slowly inserted. The needle was attached by tubing to Hamilton syringes that were placed in a microinjection pump which allowed for precise and slow infusions. Four bilateral injections of sodium azide (3 M sodium azide dissolved in phosphate buffer, pH = 7.4, 0.5 µL per injection) were made, alternating left and right hemispheres. Each injection was made over a 10 min period within the PCC within the following atlas coordinates (from Bregma, in mm): A/P -2.8 to -3.3; M/L ±0.2 to 0.4; D/V -1.2 to -1.3 (Paxinos and Watson, 1997). The needle was left in place for a few minutes after each injection and removed very slowly.

Three control animals received phosphate buffer injections in the PCC (vehicle). The remaining control rats (*n* = 9) received the same procedure without drilling or injection (sham). All control animals were under anesthesia for the same amount of time as the sodium azide-injected rats (n = 13).

At the end of surgery, the skin was sutured using 9 mm wound clips (Reflex, CellPoint Scientific, Gaithersburg, MD) and treated with a topical antibiotic containing pramoxine hydrochloride (Neosporin). A single 5 mg/kg injection of carprofen (Rimadyl, Pfizer) was administered intramuscularly as a post-operative NSAID analgesic. The animal was removed from the anesthesia system and allowed to waken, 5–10 min on average. Upon recovery, the rat was moved to its home cage.

2.3.5 Brain Procedures

2.3.5.1 Brain Processing

At the end of the last day of retraining, the brains were removed by rapid decapitation, frozen in isopentane, and stored in an ultra-low freezer at -40°C. Each brain was sectioned at 40 µM in a -17°C cryostat, collected onto glass slides in two series and kept frozen at -40°C until processed. One series was used for histochemical analysis of C.O. activity. The adjacent series was stained with cresyl violet for analysis of cell bodies and cell counting.

2.3.5.2 Cytochrome Oxidase Histochemistry

Experimental slides were processed in batches for enzyme histochemistry and each batch included two standard slides. Standards slides contained tissue sections of varying thickness (10, 20, 40, 60, and 80 µm) with known C.O. activity and were cut from frozen rat brain homogenate. The C.O. activity of the standards was determined in a previous spectrophotometric

experiment. The standards allow for quantification and comparison among batches (Gonzalez-Lima and Jones, 1994; Gonzalez-Lima and Cada, 1998).

C.O. histochemistry was performed as previously described (Gonzalez-Lima and Jones, 1994; Gonzalez-Lima and Cada, 1998). Chemicals were purchased from Sigma. Frozen sections were first incubated at 4°C for 5 min in a 0.1 M sodium phosphate buffer (PBS, pH 7.6) solution containing 0.5% glutaraldehyde and 9% sucrose, to facilitate adherence to the slides. This was followed by three baths of 9% sucrose in PBS (5 min each) at graded temperatures in order to bring the tissue from 4°C to room temperature and to remove red blood cells. Next, the slides were placed in a preincubation bath of 50 mM Tris buffer that included 0.55 g cobalt chloride, 200 g sucrose, 10 mL dimethyl sulfoxide, and 774 mL of 0.1 M hydrochloric acid for 10 min. Following a 5 min rinse in PBS, sections were incubated for 60 min at 37°C in an oxygen-saturated solution containing 0.35 g 3,3'-diaminobenzidine tetrahydrochloride, 52.5 mg cytochrome c, 14 mg catalase, 35 g sucrose, and 1.75 mL dimethyl sulfoxide in 700 mL PBS. The reaction was stopped by fixing the tissue in 9% sucrose PBS-buffered formalin (4%) for 30 min. Sections were dehydrated in baths of increasing concentrations of ethanol (30, 50, 70, 95, 95, 100, and 100%, 5 min each), cleared in xylene (3 times, 5 min each), and coverslipped with Permount.

2.3.5.3 Cytochrome Oxidase Image Analysis

C.O. activity was quantified by optical densitometry using Java software (Jandel Scientific) as detailed in Gonzalez-Lima and Cada (1998). A Kodak calibration strip with various gray levels of known optical densities (O.D.) was imaged and subsequent measurements were automatically reported to a

spreadsheet in O.D. Tissue sections were placed on a DC-powered lightbox, captured with a Javelin analog CCD camera, and digitized with a Targa-M8 frame-grabber. The field of view was approximately 0.75 × 1.0 cm. For each area of interest, O.D. was measured bilaterally across three adjacent brain sections per subject, using a brain atlas (Paxinos and Watson, 1997) to delineate the regions. For each brain region, the group average was calculated with the median value per subject.

For one standard per batch, ten measurements per thickness were measured by image analysis. Using the mean O.D. values and C.O. activity of the tissue standards, O.D. values for each area of interest were converted to units of C.O. activity. The linearity of each batch was verified by regression equations ($r^2 > .90$) and calibration curves were calculated under the assumption that increased tissue thickness is directly correlated with an increase in histochemically-revealed C.O. activity (Gonzalez-Lima and Cada, 1998). This curve predicted C.O. activity from the O.D. measures of the experimental tissues within each batch. The use of individual batch standards and accompanying regression curves aided in the control of interbatch variability. C.O. activity was reported as µmol/min/g of tissue.

Sodium azide is a specific inhibitor of C.O., and since the volume of drug injected is small (0.5 µL) and not likely to diffuse substantially, C.O. histochemistry also estimated the location of injection. Metabolic inhibition might affect other brain regions that connect with the PCC. Thus, we examined the activity in areas with major efferent and/or afferent connections. Of the regions examined, the anterior thalamic nuclei and the subiculum are the most heavily connected to the PCC (Finch et al., 1984; van Groen and Wyss, 1992a; van

Groen and Wyss, 2003). The PCC is a component of the Papez circuit, an anatomical pathway connecting many limbic structures that are implicated in spatial behavior (Mello e Souza et al., 1999; Harker and Whishaw, 2002; van Groen et al., 2004). Therefore, we also measured activity in this pathway which involves the following regions (projections are in brackets): cingulate cortex [cingulum] → entorhinal & perirhinal cortices [perforant pathway] → hippocampal proper [alveus] → subiculum [fornix] → mammillary bodies [mamillothalamic tract] → anterior thalamic nuclei [anterior thalamic radiation] → cingulate cortex. Brain regions will be referred to using the nomenclature from a rat brain atlas (Paxinos and Watson, 1997). The regions of the PCC we sampled are shown in Figure 2.

Figure 2.2   Coronal brain diagram around Bregma -2.8 mm indicating the

sampled regions of the PCC measured in the C.O. image analysis.
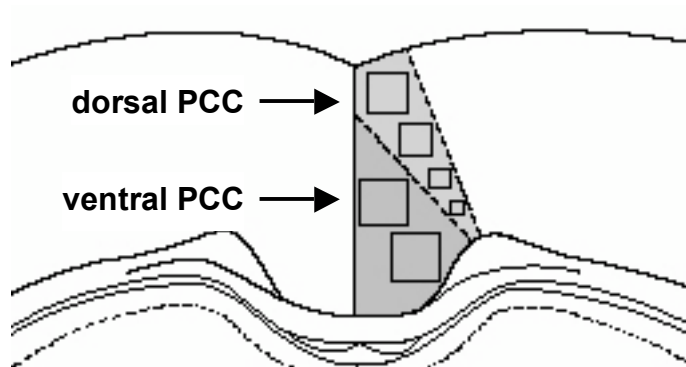
2.3.5.4 Nissl Staining

Nissl staining was used to count cell bodies, obtain stereological estimates of PCC cell density, and determine if the changes in C.O. activity were due to lower enzymatic activity alone or accompanied by neurodegeneration. For each subject, we stained the alternate slide to the one that showed the lowest C.O. activity in the PCC. Frozen brain sections were delipidized in a series of baths: 95% ethanol, 70% ethanol, distilled water, and 0.05 M sodium acetate buffer (pH 4) (2.5 min each). This was followed by staining in 0.1% cresyl violet in sodium acetate buffer at 45°C for 4 min, differentiated in 70% and 95% ethanol, and dehydrated in sequential baths of 95%, 100% and 100% ethanol (5 min each). Slides were then cleared in two washes of xylene (5 min each) and coverslipped with Permount.

2.3.5.5 Posterior Cingulate Cortex Cell Count

Cell counts were measured by an experimenter who was blind to subject assignment. Cell density (cells/volume) in the PCC was estimated from Nissl-stained sections of vehicle control (n = 3), sham control (n = 3), and sodium azide (n = 6) subjects using the optical dissector stereological method. The imaging setting consisted of a Labophot-2 binocular bright field microscope (Nikon Corporation, Tokyo, Japan) connected to a DVC-340 scan camera, DVCView 3.3 imaging software (DVC Company, Austin, TX), a Microcode II digital readout (Boeckeler Instruments, Inc., Tucson, AZ) and a PC computer. Cell density was estimated in three different PCC regions: 1) layers II/III of the dorsal PCC, 2) layers V/VI of the dorsal PCC, and 3) layers III/IV of the ventral PCC. Differential cell count was obtained based on morphological criteria for

brain cells. Neurons were identified by large ellipsoidal/pyramidal cell body, low nucleus/cytoplasm ratio, heterochromatic nucleus, and visible nucleolus; while glia appear with a small cell body, high nucleus/cytoplasm size ratio, and hyperchromatic nucleus. Cells (except those on top of the sections) were identified at 50X through the thickness of a section and were counted when they first came into focus within an unbiased counting frame (Harding et al., 1994). One sample per PCC region was obtained from each of six sections per subject within a randomly determined cerebral hemisphere. PCC cell density per region was calculated as $Nv_{cells} = \Sigma Q^-/\Sigma v_{(frame)}$, where ΣQ^- is the sum of cell counts per sample, and $\Sigma v_{(frame)}$ is the area of the unbiased counting frame (0.0396 mm^2, adjusted for 140X magnification) multiplied by the length of the analyzed region (d). The length was calculated as d = (No. of sections – 1) x No. of section series x section thickness.

2.3.5.6 *Thiobarbituric Acid Reactive Substances Analysis*

Rat brain homogenates were exposed to different concentrations of sodium azide and lipid peroxidation was quantified using the thiobarbituric acid reactive substances (TBARS) assay as previously reported (Zhang et al., 2006). The range of sodium azide concentrations was based on the final concentration (100 mM) of 3 M sodium azide after distribution in the PCC volume, which was estimated in one of the subjects from C.O. stained sections by means of the Cavalieri method. An array of grid testing points was randomly superimposed over a magnified PCC. The volume was calculated as V = $\Sigma(P)$ X a(p) X T, where $\Sigma(P)$ is the sum of grid points in the PCC, a(p) is the square of the linear distance between points on a grid divided by the square of the magnification, and T is the distance between the first and last section containing the PCC. We

43

determined the V_{PCC} = 29.4 mm^3. Three adult Sprague Dawley male rats (5

months old) were decapitated, and their brains were quickly extracted and

homogenized in a glass-glass homogenizer (20–25 strokes). Homogenates were

aliquoted in 1.5 mL Eppendorf tubes, slowly frozen in isopentane at -40°C and

stored until further use. Freeze-thaw cycles were avoided. On the day of the

experiment, homogenates were diluted at 12.5% (w/v) in PBS (pH 7.4 at room

temperature), vortexed, and kept in ice. Homogenates were combined with

sodium azide [0 mM (n = 8), 5 mM (n = 6), 25 mM (n = 2), 50 mM (n = 4) or 100

mM (n = 4)] and incubated at 37°C in the dark for 1 hr in closed 1.5 mL

Eppendorf tubes. After incubation, the proteins were precipitated by the addition

of 25% trichloroacetic acid (50/50, v/v). Samples were then vigorously vortexed

and centrifuged at 10,000 rpm for 30 min at room temperature. Supernatants

were combined with 1% thiobarbituric acid in 0.3% NaOH (50/50 v/v) and

incubated in glass test tubes at 90°C for 40 min. Samples were then maintained

at room temperature for 5 min and the absorbances were measured in a

Shimadzu spectrophotometer at λ = 532 nm using tetraethoxypropane as an

external standard (ε = 34.5 mM^{-1} min^{-1}). The levels of lipid peroxidation were

expressed as TBARS units (µmol/L).

2.3.6 Statistical Methods

Repeated-measures analysis of variance (ANOVA) containing one within-

subject variable (training day) and one between-subject variable (group) was

used to verify learning performance before surgery. Matching subjects to

treatment group based on their training performance prevented pre-treatment

group differences that might influence their post-treatment performance.

The effects of PCC hypometabolism on reference memory during the probe task were analyzed using Student's t test. Student's t tests also assessed group differences in the following measures of the probe task: total nosepokes; initial nosepokes to baited and unbaited holes; repeat nosepokes to baited and unbaited holes; total nosepokes to baited and unbaited holes; internosepoke interval between baited and unbaited holes; and latency to complete the probe. Post-training scores were evaluated with repeated-measures ANOVA followed by simple contrasts.

Group differences in brain C.O. data and cell counts in the Nissl-stained slides were examined using Student's t tests. Furthermore, the functional relationships between the PCC and other brain regions were analyzed by computing Pearson product-moment correlations within each group (Nair and Gonzalez-Lima, 1999). Finally, for the TBARS experiment, comparisons were made using one-way ANOVA followed by Dunnett's test for multiple comparisons, which compares the mean of each experimental group with the mean of the control group. All statistical testing was carried out using the SPSS 11.5 software package (SPSS, Inc., Chicago, IL). Differences were considered statistically significant at the two-tailed $p < .05$ level for all tests.

2.4 RESULTS

2.4.1 Behavioral Analysis

Two animals were excluded from the experiment. One was removed because it was not eating upon arrival to the research facility, and another died during surgery. As there was no difference between vehicle and sham control groups in reference memory performance in the probe (t(10) = 0.753, p = .469) and retraining trials (t(10) = 1.518, p = .160), these rats were treated as a single control group for subsequent analysis.

The reference memory scores during acquisition are similar to what has been shown in another study using a similar training paradigm consisting of 4 trials per day for 7 days (Lannert and Hoyer, 1998). All rats significantly improved reference memory of the baited holeboard over the 8 days of training, $F_{(7, 147)}$ = 23.80, p < .001 (Figure 3). However, there was no effect of group ($F_{(1, 21)}$ = 0.00, p > .984). This was expected since the animals were matched into treatment groups based on their training performance.

Figure 2.3   Acquisition performance in the holeboard. Means ± S.E.M. of reference memory scores of the baited pattern are plotted by day (5 trials/day).
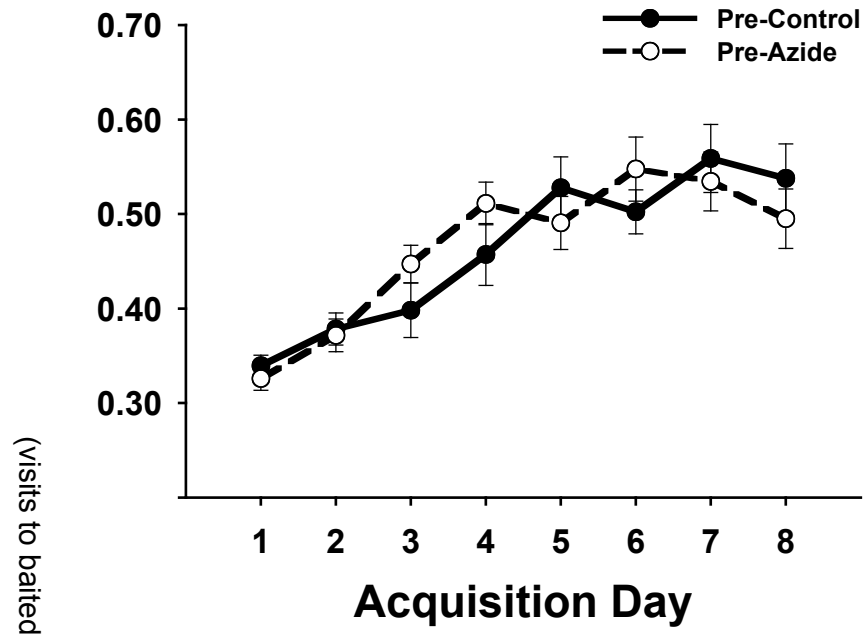
During the unbaited probe trial, the reference memory of sodium azide-injected animals was less than that of control animals (0.27 versus 0.37, respectively, Figure 4) ($t(21)$ = -1.671, $p > .05$). After comparing each subject's probe scores to their maximum training score, the mean group difference approached significance ($F_{(1, 21)}$ = 4.10, $p = .056$). When probe scores were compared to training averages within each group, only the rats treated with sodium azide showed significant impaired memory for the baited pattern in the probe trial (Figure 4; $t(10)$ = 5.395, $p < .001$). The control group did not show a significant decline in memory ($t(11)$ = 1.877).

In the probe trial, the sodium azide-treated rats spent a longer amount of time between the initial pokes into previously-baited holes ($t(21)$ = 2.51, $p = .02$) although the time to complete the trial was not different from control animals ($t(21)$ = 2.027). In addition, the total number of nosepokes of the sodium azide-treated rats was not different from control rats (26 versus 23, respectively) ($t(21)$ = 0.565). There were no group differences in the probe trial in the number of novel or repeated nosepokes in baited or unbaited holes.

Analysis of daily retraining averages by repeated measures did not reveal a significant effect of day or group. In addition, there were no group differences when daily retraining averages were analyzed with Student's t test. Therefore, sodium azide-treated rats recovered to control levels with continued training over days 13–16 (Figure 4).

Figure 2.4   Mean ± S.E.M. of reference memory before (training) and after (probe and retraining) sodium azide injection into the PCC. *significantly different from acquisition, $p < .001$.
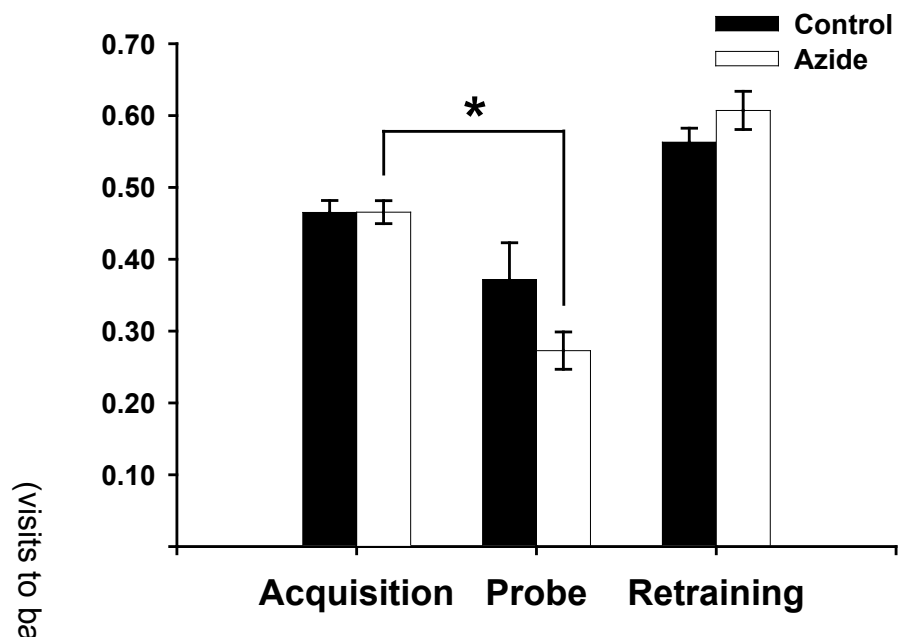
2.4.2 Brain Findings

2.4.2.1 Cytochrome Oxidase Histochemistry

Optical density of the selected regions of interest was converted to enzyme activity units (Table 2). Out of 26 regions examined, the only area to show a group difference was the PCC ($t(21) = 4.165$, $p < .001$). Further examination of this area revealed that hypometabolism due to sodium azide in the PCC was specific to the dorsal aspect of the PCC (Figure 5; $t(21) = 5.601$, $p < .001$). The rats injected with 3 M sodium azide showed a 23% decrease in C.O. activity in the dorsal PCC five days after administration. Significant decreases in activity were found from Bregma -2.3 to -4.2 mm, confirming that our injection was within the boundary of the PCC.

Table 2.2   Regional differences in cytochrome oxidase activity (MEAN ± S.E.M. µmol/min/g) in brains of rats injected with sodium azide in the PCC or sham control.

AREA OF INTEREST	abbreviation	Bregma level (mm)	CONTROL Mean ± SEM	(n)	AZIDE Mean ± SEM	(n)	
CINGULATE REGIONS							
posterior cingulate	PCC		270 ± 6	(12)	233 ± 7	(11)	*
dorsal PCC	RSA	-1.80 to -5.30	264 ± 5	(12)	204 ± 10	(11)	*
ventral PCC	RSG	-1.80 to -5.30	276 ± 7	(12)	263 ± 4	(11)	
anterior cingulate	ACC	1.60 to -1.40	251 ± 3	(10)	260 ± 5	(9)	
cingulum bundle	cb	-1.80 to -5.30	33 ± 3	(12)	29 ± 3	(11)	
THALAMIC REGIONS							
anterior dorsal	AD	-1.80	453 ± 16	(11)	451 ± 19	(11)	
anterior ventral	AV	-1.80	349 ± 5	(11)	338 ± 11	(11)	
anterior medial	AM	-1.80	275 ± 5	(11)	262 ± 9	(11)	
reticular	Rt	-1.80	299 ± 5	(11)	303 ± 8	(11)	
rhomboid/reuniens	Rh/Re	-1.80	250 ± 10	(11)	246 ± 6	(11)	
lateral dorsal	LD	-2.30	298 ± 12	(12)	292 ± 12	(11)	
HIPPOCAMPAL FORMATION							
anterior/dorsal							
CA1	CA1d	-3.80	236 ± 7	(12)	227 ± 7	(11)	
CA3	CA3d	-3.80	221 ± 6	(12)	216 ± 8	(11)	
dentate gyrus	DGd	-3.80	306 ± 7	(12)	292 ± 11	(11)	
posterior/ventral							
CA1	CA1v	-5.30	253 ± 8	(12)	252 ± 8	(11)	
CA3	CA3v	-5.30	277 ± 10	(12)	273 ± 11	(10)	
dentate gyrus	DGv	-5.30	226 ± 8	(12)	230 ± 7	(11)	
subiculum	SUB	-5.30	226 ± 13	(11)	241 ± 10	(11)	
mammillary bodies	MB	-4.80	356 ± 15	(11)	350 ± 13	(9)	
entorhinal	Ent	-4.80	148 ± 12	(12)	142 ± 11	(11)	
perirhinal	PRh	-4.80	175 ± 12	(12)	165 ± 12	(11)	
OTHER							
secondary motor cortex	M2	-0.26	276 ± 8	(10)	279 ± 8	(9)	
secondary visual cortex							
medial area	V2M	-5.30	253 ± 9	(12)	251 ± 8	(11)	
lateral area	V2L	-5.30	260 ± 8	(12)	254 ± 5	(11)	
caudate putamen	CPu	-1.80	295 ± 6	(12)	280 ± 7	(11)	
zona incerta	ZI	-3.80	219 ± 12	(12)	207 ± 14	(11)	
periaqueductal gray	PAG	-5.30	269 ± 12	(10)	271 ± 10	(10)	
raphe nuclei	RLi	-5.30	292 ± 11	(10)	303 ± 8	(10)	

*signficantly different from control (p < 0.001)

Figure 2.5   Illustrations of cytochrome oxidase-stained brain sections around

Bregma -2.80 mm. These were obtained from rats that received either vehicle

(left) or sodium azide (right) injections.

PCC

PCC

VEHICLE

AZID
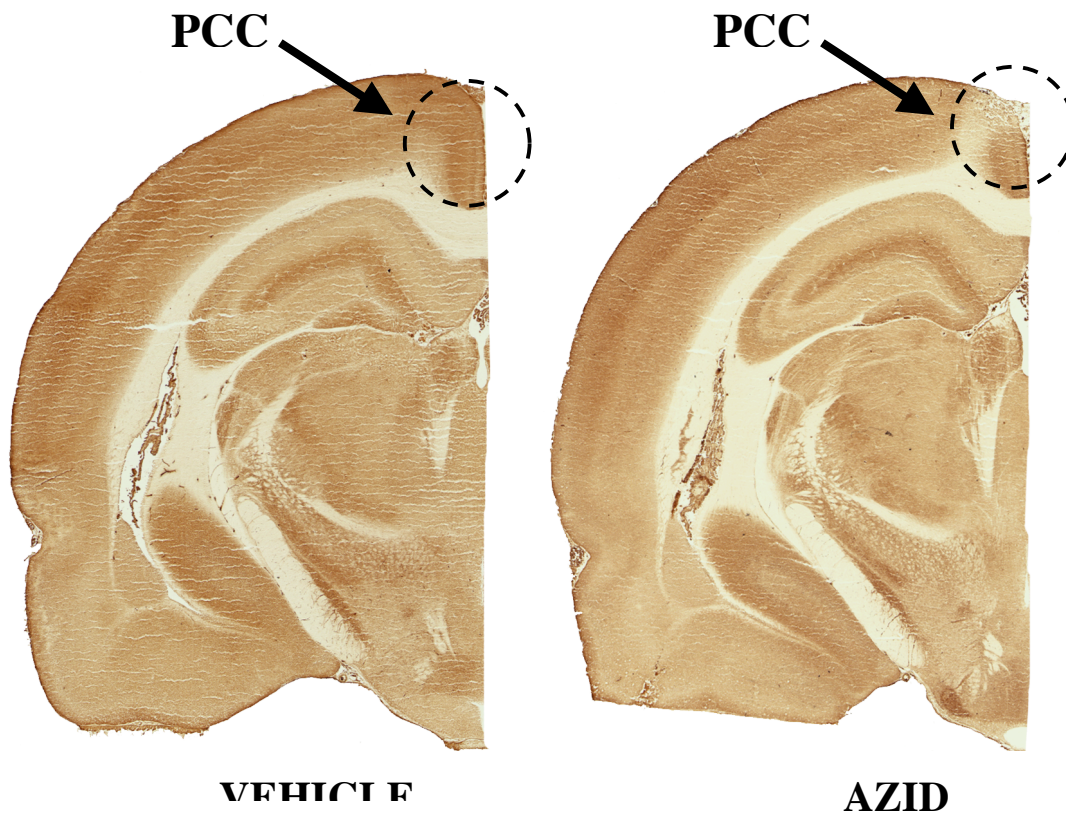
2.4.2.2 PCC-Interregional Correlations

Correlations in C.O. activity between the PCC and other brain regions were different in the two groups. In the control group, there were nine significant correlations ($p < .05$) in C.O. activity between the PCC and other regions of interest (Table 3). An interesting finding is the number of positive correlations ($n = 6$) between the PCC and hippocampal areas (DGv, CA1v, CA3v, SUB, PRh, and Ent). Significant positive correlations were also found with the CPu and secondary visual areas (V2M, V2L). In the sodium azide-treated group, there was only one significant correlation—one negative correlation between the PCC and CA3d. The positive correlations in the control group between C.O. activity in the PCC and other regions revealed functional coupling that was absent in the sodium azide-treated group. This suggests that these regions were functionally dissociated in sodium azide-treated subjects.

Table 2.3   Significant Pearson correlation coefficients (r) of C.O. activity

between the PCC and other brain regions.

PCC–Interregional Correlations

	CONTROL	AZIDE
CA3d	0.19	-0.66 *
CA1v	0.60 *	-0.16
CA3v	0.71 *	0.02
SUB	0.67 *	0.28
PRh	0.63 *	0.01
Ent	0.64 *	0.09
DGv	0.86 *	0.49
CPu	0.64 *	-0.05
V2M	0.77 *	0.39
V2L	0.73 *	0.04

significantly different from zero (p < 0.05)

2.4.2.3 *PCC Cell Count*

There were no significant differences in neuronal or glial cell density between vehicle control versus sham control rats ($p > .05$). Therefore, their scores were pooled for the following analysis. The neurotoxic effect of sodium azide in PCC was evidenced by dramatic changes in both neuronal and glial cell density. Sodium azide induced significant decreases in neuronal density and increases in glial cell density in all the analyzed PCC regions as compared to control animals (Figure 6, $p < .05$). The largest effect was observed in the ventral PCC where sodium azide produced a 64.3% decrease in neuronal density and a 4.8-fold increase in glial cell density (Figure 7). Furthermore, the majority of the remaining PCC neurons in sodium azide-treated subjects showed morphological signs of necrotic degeneration such as cell edema, vacuolization, and karyorrhexis.

Figure 2.6   Neuronal and glial cell densities in the PCC in sodium azide-injected rats and control rats. *significantly different from control values, $p < .05$.

PCC cell density
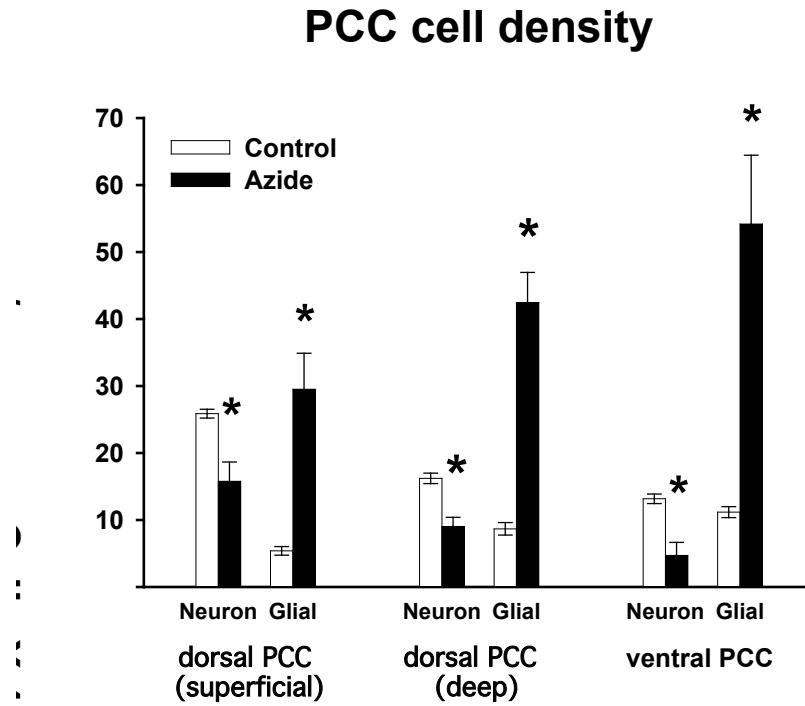
Figure 2.7   Cresyl violet-stained cells in the dorsal PCC (A) and ventral PCC (B) from rats with vehicle (left) or sodium azide injections (right). Sodium azide significantly increased gliosis and neuronal loss. Scale bar = 10 µm.

A. PCC dorsal (superficial)
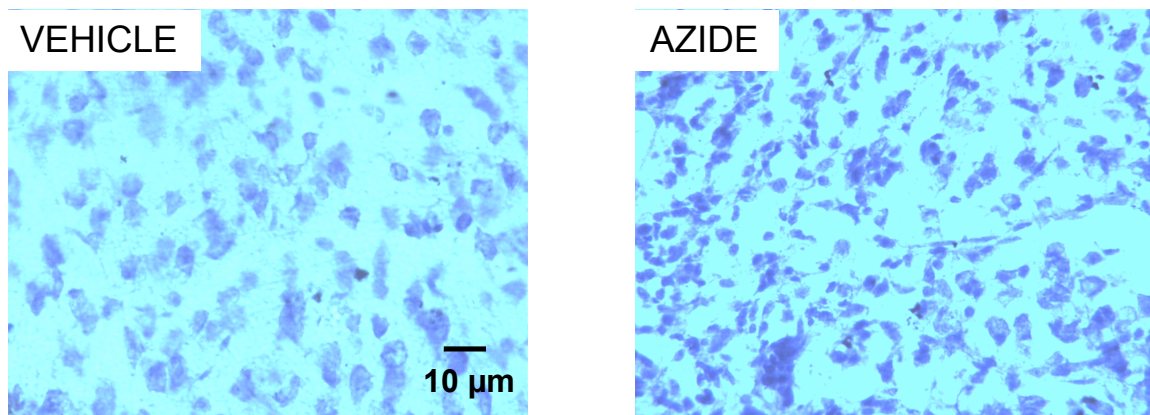
B. PCC ventral
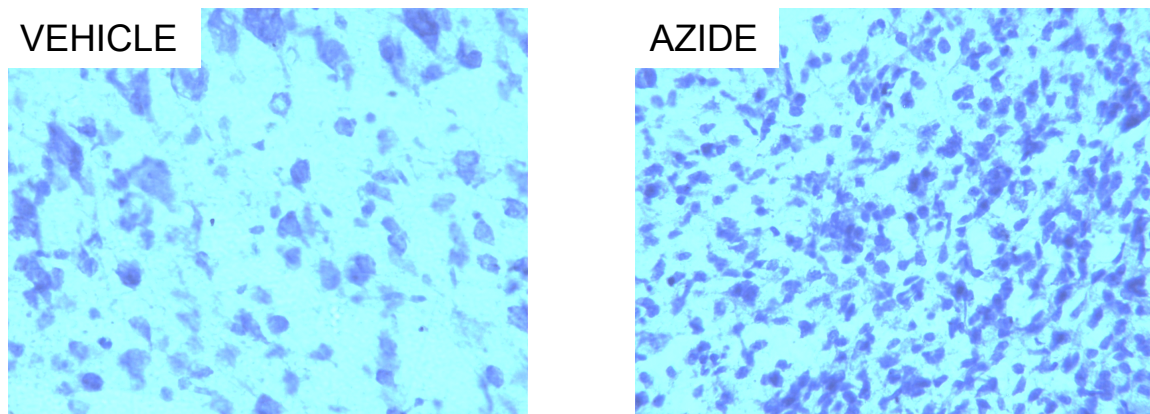
2.4.2.4 Oxidative Stress

Sodium azide potently increased brain lipid peroxidation in a concentration-dependent fashion ($F_{(4, 23)}$ = 12.8, p < .001). Compared to control, a seven-fold increase in lipid peroxidation was produced by the sodium azide concentration estimated in the PCC in the *in vivo* experiment (100 mM). A concentration twenty times lower (5 mM) produced a two-fold increase in lipid peroxidation (Figure 8).

Figure 2.8   Sodium azide treatment increases lipid peroxidation. Data
represent the Mean ± S.E.M. of TBARS reaction product in rat brain
homogenate. *significantly different from untreated control, $p < .001$, Dunnett's
test.
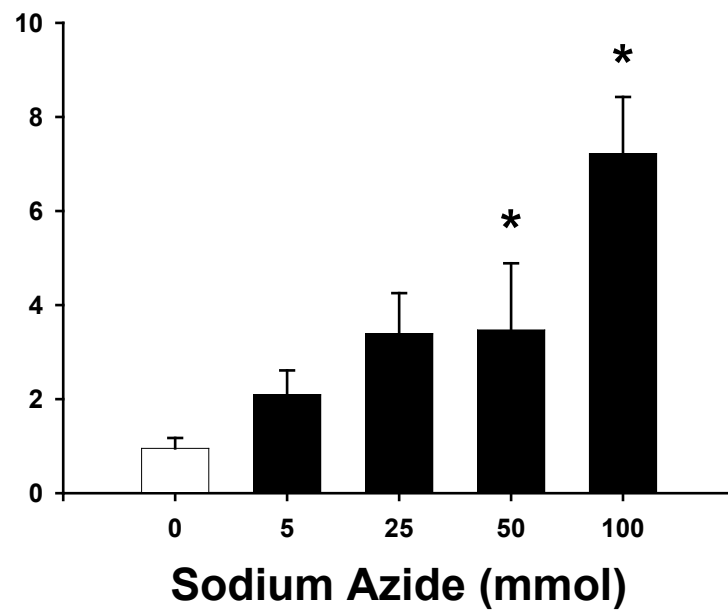
2.5 DISCUSSION

The present study confirms that the PCC is involved in spatial memory and verified that a local injection of sodium azide in this region induces neurotoxicity that is associated with inhibition of mitochondrial metabolism and oxidative damage. A major finding is that isolated hypometabolism in the PCC due to sodium azide treatment produced memory impairment in a holeboard task that required using spatial cues. The deficits in the probe trial are unlikely due to a change in response to sucrose reward. Rats with excitotoxic lesions in the PCC were not different from control animals in a sucrose consumption test (Bussey et al., 1996). Also, previous studies have shown that rats treated systemically with sodium azide have no change in sensory or motor function, or in exploratory activity in an open field chamber (Bennett and Rose, 1992; Szabados et al., 2004). However, they did have impaired memory for spatial tasks such as the eight-arm radial maze (Bennett and Rose, 1992), Morris water maze (Bennett et al., 1992), and holeboard task (Callaway et al., 2002). The present study did not find a difference in the total number of nosepokes between sodium azide-treated and control rats, which suggests that the impaired performance was due to a deficit in memory retrieval for the baited pattern and not due to differences in general activity or motivation.

The fact that sodium azide-treated rats were not different from control rats during the retraining phase in the holeboard maze may be due to the availability of a competing learning process. The baited pattern could be learned either by forming and accessing a cognitive map, or by response/procedural learning (Whishaw et al., 2001). In the present study, subjects were placed in the same corner of the holeboard for every trial and thus, rats using a response/procedural

strategy would also exhibit similar performance. Brain systems consisting of different structures are involved in processes for similar types of learning and memory ("parallel processing") (Lee and Kesner, 2003; McIntyre et al., 2003; Mizumori et al., 2004). Which neural system has more relative influence on behavioral expression may vary depending upon a number of factors such as age, experience, or incentive. If the PCC is damaged, the tendency to use cognitive maps is removed and the competing response/procedural learning may proceed. Furthermore, C.O. inhibition in the PCC was not comprehensive. Similar performance in the two groups during retraining may have resulted from the spared ventral portion of the PCC. Finally, the most anterior and posterior aspects of the PCC were also spared from the inhibitory metabolic effects of sodium azide, and some components of the stored information may have remained undisturbed. It is possible that the metabolically-normal tissue was sufficient for retraining in the maze.

C.O. histochemistry verified that the hypometabolism was localized in the PCC and that significant denervation of connecting structures did not occur by five days after sodium azide administration. The observation of hypometabolism in the dorsal, but not ventral aspect of the PCC can be explained by the depth of injection during surgery. We wanted our lesion to be specific to the PCC and avoid damage to the underlying cingulum fiber bundle. There is debate in the animal literature that previous findings of behavioral impairment from PCC damage can be, in part, due to inadvertent damage to this fiber tract (Neave et al., 1994; Warburton et al., 1998).

Correlations in metabolic activity between PCC and other brain regions were analyzed. Interestingly, most of the significant correlations found in the

control animals were in the Papez circuit (DGv, CA1v, CA3v, SUB, PRh, and Ent). This circuit was originally hypothesized to underlie emotion (Papez, 1937). It has been modified to include memory because lesions of these structures in humans and rodents often lead to disruption in learning and memory (Valenstein et al., 1987; Holdstock et al., 2000; Harker and Whishaw, 2002; van Groen et al., 2004). The PCC-interregional correlations validate the idea that decreasing the functional relationships in the Papez network can impair memory. PCC hypometabolism by sodium azide eliminated all the significant correlations between the PCC and other brain regions that were found in the control group.

The dose of sodium azide used in this study (3 M) was sufficient to produce memory impairment that was accompanied by cellular changes such as decreased C.O. activity and increased oxidative damage. Brouillet et al (1994) previously determined that a 3M intrastriatal injection of sodium azide significantly increased lactate and decreased ATP concentrations after 3 hours (Brouillet et al., 1994). These alterations may have led to the neurodegenerative effects we observed in the Nissl-stained tissue; specifically, there were significant decreases in neurons and increases in glial cells.

We also showed that lipid peroxidation, a marker of oxidative stress, is increased in sodium azide-treated brain homogenates. A defect in mitochondrial metabolism increases the generation of reactive oxygen species. Increasing evidence implicates oxidative damage in the neurodegenerative process of Alzheimer's disease (AD) (Benzi and Moretti, 1995; Reddy and Beal, 2005; Mielke and Lyketsos, 2006). Sodium azide-induced lipid peroxidation may represent a pharmacological research tool to study oxidative stress associated with neurodegenerative diseases and aging.

The PCC may be a vulnerable brain region. The PCC has a high baseline activity in healthy human subjects (Minoshima et al., 1997) and it contains numerous glutaminergic excitatory synapses. To fulfill a high energy demand, C.O. expression is upregulated (Wong-Riley et al., 1998). A high energy demand will render the PCC vulnerable to other metabolic insults such as vascular problems or C.O. inhibition. In rats, systemic administration of an N-methyl-D-aspartic acid (NMDA) antagonist produces region-specific neurotoxicity, and the PCC is the most affected region (Li et al., 2002). Likewise, the PCC would be one of the first areas affected by C.O. inhibition that compromises energy generation and eventually cell survival.

The PCC displays the largest decrement in glucose utilization in early-stage Alzheimer's disease (Minoshima et al., 1997). Laminar analysis of C.O. activity in the PCC from AD patients reveals a greater decrease in the energy-demanding superficial layers that contain synaptic neuropil (Valla et al., 2001). PCC hypometabolism appears before the onset of memory deficits in persons at genetic risk for AD, but who are not yet cognitively impaired (Reiman et al., 1996), as well as in subjects with mild cognitive impairment who later develop AD (Mosconi, 2005).

PCC hypometabolism by sodium azide-induced inhibition of C.O. activity is a good model to study early AD pathophysiology, as confounds from neurotransmitter-specific lesions are eliminated. C.O. inhibition in the PCC changed interregional correlations in brain activity and increased oxidative stress, which resulted in memory impairment in a spatial holeboard task. AD patients show disrupted correlations in metabolism between cortical regions (Horwitz et al., 1987). Therefore, sodium azide-treated rats are a useful model for

characterizing behavior and brain impairments associated with brain metabolic deficits, and for testing potential memory-enhancing drugs. Future studies will test if methylene blue, a metabolic enhancer (Callaway et al., 2004) and inhibitor of neurodegeneration (Zhang et al., 2006), can prevent the deficits caused by sodium azide-induced hypometabolism in the PCC.

CHAPTER 3: Memory Facilitation by Methylene Blue: Dose-dependent Effect on Behavior and Brain Oxygen Consumption

3.1 ABSTRACT

Methylene blue (MB) administered post-training improves memory retention in avoidance and appetitive tasks, and restores spatial memory impaired by an inhibitor of cytochrome oxidase. MB may improve memory retention by increasing brain oxygen utilization. We investigated which doses improve memory without nonspecific behavioral effects and whether MB enhances brain oxygen consumption. Different doses were evaluated 24 h after administration in the following tasks: wheel running, feeding, open field habituation, and object recognition tests. The 1–10 mg/kg MB-treated rats were not different from saline-treated rats in locomotion or feeding behavior. The 50–100 mg/kg doses decreased feeding and running wheel behavior. The 4 mg/kg dose improved behavioral habituation and object memory recognition. Dose-dependent effects of MB on brain oxygen consumption revealed that low concentrations increased brain oxygen consumption *in vitro* and 24 h after *in vivo* administration. Therefore, MB doses that facilitate memory retention are associated with increased brain oxygen consumption.

3.2 INTRODUCTION

Memory difficulties in dementia are correlated with impaired mitochondrial oxidative metabolism and brain oxygen utilization (de la Torre, 2004; Beal, 2005). Therefore a drug that increases brain mitochondrial respiration may improve memory. One candidate is methylene blue (MB), a redox compound with an affinity for mitochondria (Visarius et al., 1999). After *in vivo* administration, MB passes the blood-brain barrier and accumulates in the human brain within hours (Peter et al., 2000). MB increases cytochrome oxidase (C.O.) activity by donating electrons to the electron transport chain (Scott and Hunter, 1966; Callaway et al., 2004).

The memory-improving action of MB was first reported by Martinez et al. (1978). A low dose (1 mg/kg) injected in rats post-training enhanced retention of an inhibitory avoidance response when tested 24 h later (Martinez et al., 1978). Our laboratory also examined the effects of low dose MB (1 mg/kg and 4 mg/kg) in other appetitive and aversive tasks, and we have provided convincing evidence that MB improves memory retention (Callaway et al., 2002; Callaway et al., 2004; Gonzalez-Lima and Bruchey, 2004). Furthermore, Gonzalez-Lima and Bruchey (2004) found that rats injected with one or five daily injections of 4 mg/kg MB were not different from saline-treated rats in measures of exploration or anxiety in an open field chamber. However, these studies did not evaluate other behavioral effects of MB which could explain their results. For example, MB could simply modify baseline levels of locomotor activity and thereby increase inhibitory avoidance responses.

Although low dose MB improves memory in various tasks, it has not been evaluated for its effects on locomotor activity and feeding behavior that may

66

contribute to the modification of behavior observed in previous avoidance and appetitive tasks. For that reason, our first objective was to investigate which MB doses improve behavioral habituation and recognition memory 24 h after administration without nonspecific effects on behavior. Different doses were evaluated in wheel running, feeding, open field habituation, and object recognition tests. The first two tests measured locomotion and feeding of a sweet cookie. The second two tests measured between-days memory retention of habituation of exploratory behavior (Cerbone and Sadile, 1994) and object recognition memory (Lebrun et al., 2000).

C.O. is the terminal enzyme mediating oxygen utilization (Gonzalez-Lima and Cada, 1998). We previously demonstrated that brain C.O. activity increases 24 h after 1 mg/kg MB administration *in vivo* (Callaway et al., 2004). Improved cellular respiration in the brain would explain the enhanced memory retention seen in animals after treatment with low dose MB (Martinez et al., 1978; Callaway et al., 2002; Callaway et al., 2004; Gonzalez-Lima and Bruchey, 2004). However, there are no studies demonstrating a direct action of MB on brain oxygen utilization.

Therefore, our second objective was to investigate brain oxygen consumption after *in vitro* administration of low concentrations of MB (0.5, 5, and 10 µM) to rat brain homogenates. These *in vitro* concentrations correspond to the 1–4 mg/kg doses (Peter et al., 2000) that improve memory retention (Martinez et al., 1978; Callaway et al., 2002; Callaway et al., 2004; Gonzalez-Lima and Bruchey, 2004). A final experiment measured oxygen metabolism in rat brains 24 h after *in vivo* treatment with 1 mg/kg MB. There is a tight coupling between oxygen consumption and neuronal activity (Sokoloff, 1989). Measuring

brain oxygen consumption could help to understand the cellular mechanisms underlying the effect of MB on memory.

3.3 METHODS

3.3.1 Subjects

The experiments were performed in accordance with NIH guidelines for the use of experimental animals and were approved by the University of Texas Institutional Animal Care and Use Committee. All rats were purchased from Harlan (Houston, TX). They were housed on a 12 h light-dark cycle with food and water access *ad libitum*. For the behavioral experiments, subjects were 36 male Long-Evans rats weighing an average of 366 ± 14 g at the beginning of behavioral testing. An additional ten 7-month old male Long-Evans rats were used for the *in vitro* oxygen assays.

A previous study indicated that 1 mg/kg MB increased in C.O. activity 24 h after administration in Sprague Dawley rats (Callaway et al., 2004). Therefore, twenty-two adult male Sprague Dawley rats weighing an average of 276 ± 2 g were used to determine if the C.O. increase 24 hr after MB treatment is related to an increase in oxygen consumption *in vivo*.

3.3.2 MB Administration

Rats were counterbalanced into five treatment groups of saline, 1, 4, 10, or 100 mg/kg MB (Faulding Pharmaceuticals, Paramus, NJ). The injections were performed intraperitoneally (ip). All behavioral experiments were conducted during the light phase. Behavior was measured 24 h after MB administration with the exception of the running wheel, which lasted for a continuous 24 h period.

3.3.3 Behavioral Procedures

3.3.3.2 Running wheel

Rats were injected with MB or saline, and placed in the holding compartment of a standard activity wheel. The door between the holding cage and wheel remained open to allow access to food and water *ad libitum*. The number of revolutions was recorded 24 h later.

3.3.3.3 Feeding test

Before the feeding experiment, rats were given vanilla wafers (Nabisco Brands, Inc., East Hanover, NJ) in their home cage in order to avoid neophobia. Rats were injected with MB or saline 24 h before testing. Trials were conducted in a box (43.2 cm X 21.6 cm X 30.5 cm) with clear plastic sides. One vanilla wafer softened with approximately 5 mL of distilled water was placed in a plastic weigh boat on a wire mesh floor. Subjects were placed in the box facing the wafer and the experimenter left the room. The rats were removed after 5 min and the remaining wafer weight was recorded. Scattered food was collected and included in the calculations.

3.3.3.4 Open field Habituation Test

An automated activity monitoring system from MED Associates (St. Albans, VT) recorded various motor indices of exploration. The 43.2 cm^2 chamber consisted of clear plastic sides 30.5 cm high and a plexiglass floor. Activity was detected by parallel beam arrays of infrared motion detectors (16 X 16, 2.5 cm apart). Two arrays located 2.5 cm above the floor detected ambulatory and stereotypic measures, and a third array positioned 17.2 cm above the chamber floor detected rearing. The measures included ambulatory

counts, time, and distance (number of horizontal beam breaks, and the calculated time and distance traveled); stereotypic time and counts (duration and frequency of short movements without ambulation of the rat, including grooming, turning, and tailflick behavior); vertical counts and time (frequency and duration of vertical beam breaks, which were produced by rearing on hindlimbs); resting time (time spent with no new beam breaks); and center crossings (number of crossings into the central 38% area of the open field).

Exploratory behavior was assessed in a dimly-lit, sound-proofed testing room. Rats were habituated to the room for a 5 min period. They were then placed in the chamber facing one corner and their behavior was recorded for 5 min. Immediately after the session, they were administered MB or saline and returned to their home cage for 24 h. The following day, the rats received another 5 min habituation period in the testing room followed by a second 5 min session in the open field chamber. The chambers were cleaned with a mild detergent between animals (Bio-Clean, Stanbio Laboratories, Boerne, TX).

3.3.3.5 Object Recognition Test

Previous studies of the object recognition test indicate that a 24 h intertrial interval results in loss of memory for the object (Bartolini et al., 1996; Pitsikas et al., 2002). Therefore, we expected that saline-treated rats would explore the objects equally and that MB would improve memory for the familiar object on day 2. The object recognition test was conducted in the same chamber used for the open field test. Since all animals previously received two days of 5 min open field trials, they were already familiar with this environment and did not require more pre-exposure. The objects were unopened aluminum cola cans, large metal clamps, and 50 mL clear centrifuge tubes filled with blue paper. The

objects were suspended so as to not interfere with the infrared beams or be displaced by the animals. The MED Associates activity monitoring program recorded time near the object, which was defined as the time spent in the corner (10 X 10 cm corner area) where the objects were suspended.

The first day consisted of a 3 min trial in which animals freely explored two identical objects that were suspended in opposite corners of the open field. The arena was cleaned with diluted Bio-Clean between each trial and the objects were wiped with 70% ethanol to minimize olfactory cues. Immediately following the exploratory session, subjects were returned to their home room and injected with MB or saline. After 24 h, rat received a second trial. They were placed in the same open field except that one object from day 1 was replaced with a novel object. Animals were allowed to explore both objects for 3 min. Object recognition was analyzed using the difference in time spent near the novel versus familiar object.

3.3.4 Brain Oxygen Assays

3.3.4.1 Fiber Optic Oxygen Sensor

Dissolved oxygen concentration was measured with a fiber optic oxygen sensor system (Ocean Optics, Dunedin, FL). The system is as accurate as polarographic techniques and it has a faster response time but it does not consume oxygen or require frequent calibrations (Shaw et al., 2002). It consists of a fluorescence probe connected to a light source and spectrometer. Ocean Optics software converts partial pressure in the tissue samples to molar percentage. The sensor was calibrated at Ocean Optics and a single-point update was completed immediately before the study in a 37°C incubator.

3.3.4.2 in vitro Procedures

The dose-dependent effects of MB on oxygen metabolism were studied using different MB concentrations added to rat brain homogenates. MB enters cellular membranes after it is reduced to leucomethylene blue (LMB) by the capillary endothelium (Merker et al., 1997); therefore, LMB was used to facilitate entry into the cells in the brain homogenates *in vitro*. MB was reduced with 45 mM ascorbic acid in distilled water and a minimal amount (< 2 mM) of HCl was added to speed the reaction (Snehalatha et al., 1997; Mowry and Ogren, 1999). Three LMB concentrations were used (0.5, 5.0, and 10.0 µM) that approximated the levels found in plasma after a single 100 mg intravenous injection in humans (Peter et al., 2000). Samples were run 9 times per concentration in a counter-balanced approach.

The brain homogenization and *in vitro* procedures were similar to those in a previous study (Callaway et al., 2004). Following decapitation, the brains were quickly extracted, mixed thoroughly to form one homogenate, divided into centrifuge tubes, spun briefly at a low rpm, and frozen in isopentane. On the day of the assay, the homogenized brains were mixed in isolation buffer (0.32 M sucrose, 1 mM EDTA, 8.4 mM Trizma HCl, and 1.6 mM Trizma base) to produce a 20% tissue mixture. To solubilize membranes, 10% deoxycholate was added for a final concentration of 0.25% tissue and 0.5% deoxycholate.

LMB (990 µL) was warmed to 37°C. Ten microliters of tissue solution were added, inverted twice to mix, and placed in a 37°C chamber for 5 min measurements. Control samples contained 10 µL of tissue solution and 990 µL of 0.05 M potassium phosphate buffer (0.02 M KH_2PO_4 and 0.24 M Na_2HPO_4). All final solutions had a pH of 7.2 ± 0.1.

3.3.4.3 in vivo Procedures

Rats were injected with 1 mg/kg MB ip and killed 1 h (n = 5), 2 h (n = 5), or 24 h (n = 6) later. Controls subjects (n = 6) were rats that received an equivalent volume of saline intraperitoneally and killed 2 h later. Following decapitation, the brains were quickly extracted, homogenized, frozen in isopentane, and stored at -40°C. For each subject, approximately 50 μL of brain tissue homogenate was placed in a microcentrifuge tube, warmed to 37°C in a water bath, and placed in a 37°C incubator for analysis. Each sample was measured for 5 min with the oxygen sensor described above.

3.3.5 Statistical Methods

SPSS software (version 11.5, SPSS, Chicago, IL) was used for all statistical analysis. Parametric data were analyzed using analysis of variance (ANOVA) to test the significance of mean group differences for the open field measures and oxygen probe data. This was followed by Dunnett's post-hoc t tests to compare each treatment group to the control group. Nonparametric data from the running wheel and feeding tests were analyzed with Mann–Whitney U tests for independent group mean comparisons. The Wilcoxon signed-ranks test was used for paired data in the object recognition test. The specific tests and two-tailed p levels are reported in the results. Comparisons were considered significant at the p < .05 level.

3.4 RESULTS

3.4.1 Behavioral Effects of MB

3.4.1.1 General Observations after in vivo Administration

Shortly after injection, the 100 mg/kg dose produced piloerection and uncoordinated movement in the first three subjects injected. One of these rats was found dead in the running wheel the following day. This dose was discontinued from further use and the other two rats injected with 100 mg/kg were excluded from further testing. Three subjects injected with 50 mg/kg were examined in the running wheel and wafer feeding tests. However, because of decreased daily food consumption in these rats, they were excluded from the open field habituation and object recognition tests. The rats injected with saline or 1–10 mg/kg MB did not show adverse effects from the injections.

3.4.1.2 Running Wheel and Feeding Tests

Group differences were examined with Mann–Whitney U tests, comparing each MB group to the saline-treated group (Table 1). In the running wheel, rats given the highest doses of MB (50 and 100 mg/kg) were significantly less active than saline-treated rats, as indicated by fewer median revolutions (35 versus 279, respectively) ($U(14) = 9.0$, p = .038). Rats treated with 1–10 mg/kg MB were not different from saline-treated rats in the running wheel.

In the feeding task, 1–10 mg/kg MB-treated rats ate a similar amount of wafer as those treated with saline. However, the rats injected with 50 mg/kg only ate an average of 0.03 g versus a 0.52 g average in the other groups. Due to the small sample size in the 50 mg/kg group ($n = 3$), the group difference was not significant ($U(14) = 5.0$, $p = .088$).

Table 3.1   Running wheel and feeding test results 24 h after saline or MB
treatment.

MB Dose (mg/kg)	n	Running Wheel (revolutions)			n	Feeding Test (grams)		
		Mean ± S.E.M.	Median	Range		Mean ± S.E.M.	Median	Range
saline	11	318 ± 72	279	28 – 718	11	0.60 ± 0.23	0.10	0 – 1.8
1	4	166 ± 104	92	9 – 470	6	0.48 ± 0.30	0.48	0 – 1.8
4	5	453 ± 112	362	253 – 843	6	0.48 ± 0.28	0.48	0 – 1.5
10	7	268 ± 97	103	78 – 761	7	0.53 ± 0.31	0.53	0 – 1.7
50	3	64 ± 46	35 *	3 – 154	3	0.03 ± 0.04	0.03	0 – 0.1
100	2	116 ± 111	116 *	5 – 227				

50–100 mg/kg MB vs saline, p < .05

3.4.1.3 Open Field Habituation Test

No significant group differences were found on day 1 using ANOVA (Table 2). Previous studies suggest that decreased exploratory activity in a familiar environment is indicative of habituation (for review, see Cerbone and Sadile, 1994). On day 2, 24 h after MB or saline treatment, 4 mg/kg-treated rats were less ambulatory (15 ± 3 s) as compared to saline-treated rats (27 ± 2 s). Dunnett's-corrected comparisons verified that 4 mg/kg MB-treated rats showed significantly less ambulatory time (p = .006), ambulatory distance (p = .029), and ambulatory counts (p = .034) as compared to saline-treated rats. Likewise on day 2, 4 mg/kg MB-treated rats rested longer than saline-treated rats ($F_{(3, 24)}$ = 6.43, p = .025). The habituation effect was confirmed as a between-days difference in ambulatory distance by accounting for baseline performance on day 1 ($F_{(3, 24)}$ = 3.02, p = .049). Percent decreases from day 1 to day 2 in ambulatory distance were 5% for saline-treated rats, 18% for 1 mg/kg MB-treated rats, and 26% for the 4 mg/kg MB-treated group. The 10 mg/kg MB group showed a 25% increase, but it was not statistically significant. No significant group differences were found in measures of rearing (vertical time or counts) on day 2. In addition, there were no group differences in the number of crossings into the center of the chamber. This signifies that MB did not affect center avoidance, an indicator of anxiety.

Table 3.2   Means + S.E.M. of activity measures in 5 min open field sessions

before treatment (Day 1) and 24 hours after saline or MB treatment (Day 2).

MEASURE	Saline		1 mg/kg	
	Day 1	Day 2	Day 1	Day 2
Ambulatory distance (cm)	1343 ± 135	1268 ± 114	1558 ± 102	1277 ± 80
Ambulatory time (s)	26 ± 3	27 ± 2	31 ± 3	27 ± 2
Ambulatory counts	585 ± 70	605 ± 70	715 ± 58	578 ± 49
Vertical time (s)	54 ± 5	55 ± 8	46 ± 9	34 ± 5
Vertical counts	38 ± 3	31 ± 3	38 ± 3	27 ± 5
Stereotypic time (s)	82 ± 4	73 ± 3	84 ± 3	76 ± 5
Stereotypic counts	1455 ± 90	1249 ± 67	1521 ± 53	1336 ± 97
Resting time (s)	188 ± 6	196 ± 5	179 ± 4	194 ± 5
Center crossings (38% of chamber)	128 ± 17	120 ± 15	131 ± 5	107 ± 8

MEASURE	4 mg/kg			10 mg/kg	
	Day 1	Day 2		Day 1	Day 2
Ambulatory distance (cm)	1123 ± 126	828 ± 152	*	1259 ± 253	1572 ± 82
Ambulatory time (s)	22 ± 3	15 ± 3	*	25 ± 5	33 ± 3
Ambulatory counts	494 ± 54	354 ± 75	*	569 ± 126	715 ± 56
Vertical time (s)	71 ± 12	60 ± 16		43 ± 9	52 ± 5
Vertical counts	49 ± 8	33 ± 8		40 ± 9	40 ± 4
Stereotypic time (s)	75 ± 5	64 ± 4		77 ± 7	81 ± 3
Stereotypic counts	1300 ± 108	1085 ± 89		1345 ± 142	1454 ± 75
Resting time (s)	199 ± 7	218 ± 7	*	193 ± 14	181 ± 3
Center crossings (38% of chamber)	131 ± 18	95 ± 22		133 ± 23	150 ± 7

*significantly different from saline, p < .05

3.4.1.4 Object Recognition Test

There were no significant differences in the amount of time rats spent exploring each identical object on day 1. On day 2, all rats distinguished between the two objects as shown by a longer exploration time with the novel object (p = .002, Wilcoxon signed-ranks test). Day 2 group averages (Table 3) showed that saline-treated rats explored the novel object 5 sec longer than the familiar object. The effects of MB on object recognition varied in a dose-dependent manner. On average, rats treated with 1 mg/kg MB explored the novel object 2 s longer than the familiar object, the 4 mg/kg MB-treated rats spent almost 10 s more exploring the novel object, and the 10 mg/kg MB-treated group spent 16 s longer in close proximity to the novel object. The 4–10 mg/kg MB-treated groups showed a statistically reliable difference (both groups: p = .028, Wilcoxon signed-ranks test).

Table 3.3   Dose-response effects of MB on object recognition memory.

MB dose		Familiar Object	Novel Object
(mg/kg)	n	Mean ± S.E.M.	Mean ± S.E.M.
0	10	5.01 ± 1.45	10.06 ± 2.45
1	6	6.65 ± 1.41	8.65 ± 3.12
4	6	3.63 ± 1.36	13.16 ± 4.58 *
10	6	1.93 ± 0.83	17.55 ± 12.46 *

novel significantly different from familiar, p < .05

3.4.2 Effects of MB on Brain Oxygen Consumption

3.4.2.1 Dose-dependent Effects after in vitro Administration

The values obtained from our control group indicated a partial pressure baseline measure of 28 mmHg, which is consistent with other studies of brain oxygen tension (Doppenberg et al., 1998; Duong et al., 2001). Repeated-measures ANOVA demonstrated that oxygen concentration decreased over time in all groups (Figure 1; $F_{(4, 128)}$ = 712.96, $p < .001$). This was expected because respiratory substrates were not added to the samples and, therefore, consumption occurs only to the extent of the oxygen concentration in the samples. There was a main effect of LMB ($F_{(3, 32)}$ = 10.18, $p < .001$, repeated-measures ANOVA). Dunnett-corrected comparisons showed significant differences between control and 5 µM LMB ($p = .004$), and control and 10 µM LMB ($p < .001$). The difference in starting points suggests that LMB increases oxygen metabolism within the first min post-administration *in vitro*.

Figure 3.1   Effects of LMB on brain oxygen consumption *in vitro*. *significantly

different from control, *p* < .01.
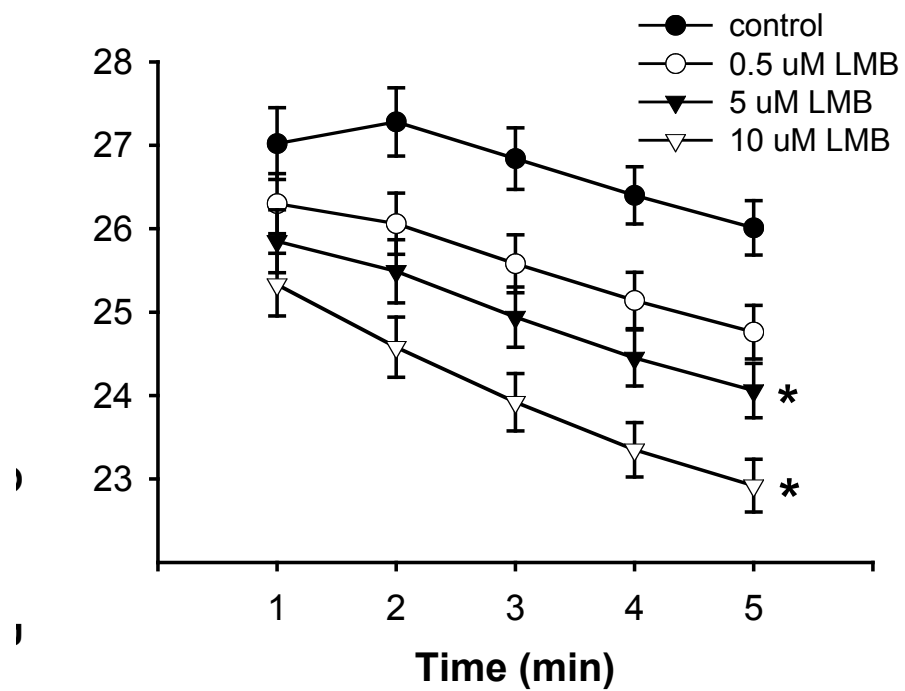
3.4.2.2 Time-dependent Effects after in vivo Administration

There was a significant effect of time after MB administration on oxygen consumption ($F_{(3, 18)}$ = 9.59, p = .001, repeated-measures ANOVA). Brain oxygen concentration was significantly lower 24 h after treatment with MB versus saline (Dunnett's p = .001). There were no differences 1 or 2 h following MB administration (Figure 2).

Figure 3.2   Effects of 1 mg/kg MB on brain oxygen consumption at 1, 2, and 24 h after administration *in vivo*. *significantly different from saline-treated rats, p = .001.
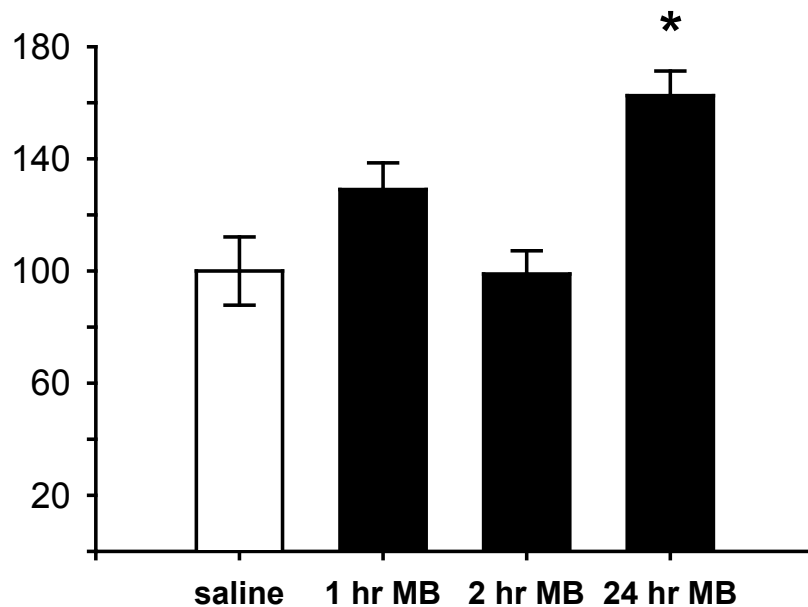
3.5 DISCUSSION

This study was the first to determine that low dose MB improves between-days memory retention in habituation and object recognition tasks without nonspecific effects on motor activity, feeding, and anxiety. It is also the first to demonstrate that MB enhances brain oxygen consumption. Previous studies in normal rats have shown that low dose MB enhances memory retention of: (1) an inhibitory avoidance response (Martinez et al., 1978), (2) a baited holeboard pattern (Callaway et al., 2004), and (3) an extinguished conditioned response (Gonzalez-Lima and Bruchey, 2004). However, these previous studies could also be explained by nonspecific drug effects on motor activity or feeding behavior rather than memory effects.

The present results demonstrated that 1–10 mg/kg doses of MB improved memory retention without disrupting general activity, anxiety, or sweet-seeking feeding behavior in rats. The 4 mg/kg dose was specifically selected for testing because humans have taken 300 mg/day of MB for one year without significant side effects (Naylor et al., 1986). This dose corresponds to 4.3 mg/kg for a 70 kg person.

For the memory tests, rats were injected with 1–10 mg/kg MB after the end of the training session in day 1 and tested for improved memory retention 24 h later. Post-training MB administration was chosen in order to target the processes of memory consolidation and to enhance brain metabolic processes underlying the retention of the memory when tested 24 h later (McGaugh, 2000; Cooke et al., 2004). Therefore, MB could not interfere with acquisition learning because it was administered after training.

83

3.5.1 Behavioral Effects of MB

Low dose MB significantly improved memory in the object recognition task. Although all groups explored the novel object longer than the familiar one, the difference was significant only in the rats injected with 4–10 mg/kg MB. In the open field test, the lower 1–4 mg/kg MB doses generally improved the habituation effect. The only dose to improve memory in both tasks was 4 mg/kg MB. The higher 10 mg/kg MB dose produced increased exploration in the open field chamber and high variance in the object recognition test. This suggests that MB shows the same bell-shaped dose effects on memory as other cognitive enhancers (Flood et al., 1981; Baxter et al., 1994).

One alternative interpretation of the memory experiments is that MB could simply modify locomotor activity, thereby creating a habituation or object recognition effect. However, locomotor behavior during a 24 h session in the running wheel was not different in the 1–10 mg/kg MB groups as compared with the saline group. This suggests that MB has a specific effect on memory which could not be explained by a nonspecific locomotor effect. Furthermore, a nonspecific modification of locomotor behavior would not account for the longer amount of time spent exploring the novel object in the MB-treated groups.

Another possibility is that low dose MB may be anxiolytic and thus stimulate exploratory behavior. Anxiety in rats is associated with increased thigmotaxic behavior (more activity in the periphery of the chamber) and center avoidance (less crossings into the center of the chamber) (Treit and Fundytus, 1988). In our study, there were no differences in center crossings in the open field in rats given 1–10 mg/kg MB. This implies that low dose MB does not affect anxiety-related behaviors. In addition, Gonzalez-Lima and Bruchey (2004) found

84

no evidence of nonspecific effects on measures of exploration and anxiety in rats treated with one or five daily injections of 4 mg/kg MB. Therefore, the effects following post-administration of 4 mg/kg MB on habituation and object recognition are the result of enhanced memory retention. This improvement is consistent with a Pavlovian study showing that 4 mg/kg MB improved retention of extinction memory during the post-extinction phase (Gonzalez-Lima and Bruchey, 2004).

3.5.2 Effects of MB on Brain Oxygen Consumption

Oxidative metabolism examined *in vitro* with an optical oxygen sensor revealed a dose-dependent effect of MB. Both 5 µM and 10 µM LMB significantly increased oxygen consumption. The effect of 0.5 µM LMB did not reach statistical significance after Dunnett correction. We previously demonstrated that 0.5 µM MB increased C.O. activity while 5 µM had no effect and 10 µM decreased activity (Callaway et al., 2004). One important difference in the two methods employed is that the reduced form (LMB) was used in the oxygen recordings but the oxidized form (MB) was used in the C.O. activity measurements. The reduced form is favored for entry into the cell (Merker et al., 1997). Because there were only a few seconds of incubation with MB or LMB in both protocols, the amount entering the cell in the C.O. activity measurements was probably lower than that applied in the oxygen probe protocol and therefore not directly comparable. With a short incubation period, 5 µM MB may enter at a concentration closer to 0.5 µM LMB. At these concentrations, no differences were found in either measurement.

It is also possible that increasing the amount of MB changes its mechanism within the electron transport chain. MB may directly reduce oxygen at higher concentrations (10 µM MB, 5 µM LMB) and prevent C.O. from donating

its electrons to oxygen, thereby inhibiting C.O. activity. A direct action on oxygen would explain the decrease in the rate of cytochrome c oxidation with 10 µM MB and the increase in oxygen consumption observed with 5 µM LMB.

Callaway et al. (2004) showed that C.O. activity increased 24 h after a single 1 mg/kg MB injection, but not after 1 or 2 h post-administration. In the present experiment, 1 mg/kg MB increased oxygen utilization 24 h after *in vivo* administration. Oxygen consumption was not different 1 or 2 h after MB treatment. The results from the respiratory metabolism experiments agree with Visarius et al. (1997) who showed that 0.5–2 µM MB stimulates cellular respiration in rat liver. Taken together, these studies indicate that improved brain energy metabolism is a mechanism whereby MB increases memory retention.

Brain C.O. activity can be partially inhibited by chronic sodium azide administration (Cada et al., 1995; Berndt et al., 2001). Systemic administration in rats causes memory deficits in the Morris water maze (Bennett et al., 1992) and the holeboard maze (Callaway et al., 2002). When low dose MB was administered to rats treated with sodium azide, their impaired memory retention was normalized to levels comparable to control rats (Callaway et al., 2002). The following study will determine whether 4 mg/kg MB can reverse spatial memory impairment caused by focal administration of sodium azide in the PCC.

Chapter 4: Methylene Blue Prevents Memory Impairment in a Spatial Task Caused by PCC Hypometabolism

4.1 ABSTRACT

Hypometabolism in the posterior cingulate cortex (PCC) in patients with mild cognitive impairment is a major risk factor for developing Alzheimer's disease. In rats, PCC metabolic inhibition produces spatial memory deficits, oxidative damage, and neurodegeneration. Methylene blue (MB) is a chemical compound that enhances memory, increases cytochrome oxidase (C.O.) activity and oxygen consumption, and has antioxidant properties. This study tested the neuroprotective and memory-enhancing properties of MB in rats that received an injection of sodium azide, an inhibitor of C.O., directly in the PCC. Sodium azide administration resulted in impaired spatial memory in a holeboard food-search task. In addition, sodium azide-treated rats had significantly fewer correlations in C.O. activity between the PCC and other brain region as compared to the control rats. Co-administration of 4 mg/kg MB prevented the memory impairment and maintained several of the significant brain interregional correlations that were found in the control group. Specifically, correlations in C.O. activity between the PCC and hippocampal areas, and between the PCC and secondary motor cortex, were preserved. Our results suggest that memory impairment associated with PCC hypometabolism can be prevented by interventions that strengthen the functional connectivity of the PCC or that optimize the metabolic function of regions that mediate spatial memory.

4.2 INTRODUCTION

Patients with neurodegenerative disorders such as Parkinson's, Huntington's and Alzheimer's disease (AD) commonly show impaired mitochondrial metabolism (Cassarino and Bennett, 1999; Beal, 2005; Petrozzi et al., 2007). Selective hypometabolism in the posterior cingulate cortex (PCC) is a major risk factor in subjects with mild cognitive impairment to develop AD (Mosconi, 2005; Borroni et al., 2006). In both peripheral and brain tissue from AD patients, there is a specific impairment in the activity of cytochrome oxidase (C.O.), the rate-limiting enzyme in the mitochondrial respiratory chain (Parker et al., 1994a; Parker et al., 1994b; Gonzalez-Lima and Cada, 1998; Cardoso et al., 2004a). However, hypometabolism in the brains of AD subjects is not widespread. C.O. inhibition has been found in the PCC, an area of the brain involved in spatial memory (Valla et al., 2001). However, the adjacent motor cortex was not affected. A recent paper reported a significant decrease in C.O. activity in peripheral tissue from subjects with mild cognitive impairment (Valla et al., 2006a). Therefore, C.O. inhibition may not only determine the progression to AD, but perhaps also determine the initiation to AD.

C.O. is the terminal enzyme in the mitochondrial electron transport chain. It catalyzes electron transport to oxygen while concurrently generating ATP (Gonzalez-Lima and Cada, 1998). C.O. activity is tightly correlated with metabolic neural activation (Wong-Riley et al., 1998). Experimental inhibition of C.O. activity with sodium azide causes memory impairments in animals. For example, systemic treatment in rats causes memory deficits in spatial tests such as the Morris water maze, radial arm maze, and holeboard task (Bennett et al., 1992; Bennett and Rose, 1992; Callaway et al., 2004). Rats receiving focal

administration of sodium azide directly into the PCC have memory deficits in a holeboard task and impaired PCC metabolism (chapter 2). C.O. inhibition leads to decreased oxygen consumption, ATP, and increased free radical formation (Brouillet et al., 1994; Swerdlow et al., 1997; chapter 2; Riha et al., 2005/chapter 3).

Drugs that reverse the effects of C.O. inhibition should improve memory retention in conditions involving impaired energy metabolism (Beal, 2005). A candidate drug is methylene blue (MB), an auto-oxidizable compound that enhances electron flow in the mitochondrial respiratory chain (Scott and Hunter, 1966) and displays antioxidant effects. MB is an FDA-approved drug indicated for the treatment of methemoglobinemia (Wright et al., 1999). MB possesses ideal pharmacokinetics for targeting neural tissue. MB crosses the blood-brain-barrier and accumulates in mitochondria (Merker et al., 1997; Visarius et al., 1999; Peter et al., 2000) where it has a variety of cellular effects.

MB restores inhibition of oxygen consumption caused by rotenone, an inhibitor of the first enzyme in the mitochondrial electron transport chain (Lindahl and Oberg, 1961; Zhang et al., 2006). Moreover, MB prevents superoxide free radicals formed during reperfusion after ischemia (Kelner et al., 1988; Salaris et al., 1991). MB also decreases free radical-induced lipid peroxidation (Salaris et al., 1991; Zhang et al., 2006). Low concentrations (1-10 μM) of MB stimulate cellular respiration in rat liver (Visarius et al., 1997) and brain (Riha et al., 2005/chapter 3). Low dose MB increases brain C.O. activity *in vitro* and after 24 hours administration *in vivo* in rats (Callaway et al., 2004; Gonzalez-Lima and Bruchey, 2004). MB administration prevented cell death, decreased lipid

peroxidation, and increased oxygen consumption in mice displaying retinal degeneration caused by rotenone (Zhang et al., 2006)

The ability of low dose MB to increase C.O. activity and mitochondrial respiration can explain the reports of memory improvement in rats treated with MB. *In vivo*, 1-4 mg/kg MB improves memory in an inhibitory avoidance task (Martinez et al., 1978), an appetitive food-search task (Callaway et al., 2004), and a discrimination task (Wrubel et al., 2007). Other studies have demonstrated that 4 mg/kg MB improves memory retention in an object recognition test, habituation in a familiar environment, and extinction of fear in rats (Gonzalez-Lima and Bruchey, 2004; Riha et al., 2005/chapter 3). MB not only improves memory in normal rats, but also in rats with metabolic impairments. For example, low dose MB prevented memory impairments in rats that were given system administration of sodium azide (Cada et al., 1995; Callaway et al., 2002).

We hypothesized that low dose MB will prevent the memory deficits caused by isolated hypometabolism in the PCC. Rats were trained in a baited holeboard food-search task. After learning the task, two groups received bilateral injections of sodium azide directly in the PCC. This was followed by systemic administration of 4 mg/kg MB or saline. One day after surgery, the rats were tested in the holeboard chamber for memory retention of the previously-baited pattern. In addition, locomotor activity was evaluated to determine if there were nonspecific effects from sodium azide (AZ) or sodium azide plus MB (AZ+MB) treatment that would confound holeboard performance. Finally, histochemistry of C.O. activity determined if there are metabolic changes in the brain due to treatment. It is well-established that low dose MB improves memory. The current experiment will further evaluate MB as a memory-enhancing compound

and provide evidence as to the mechanism by which MB prevents memory

deficits.

4.3 METHODS

4.3.1 Subjects

For the holeboard study, subjects were 30 adult male Sprague Dawley rats (Harlan, Houston, TX) weighing 219–255 g on the first day of training. They were single-housed on a 12 h light-dark schedule and allowed to drink water *ad libitum*. For motivational purposes, rats were placed on a food restriction protocol that ensured they did not weigh less than 85% of free-feeding rats of a similar age. They were fed daily at the end of their light cycle. Beginning five days before training, animals were weighed and handled daily for 5 min. On each of the two days before habituation, two sucrose food pellets (45 mg, Noyes, Lancaster, NH) were placed in their home cage. These sucrose pellets were the same reinforcers used for training in the holeboard chamber. All procedures were approved by the institutional animal care and use committee (IACUC) at the University of Texas at Austin. The experiments were conducted in a facility accredited by the Association for Assessment and Accreditation of Laboratory Animal Care (AAALAC) International.

4.3.2 Behavioral Procedures

4.3.2.1 Apparatus

The holeboard and locomotor tests were conducted in automated open field chambers purchased from MED Associates (St. Albans, VT). The testing environments were composed of clear Plexiglas sides 30.5 cm high and a white fiberglass floor (43.2 cm^2). Parallel arrays of infrared motion detectors (16 X 16, 2.5 cm apart) detected nosepokes in the holeboard task and locomotor activity in the open field test.

For the holeboard task, a top floor was placed in the chamber 2 cm above a bottom insert. The top holeboard floor was made of metal and contained 16 holes (4 X 4, 3.2 cm^2). The outer holes were 8.6 cm from the wall and the rows were 4.5 cm apart. The bottom insert contained a bottom tray, wire screen, and a top tray. The bottom tray had 16 holes of the same dimensions as the top task floor. Five inaccessible sucrose pellets were placed in each hole. The top tray secured the wire screen over the bottom tray. The underlying food pellets controlled for odor that may emanate from the baited holes. Thus, an animal should not be able to successfully detect the baited holes based on odor cues.

4.3.2.2 Habituation & Training

Animals were run in cohorts of 4–5 rats, resulting in a total number of 6 cohorts. Cohorts were transported from their homeroom to the testing room in clear plastic cages placed on a metal cart. Each subject was alternatively run until all rats in that cohort finished their daily trials. The holeboard procedure was performed in a dimly-lit room (33 lux) with proximal spatial cues placed around the chamber.

Animals were first exposed to the chamber during habituation. One sucrose pellet was placed in each hole for the habituation trials. Before each trial, the chamber and holes were cleaned with a mild detergent (Bio-Clean, Stanbio Laboratories, Boerne, TX). The holeboard insert was rotated between trials to further mask odor cues. Rats were placed in the northeast corner of the chamber. A trial began when the subject initiated the first nosepoke, and lasted for 5 min or until all bait was consumed. Habituation trials were continued until rats consumed at least 15 pellets in one trial. This criterion was reached in 2 to 4 trials.

Holeboard training began the day following habituation. The rats were run in the same cohort as in their habituation trials. Four holes were baited in a consistent pattern for all subjects throughout training (Figure 1). A trial started as soon as the first hole was nosepoked and ended immediately after the last bait was consumed, or after 5 minutes elapsed. The rats received 5 trials per day.

Figure 4.1   Schematic drawing of the holeboard task floor. Filled circles indicate baited holes; empty circles indicate unbaited holes.
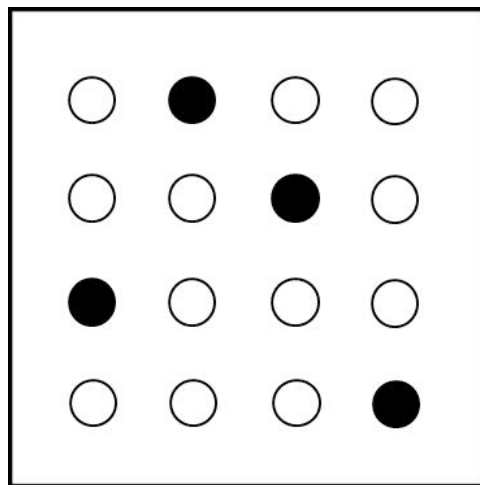
Training continued for at least 8 days. Training was stopped when 60% reference memory was attained or for a maximum of 14 days of training. The intertrial interval was approximately 9 min. Training scores were averaged each day. Rats were matched into treatment groups based on their averaged reference memory scores across all days of training. Surgery was performed the day after each rat's last training trial. Following a 24 h recovery period, subjects received an unbaited probe trial to test for memory retention.

MED Associates software measured various parameters in the holeboard task: baited holes visited, nonbaited holes visited, repeat visits to both types of holes, and latency to complete the trial. Reference memory was calculated as the ratio of visits to baited holes divided by number of visits to all holes. The holeboard probe tests were also videotaped.

4.3.2.3 Locomotor Activity

Locomotor activity was assessed in an open field chamber located in the same room as the holeboard task. The overhead light used during the trials measured 560 lux. Distal spatial cues were present in the room. Subjects were individually transported to the room in opaque cages made of a different material than those used for the holeboard trials. Experimenters carried the cages by hand using a different path than the one used during transport during holeboard training. The above procedures were employed to make the context as different as possible from the holeboard task. One 5 min trial was conducted on post-training days 5–7. Following the unbaited probe trial, animals were brought back to their home room. The behavior room was prepared for locomotor testing and animals were run in the chamber for a second 5 min trial. The open field chamber was cleaned between trials with Betadine (Purdue Pharma, Stamford,

CT). Med Associates software calculated ambulatory time, stereotypic time, and vertical counts. Ambulatory time was defined as the number of seconds the rat was in ambulation. Stereotypic time referred to the amount of time the rat broke the infrared beams without ambulating. For example, scratching, grooming, and turning in a tight circle are counted as stereotypic behaviors. Vertical counts were measured by beam breaks and indicated the number of times the animal reared.

4.3.3 Surgery

Rats were anesthetized by first placing them in a hostcage containing 97% breathing air and 3% isoflurane (Aerrane, Baxter Pharmaceutical Products, Deerfield, IL). After the initial induction, the rat was moved to a heated surgical bed on a Stoelting stereotaxic frame, and secured in the flat skull position using ear bars and an incisor bar. A nosecone positioned over the incisor bar was connected to a vaporizing machine that provided a steady flow of anesthesia (E-Z Anesthesia, Euthanex Corp, Palmer, PA). The subjects were continuously monitored for anesthesia state and the percentage of isoflurane was adjusted if necessary.

The head was shaved and disinfected with Nolvasan (Wyeth, Madison, NJ). Lacrilube (Allergan, Irvine, CA) was applied on the eyes to prevent drying. One injection of an NSAID was given intramuscularly to alleviate pain (Rimadyl, 5 mg/kg, Pfizer). A small mid-sagittal incision was made on top of the head and was kept open with a retractor. The periosteum was removed by scraping with cotton swabs. Two small bilateral holes (0.8 mm^2) were drilled over the PCC on each side of the midline suture. The rats in the AZ and AZ+MB groups were injected with 3 M sodium azide dissolved in phosphate buffer (pH 7.4). This

concentration was previously determined to be effective at impairing spatial memory in the holeboard and energy metabolism (Brouillet et al., 1994; Chapter 2). Four bilateral injections were made in the following atlas coordinates (from Bregma, in mm): A/P -2.8 to -3.3; M/L ±0.2 to 0.4; D/V -1.2 to -1.3, alternating left and right sides (Paxinos and Watson, 1997). A flowmeter delivered each injection at a rate of 0.05 µL/min for 10 min. After each infusion, the needle was kept in place for a few minutes and slowly removed.

After the injections, the skin was sutured with wound clips (Reflex, CellPoint Scientific, Gaithersburg, MD) and Neosporin was applied to the wound. Subjects in the AZ+MB group (n = 9) were injected intraperitoneally with 4 mg/kg MB (Faulding Pharmaceuticals, Paramus, NJ) at the end of surgery. The control group (n = 10) and AZ group (n = 10) received an equivalent volume of 0.9% saline intraperitoneally. After recovering from surgery (5–10 minutes), the rats were returned to their home cage and monitored to ensure full recovery. The control rats received the same surgical treatment and spent an equivalent amount of time under anesthesia, but they did not receive a craniotomy.

4.3.4 Brain Procedures

4.3.4.1 Brain Processing:

After the second assessment of locomotor activity, the rats were killed by decapitation. Their brains were quickly extracted, frozen in isopentane, and stored in an ultra-low freezer at -40°C. The brains were cut in 40 µm coronal sections in a -17°C cryostat and collected onto glass slides. Two adjacent series were created. One was stained for C.O. activity for quantitative histochemical analysis and the other was stained with cresyl violet for cell counting. The slides were kept in an ultra-low freezer at -40°C until processed.

4.3.4.2 Cytochrome Oxidase Histochemistry

The brains were stained in batches for C.O. histochemistry. Each batch included two standard slides that contained tissue sections of varying thickness (10, 20, 40, 60, and 80 μm). The standards were cut from frozen rat brain homogenate with known C.O. activity that was determined in a previous experiment. The details of quantitative C.O. histochemistry have been published (Gonzalez-Lima and Jones, 1994; Gonzalez-Lima and Cada, 1998).

All chemicals were purchased from Sigma. Fresh-frozen brain sections were immediately placed in a cold bath of 0.5% glutaraldehyde and 9% sucrose phosphate buffer solution (PBS, 0.1 M, pH 7.4) for 5 min. Next, they were immersed in three changes of sucrose PBS for 5 min each. These washes were at graded temperatures in order to slowly increase the temperature of the tissue. Then, they were placed for 10 min in a preincubation intensification Tris buffer containing 774 mL of 0.1 N HCl, 10 mL dimethylsulfoxide, 12 g trizma base, 200 g sucrose, and 0.55 g cobalt chloride in 1226 mL double-distilled water. After a rinse in PBS without sucrose, the tissue was stained for C.O. activity in an oxygen-saturated solution at 37°C for 60 min. The incubation solution contained 0.35 g 3,3'-diaminobenzidine tetrahydrochloride, 52.5 mg cytochrome c (from horse heart), 14 mg catalase, 35 g sucrose, and 1.75 mL DMSO in 700 mL PBS. The incubation was followed by 30 min in a bath of 4% formalin in sucrose PBS in order to stop the reaction and fix the tissue. Subsequently, the slides were slowly dehydrated by passing through increasing concentrations of ethanol washes (30, 50, 70, 95, 95, 100 and 100%) for 5 min each. Finally, the tissue was cleared in xylene (3 times, 5 min each) and coverslipped with Permount.

4.3.4.3 Cytochrome Oxidase Image Analysis:

The C.O. content in nerve tissue is closely correlated with the optical density (O.D.) of histochemically-stained sections (Hevner and Wong-Riley, 1989). O.D. of the stained brain standards and the brain sections were measured using a computer-assisted image analysis system consisting of a DC-powered lightbox, a CCD camera (Javelin Electronics, Torrance, CA), a Targa M8 image capture board, and JAVA imaging software (Jandel Scientific, Corte Madera, CA). Java calibrated gray level values from a Kodak step tablet into known O.D. and subsequent measurements were recorded as O.D. (Gonzalez-Lima and Cada, 1998).

For each section thickness of one brain standard per batch, ten O.D. measurements were averaged and the mean values were used to obtain a regression equation. Using this equation, O.D. values were converted to units of C.O. activity (μmol/min/g tissue). Regression equations calculated from standard O.D. values confirmed the linearity of the C.O. histochemical reaction ($r^2 > .94$).

For each subject, the O.D. of each region of interest was measured bilaterally in three adjacent sections. The field of view of each sample area was approximately 0.75 X 1.0 cm. The median values for each region per subject were averaged to obtain the group average. PCC activity in the dorsal and ventral aspects were analyzed throughout the entire rostral to caudal extent (-1.8 to -5.3 mm from Bregma). In addition, we also analyzed brain regions that connect to the PCC.

The PCC is one of the regions included in the Papez circuit, which has been proposed to mediate emotion as well as processes of learning and memory (Papez, 1937; Vertes et al., 2001). Therefore, we also measured activity in

regions of the Papez circuit. These include: the cingulate, entorhinal, and perirhinal cortices, hippocampus proper, subiculum, mammillary bodies, and anterior thalamic nuclei. A brain atlas was used to delineate brain structures (Paxinos and Watson, 1997).

4.3.4.4 Nissl Staining

To determine if either AZ or AZ+MB treatment resulted in a change in the number of neuronal or glial cells, the second series of brain sections was stained with cresyl violet and used for cell count measurements in the PCC. For each subject, the alternate slide to the one showing the least C.O. activity in the PCC was chosen for Nissl staining. The procedure began with placing fresh-frozen tissue in a series of baths for 2.5 min each: 95% ethanol, 70% ethanol, double-distilled water, and sodium acetate buffer (0.05 M, pH 4). Next, the tissue was stained with 0.1% cresyl violet in sodium acetate buffer for 4 min at 45°C. Slides were then placed in alternating series of 70% and 95% ethanol baths (5 min each) until visualization was optimal. This was followed by dehydration in ethanol (95, 100, and 100%, 5 min each). Finally, slides were cleared in xylene and coverslipped with Permount.

4.3.4.5 Posterior Cingulate Cortex Cell Count

Neuronal and glial cell counts were measured using a Labophot-2 binocular bright field microscope (Nikon Corporation, Tokyo, Japan) connected to a DVC-340 scan camera, DVCView 3.3 imaging software (DVC Company, Austin, TX), a Microcode II digital readout (Boeckeler Instruments, Inc., Tucson, AZ), and a PC computer. An unbiased optical disector stereological method (Harding et al., 1994) was used to estimate cell density (cells/volume) in the PCC in Nissl-stained sections from control ($n = 6$), AZ ($n = 6$), and AZ+MB ($n = 6$)

groups. Cell density was estimated in three different PCC regions: 1) layers II/III of the dorsal PCC, 2) layers V/VI of the dorsal PCC, and 3) layers III/IV of the ventral PCC. Cells were differentiated based on morphological criteria for brain cells. Neurons were identified by large ellipsoidal/pyramidal cell body, low nucleus/cytoplasm ratio, heterochromatic nucleus, and visible nucleolus. Glia were distinguished as cells with a small cell body, high nucleus/cytoplasm size ratio, and hyperchromatic nucleus.

Cells were identified with a 50X oil immersion objective throughout the thickness of a section and were counted when they first came into focus within an unbiased counting frame (Harding et al., 1994). Cells on the surface of the section were excluded from analysis. For each PCC region, cells were counted from each of six sections per subject within a randomly chosen hemisphere. Cell density was defined as $Nv_{cells} = \Sigma Q^-/\Sigma v_{(frame)}$, where ΣQ^- is the sum of cell counts per sample and $\Sigma v_{(frame)}$ is the area of the unbiased counting frame (0.0396 mm^2, adjusted for 140X magnification) multiplied by the length of the analyzed region (d). The length was calculated as d = (No. of sections – 1) x No. of section series x section thickness. Cell counts were measured by an experimenter blind to the treatments.

4.3.5 Statistical Methods

Reference memory scores were used to evaluate group differences in the holeboard task. Scores were calculated as the ratio of total visits to baited holes divided by the total number of visits to all holes. A repeated-measures analysis of variance (ANOVA) evaluated learning in the holeboard for the first eight days of training. ANOVA compared group differences throughout training days 9–14 and compared various measures in the probe test. Reference memory in the

probe test was examined by ANOVA followed by planned comparisons. Repeated-measures ANOVA (day X group) was used to assess locomotor activity in the open field. All significant group differences were further explored with Bonferroni-corrected comparisons.

C.O. activity and cell counts between the three experimental groups were evaluated using ANOVA followed by tests for simple effects for each region of interest. Within-group Pearson product moment correlations were computed to analyze the relationship in C.O. activity between the PCC and other brain regions (Nair and Gonzalez-Lima, 1999). For all tests an alpha level of .05 (two-tailed) was the criteria of statistical significance. All tests were performed using SPSS 11.5 software (SPSS, Inc., Chicago, IL).

4.4 RESULTS

4.4.1 Behavioral Analysis

4.4.1.1 Holeboard Performance

One rat failed to reach the criterion during habituation trials and was excluded from the study. During the first eight days of training, all rats learned the holeboard pattern (Figure 2, $F_{(7, 182)}$ = 20.99, p < .001). After day 8 of training, there were different numbers of subjects per group per day. Consequently, group scores across days 9–14 were averaged and evaluated with ANOVA. There were no group differences in holeboard training within the first 8 days ($F_{(2, 26)}$ = 0.266) or in the remaining 9-14 days of training ($F_{(2, 24)}$ = 2.95). In addition, there were no group differences in reference memory for the last day of training or in the maximum training score.

Figure 4.2   Learning curves in the holeboard task before treatment. Sample sizes are noted in parenthesis beneath each daily average.
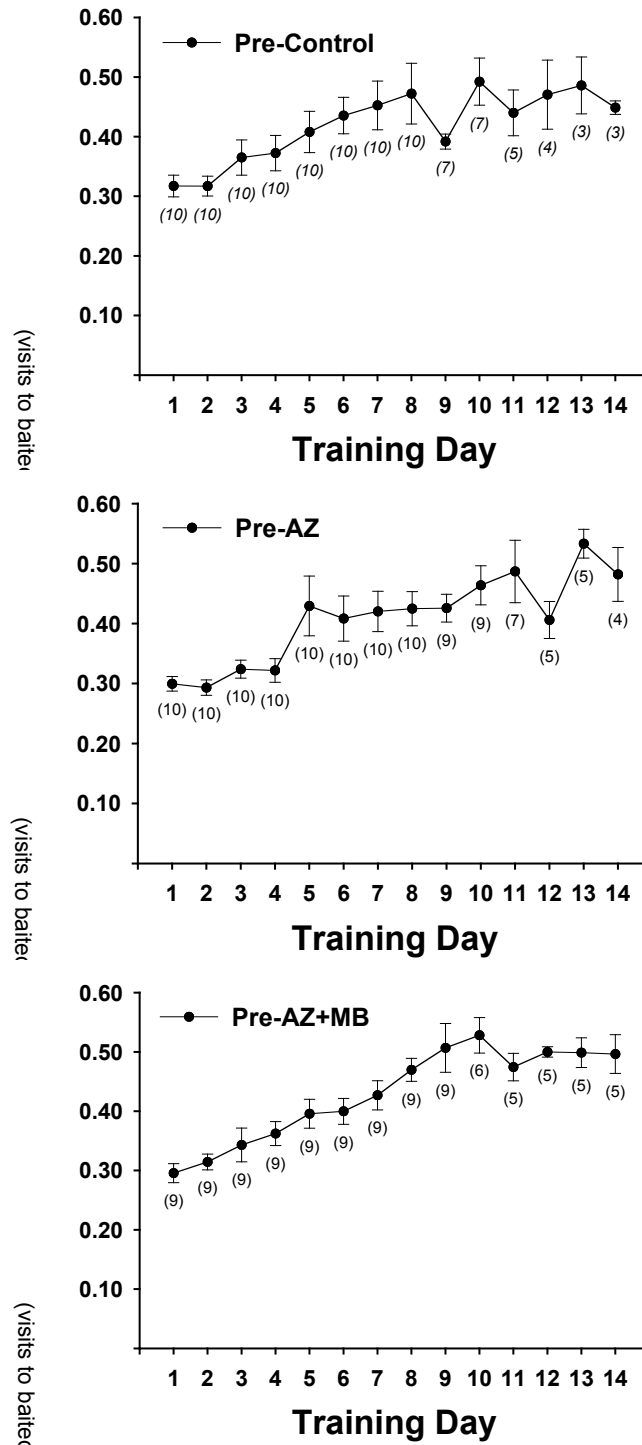
There was a significant group difference in reference memory in the holeboard task ($F_{(2, 26)}$ = 6.78, *p* = .004; Figure 3). The AZ group had 16% worse reference memory than the control group (Bonferroni *p* = .092, ns). Mean ratios ± S.E.M. of the AZ and control groups were 0.255 ± 0.018 and 0.304 ± 0.014, respectively. The effect size of sodium azide was .97. In addition, the AZ+MB group showed significantly better memory for the baited pattern (0.336 ± 0.015) as compared to the AZ group (Bonferroni *p* = .004). Furthermore, AZ+MB-treated rats showed similar reference memory as control rats. The AZ group also showed the largest difference from their training average. They showed a 37% reduction in reference memory as compared to the control group (27%) or the AZ+MB group (20%).

Planned comparisons using Student's t test revealed that the AZ-treated rats had significantly worse memory than rats in the control group (*t*(18) = -2.197, *p* = .041) and AZ+MB-treated group (*t*(17) = -3.472, *p* = .003). However, there was not a significant mean difference between the AZ+MB-treated rats and the control rats (*t*(17) = 1.557, *p* = .138).

There were no significant mean group differences in the probe test for the following measures: the number of initial or repeated nosepokes into previously-baited holes or previously-nonbaited holes; total entries into previously-baited or previously-nonbaited; or total entries. The time to complete the probe test was not different between groups.

Figure 4.3   Mean ± S.E.M. of reference memory before (training) and after PCC hypometabolic induction (probe). *significantly different from control and AZ+MB, *p* < .05.
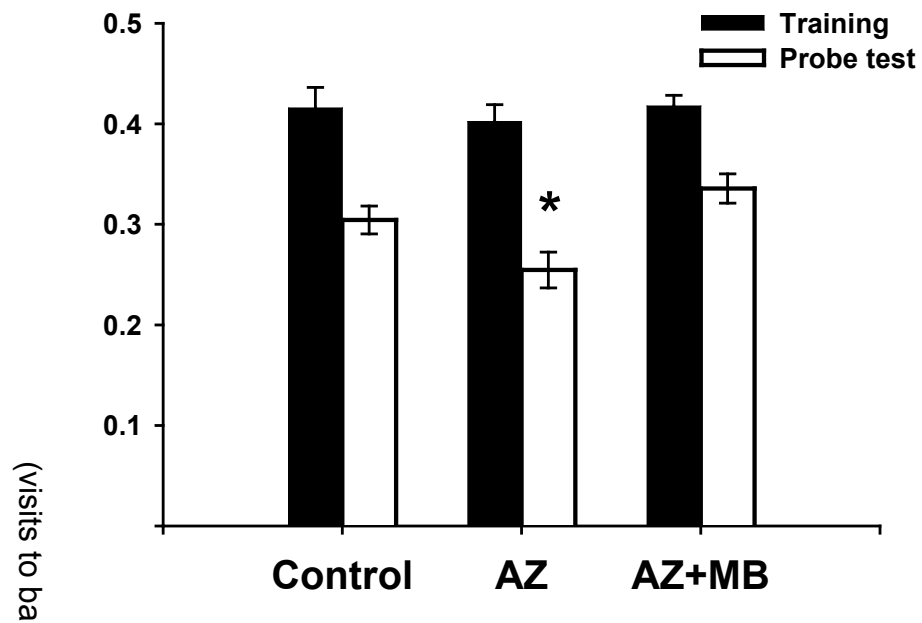
4.4.1.2 Locomotor Activity

There was a significant group effect for ambulatory time in the open field chamber ($F_{(2, 26)}$ = 3.66, p = .04). However, post-hoc analysis did not reveal differences between any of the groups. Examining the scores in Table 1 suggests that the significant result in the omnibus test is due to the higher baseline activity in AZ-treated rats (both before and after administration). All groups significantly decreased the amount of time performing stereotypic behaviors in the second trial, as compared to the first trial ($F_{(1, 26)}$ = 63.89, p < .001). There was not a significant effect of drug treatment for stereotypic time or number of rearings ($F_{(2, 26)}$ = 0.994 and $F_{(2, 26)}$ = 0.853, respectively).

Table 4.1   Locomotor activity in the open field chamber before (Pre) and after (Post) drug treatment.

MEASURE	CONTROL			AZ			AZ + MB		
	Pre	Post	*(n)*	Pre	Post	*(n)*	Pre	Post	*(n)*
ambulatory time (s)	35 ± 3	32 ± 2	*(10)*	41 ± 2	43 ± 4	*(10)*	36 ± 2	32 ± 4	*(9)*
stereotypic time (s)	82 ± 3	71 ± 3	*(10)*	79 ± 2	68 ± 3	*(10)*	83 ± 2	72 ± 2	*(9)*
vertical counts	58 ± 4	49 ± 4	*(10)*	55 ± 3	55 ± 3	*(10)*	50 ± 3	49 ± 5	*(9)*

4.4.2 Brain Findings

4.4.2.1 Cytochrome Oxidase Histochemistry

C.O. activity was quantified in the PCC, as well as in brain regions that have anatomical connections with the PCC or are included in the Papez circuit. The PCC was the only region that showed a mean group difference in C.O. activity (Table 2, $F_{(2, 26)}$ = 14.82, p < .001). Both the AZ and AZ+MB groups were significantly different from the saline group (Bonferroni-corrected p < .01). Rats treated with sodium azide showed a 17% decrease of C.O. activity in the PCC as compared to control rats, while the AZ+MB group had a 28% decrease. Co-administration of MB did not prevent the decrease in C.O. activity caused by sodium azide; PCC activity in the AZ+MB rats was similar to that in AZ rats (Figure 5). Detailed analysis within the PCC revealed group differences in both the dorsal PCC and ventral PCC aspects (dorsal: $F_{(2, 26)}$ = 16.73, p < .001 and ventral: $F_{(2, 26)}$ = 12.55, p < .001). Post-hoc analysis showed that while both AZ- and AZ+MB-treated rats were not different from each other, both had significantly less C.O. activity within the dorsal PCC area than the control rats (p < .001). Within the ventral PCC area of the PCC, the AZ+MB-treated rats had lower activity than both control rats and AZ-treated rats (p < .001 and p = .018, respectively). The AZ-treated rats were not significantly different from the control animals in the ventral PCC.

Table 4.2   Mean ± S.E.M. of C.O. activity (µmoles/min/g tissue) in control rats and in rats injected with sodium azide in the PCC with (AZ+MB) or without MB treatment (AZ).

AREA OF INTEREST	abbreviation	Bregma level (mm)	CONTROL Mean ± SEM (n)	AZ Mean ± SEM (n)	AZ + MB Mean ± SEM (n)
CINGULATE REGIONS					
posterior cingulate	PCC		299 ± 7 (10)	249 ± 11 (10) *	215 ± 14 (9) *
dorsal PCC	RSA	-1.80 to -5.30	285 ± 8 (10)	208 ± 14 (10) *	188 ± 15 (9) *
ventral PCC	RSG	-1.80 to -5.30	313 ± 6 (10)	284 ± 8 (10)	242 ± 15 (9) * †
anterior cingulate	ACC	1.60 to -1.40	304 ± 5 (10)	297 ± 4 (10)	292 ± 5 (9)
cingulum bundle	cb	-1.80 to -5.30	6 ± 5 (10)	-6 ± 4 (10)	-6 ± 3 (9)
THALAMIC REGIONS					
anterior dorsal	AD	-1.80	555 ± 35 (10)	542 ± 45 (10)	540 ± 30 (9)
anterior ventral	AV	-1.80	343 ± 20 (10)	362 ± 21 (9)	335 ± 25 (9)
anterior medial	AM	-1.80	239 ± 7 (9)	244 ± 10 (9)	234 ± 7 (9)
reticular	Rt	-1.80	249 ± 7 (10)	267 ± 7 (10)	258 ± 7 (9)
rhomboid/reuniens	Rh/Re	-1.80	240 ± 7 (10)	259 ± 8 (10)	244 ± 9 (9)
lateral dorsal	LD	-2.30	319 ± 8 (10)	325 ± 11 (10)	315 ± 5 (9)
HIPPOCAMPAL FORMATION					
anterior/dorsal					
CA1	CA1d	-3.80	243 ± 6 (10)	244 ± 9 (10)	231 ± 8 (9)
CA3	CA3d	-3.80	241 ± 7 (10)	246 ± 6 (10)	242 ± 8 (9)
dentate gyrus	DGd	-3.80	323 ± 8 (10)	327 ± 4 (10)	321 ± 3 (9)
posterior/ventral					
CA1	CA1v	-5.30	198 ± 10 (10)	210 ± 7 (10)	215 ± 9 (9)
CA3	CA3v	-5.30	238 ± 8 (9)	248 ± 7 (10)	251 ± 8 (9)
dentate gyrus	DGv	-5.30	192 ± 7 (10)	202 ± 7 (10)	210 ± 7 (9)
subiculum	SUB	-5.30	188 ± 11 (10)	197 ± 9 (10)	189 ± 13 (9)
mammillary bodies	MB	-4.80	296 ± 11 (7)	296 ± 8 (8)	316 ± 18 (7)
entorhinal	Ent	-4.80	165 ± 8 (9)	179 ± 8 (10)	179 ± 7 (9)
perirhinal	PRh	-4.80	170 ± 8 (10)	183 ± 6 (10)	188 ± 9 (9)
OTHER					
secondary motor cortex	M2	-0.26	268 ± 6 (10)	258 ± 2 (10)	270 ± 8 (9)
secondary visual cortex					
medial area	V2M	-5.30	251 ± 13 (10)	207 ± 12 (8)	240 ± 11 (9)
lateral area	V2L	-5.30	249 ± 14 (10)	244 ± 10 (9)	261 ± 10 (9)
caudate putamen	CPu	-1.80	209 ± 8 (10)	198 ± 9 (10)	215 ± 9 (9)
zona incerta	ZI	-3.80	283 ± 8 (10)	293 ± 7 (10)	269 ± 8 (9)
periaqueductal gray	PAG	-5.30	224 ± 8 (9)	231 ± 7 (10)	223 ± 5 (9)
raphe nuclei	RLi	-5.30	168 ± 8 (6)	172 ± 15 (9)	130 ± 24 (7)

*signficantly different from control ($p < .01$)

†signficantly different from AZ ($p < .05$)

Figure 4.4   Representative sections of C.O.-stained brains around Bregma -2.80 mm one day after treatment.

A. Control

2. AZ group
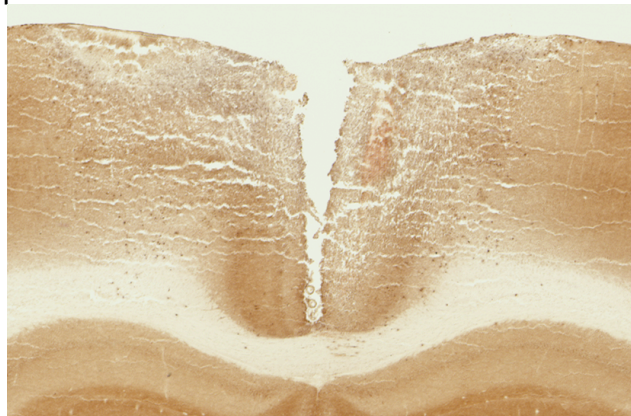
3. AZ+MB group
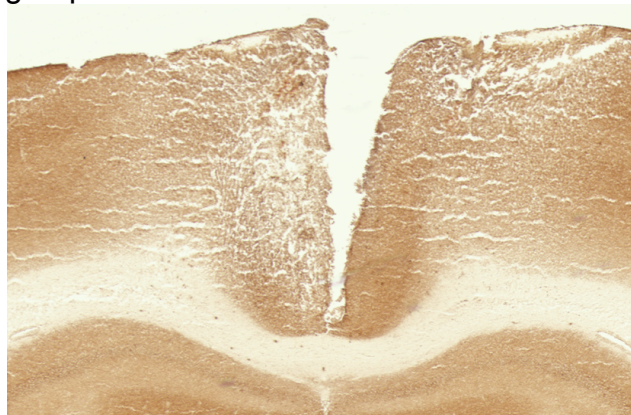
4.4.2.2 PCC-Interregional Correlations

The significant values obtained from the correlational analysis of brain activity were positive in all three groups (Table 3). Correlational analysis of brain C.O. activity between the PCC and other brain regions showed 12 significant correlations in the control group. Sodium azide administration in the PCC decreased the total number of correlations. There were seven and five significant correlations in the AZ and AZ+MB groups, respectively.

Generally, AZ-treated rats showed significant positive correlations that were not found in the control group or in the AZ+MB group (Figure 5). For example, the control group showed that brain activity in the PCC was correlated with the thalamic nuclei, anterior hippocampus proper, anterior cingulate cortex, and secondary visual cortices. However, the AZ group showed positive correlations between the PCC and the perirhinal, entorhinal and secondary motor cortices. In contrast, MB co-administration with sodium azide maintained some of the significant correlations found in the control group; specifically, those in the anterior hippocampus proper and V2M. Maintaining these correlations may underlie the preservation in memory observed in sodium azide-treated rats that also received MB.

Another interesting finding is that the AZ+MB-treated rats showed different correlations between the PCC and connecting brain regions as compared to the AZ-treated rats (Figure 5). The largest effects were in the following areas: RLi, M2, ATN, Rhinal Ctx, CPu, and ZI. In addition, several of the correlations in the AZ+MB group were very different from the control group. This suggests that the AZ+MB-treated rats were using a different, but equally efficient, strategy for memory retrieval.

111

Table 4.3   Significant Pearson correlation coefficients (r) of C.O. activity between the PCC and other brain regions. Abbreviations are defined in Table 2.

PCC-Interregional Correlations

	CONTROL	AZ	AZ+MB
AD	-0.32	0.71 *	-0.21
AM	0.67 *	0.19	0.45
Rt	0.72 *	-0.13	-.001
Rh/Re	0.68 *	0.24	0.46
LD	0.91 *	0.58	0.18
DGd	0.75 *	0.10	0.70 *
Ca1d	0.64 *	0.25	0.77 *
ZI	0.81 *	0.13	0.85 *
PRh	0.37	0.79 *	0.07
Ent	0.30	0.93 *	0.29
DGv	0.38	0.67 *	0.17
Ca1v	0.78 *	0.65 *	0.44
Ca3v	0.33	0.79 *	0.26
Rli	0.08	0.16	0.78 *
V2M	0.83 *	0.53	0.88 *
V2L	0.87 *	0.61	0.55
ACC	0.76 *	0.46	0.45
M2	0.56	0.68 *	0.01
CPu	0.66 *	0.54	0.14

significantly different from zero (p < .05)

Figure 4.5   Functional coupling of the PCC as observed with pairwise correlations. Arrow width is proportional to the magnitude of the Pearson correlation. Positive correlations are shown as solid arrows and negative correlations are represented as segmented arrows. ATN = AV + AD + AM. Rhinal Ctx = Ent + PRh. Abbreviations are defined in Table 2. *significantly different from zero, $p < .05$.

A. Control group
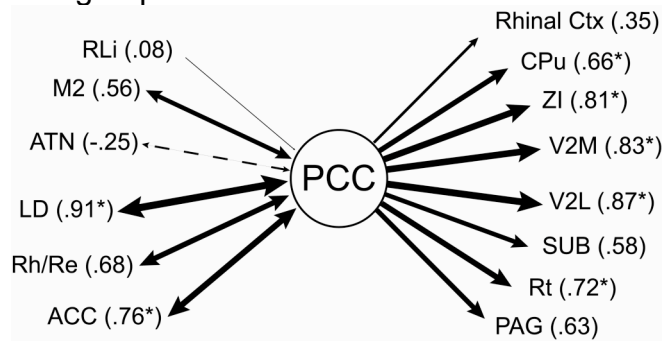
B. AZ group
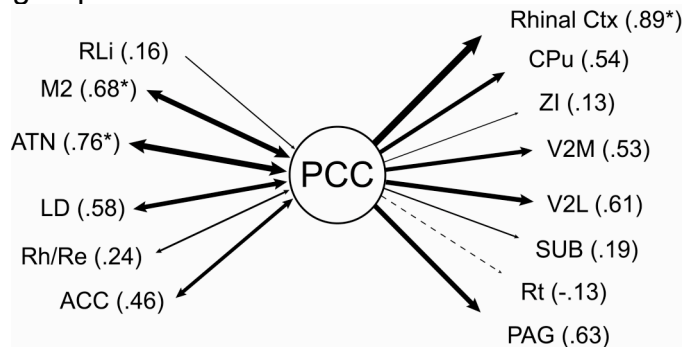
C. AZ+MB group
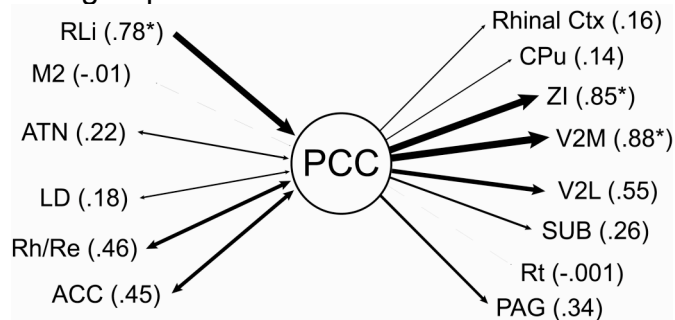
4.4.2.3 PCC Cell Count

Sodium azide treatment resulted in significantly fewer neurons and increased glia in all regions (Bonferroni $p < .05$). Neuronal loss was the greatest in the superficial region of the dorsal PCC (Figure 6). The AZ group had a 76% decrease in neurons as compared to the control group ($F_{(2, 15)} = 12.93$, Bonferroni-corrected $p = .001$). Thus, the decrease in C.O. activity in the PCC might be due, in part, to cell death. The largest increase in glia was found in the deep region of the dorsal PCC. In this region, sodium azide treatment increased the number of glia by 200% compared to control animals ($F_{(2, 15)} = 7.314$, Bonferroni-corrected $p = .021$). AZ+MB-treated rats also had significant differences in cell counts in all regions as compared to control rats. Cell density decreases in the AZ+MB group were similar to those observed in the AZ group in all regions ($p = 1.0$). This indicates that MB co-administration did not confer neuroprotection against sodium azide-mediated toxicity.

Figure 4.6   Neuronal and glial cell densities in the PCC in control, AZ and

AZ+MB groups. *significantly different from control, $p < .05$.
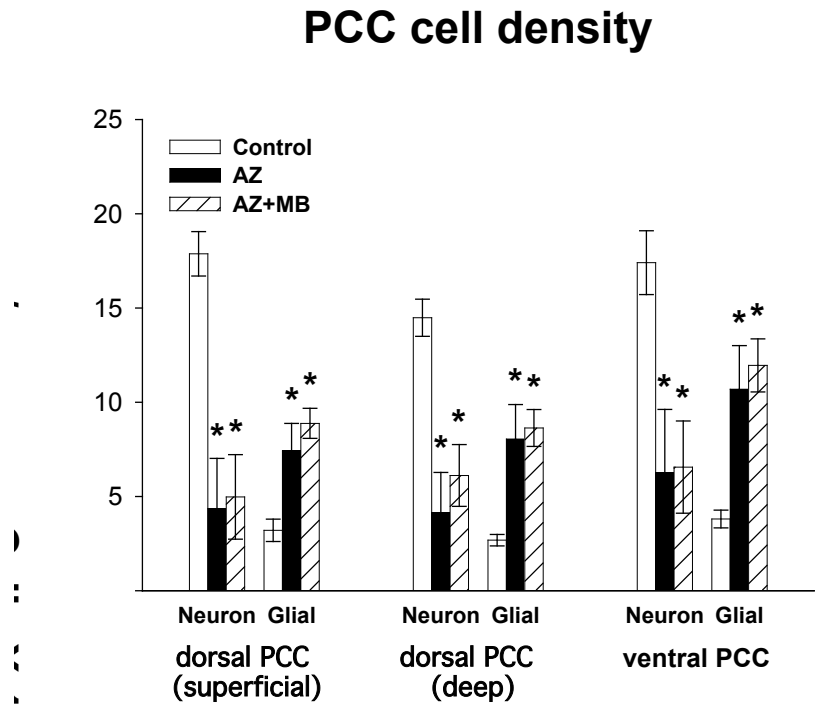
4.5 DISCUSSION

The present study demonstrated that a single systemic injection of 4 mg/kg MB prevented the memory deficits that occurred from PCC hypometabolism. MB likely increased the functional interactions between brain regions that mediate spatial memory retention. PCC hypometabolism was induced by a local injection of sodium azide, a mitochondrial inhibitor of C.O. activity, in the PCC. The AZ-treated rats had lower reference memory scores than both control and AZ+MB-treated rats. However, the AZ+MB-treated group had reference memory scores similar to those of control subjects.

Rats were treated with sodium azide after they learned the baited holeboard pattern. Thus, the memory retention deficits were not confounded by hypometabolism during the learning phase. In addition, neither AZ- nor AZ+MB-treated rats were different from control rats in exploratory activity in an open field chamber. Finally, there were no significant group differences in the total number of nosepokes or in latency to complete the task. Therefore, memory impairment in the AZ group was due to the inability to retrieve the previously-baited pattern, and not due to motor deficits. Similarly, the memory-enhancing effect of MB cannot be explained by a change in exploratory activity.

The systemic effects of MB were not mediated by an increase in neural metabolic activity in the PCC or in other brain regions. This is supported by the fact that PCC C.O. activity levels in the AZ+MB group were lower than the control group and similar to the AZ-treated group. Furthermore, there were no between-group differences in C.O. activity in other measured brain regions. This also suggests that sodium azide is a strong inhibitor of C.O. and that MB did not

116

displace the binding of sodium azide to C.O., which might prevent the memory impairment due to sodium azide.

The MB effect on reference memory does not seem to be mediated by a direct neuroprotective effect against sodium azide toxicity. Neural cell density in the PCC was significantly decreased in both AZ- and AZ+MB-treated animals as compared to control animals. Moreover, this decrease was accompanied by massive gliosis in both treatment groups. Therefore, the overall decrease in neuronal density, even in the presence of MB, suggests that prevention of cell death in the PCC was not a mechanism mediating the effects of MB on memory.

A plausible explanation for the memory-enhancing effect of MB may be through its metabolic-enhancing effects on regions functionally connected with the PCC or other brain regions involved in reference memory. This possibility is supported by the correlations between the PCC and connecting brain regions. The AZ+MB group showed correlations that were quite different from the control and AZ-treated groups. This suggests that an alternative network, such as one that does not require the PCC, was recruited in the AZ+MB-treated rats. Furthermore, the data showed that MB preserved some of the significant correlations observed in the control group. In the control group, C.O. activity in the PCC was positively correlated with the activity in the thalamic nuclei, hippocampus proper, anterior cingulate cortex, and secondary visual cortices. The anterior thalamus, hippocampus proper, and cingulate cortices are included in the Papez circuit, a proposed pathway underlying learning and memory (Papez, 1937; Vertes et al., 2001). Treatment with sodium azide and MB changed these functional interactions. Sodium azide decreased the number of significant correlations as well as created significant correlations not found in the

control group. Conversely, co-administration of MB maintained some of the significant correlations observed in the control group. Specifically, the correlations were between the PCC and the hippocampus, and the PCC and secondary visual cortex.

The only new correlation in the AZ+MB group was a significantly positive correlation between the PCC and the raphe nucleus. Both of these regions had lower C.O. activity than the control and AZ groups. Serotonin generally inhibits cortical activity. By inhibiting monamine oxidase activity in the raphe nucleus, MB may enhance the serotonin-inhibiting effects in the PCC and thereby, indirectly inhibit C.O. activity in the PCC (Lerch et al., 2006).

MB administration increases oxygen consumption both *in vitro* and *in vivo* (Lindahl and Oberg, 1961; Riha et al., 2005; Zhang et al., 2006). Previous studies found that MB improved oxygen consumption when complex I of the mitochondrial respiratory chain was inhibited (Lindahl and Oberg, 1961; Zhang et al., 2006). It is possible that MB has the same effect of increasing oxygen consumption when C.O. is inhibited. We did not measure oxygen consumption in the PCC after MB treatment in this study. MB may have a greater affinity for transferring electrons directly to oxygen in cellular systems with exogenous mitochondrial inhibitors. Future studies will attempt to resolve the mechanism of action of MB in relation to memory improvement during metabolic inhibition. A drug that increases cellular respiration will likely improve learning and memory in patients with conditions characterized by metabolic defects such as AD.

Chapter 5: General Discussion

There is a need to create animal models that exhibit the early pathophysiology of AD. Animals that mimic the abnormalities observed in early stage AD will help us to understand the mechanisms underlying progressive neurodegeneration. Drugs approved for AD have only a modest effect on memory, so an appropriate model will allow us to test novel and effective therapeutic drugs.

Human functional imaging in AD patients reveals that the first brain region to show decreased metabolism is the PCC (Minoshima et al., 1997; Johnson et al., 2006). PCC hypometabolism is also a predictor for patients with MCI to later develop AD (Mosconi, 2005). In particular, mitochondrial cytochrome oxidase (C.O.) activity is decreased within the PCC in AD (Valla et al., 2001). C.O. activity is an indicator of neuronal activity and therefore, C.O. inhibition may contribute to the decreased signals observed during functional neuroimaging of AD patients.

Evidence from human and animal studies illustrates that the PCC contributes to a network supporting spatial orientation and memory (Cammalleri et al., 1996; Berthoz, 1997; Whishaw et al., 2001; Harker and Whishaw, 2002). Functional impairment in this region may underlie the spatial orientation and memory deficits reported in AD patients (de la Torre, 2000; Holroyd and Shepherd, 2001).

Inhibition of brain C.O. activity and resulting learning and memory impairments can be modeled in rats. Two-week administration of sodium azide

through a continuous-release osmotic pump at a dose of 1 mg/kg/hr partially inhibits C.O. activity (Bennett et al., 1992; Cada et al., 1995; Berndt et al., 2001). This degree of C.O. inhibition resulted in memory deficits in active avoidance and spatial tasks such as the Morris water maze, radial arm maze, and holeboard task (Bennett et al., 1992; Bennett and Rose, 1992; Bennett et al., 1996a; Callaway et al., 2002; Luques et al., 2007). These behavioral studies did not analyze regional brain C.O. activity associated with these deficits. Interestingly, the memory deficits in the holeboard task were reversed with methylene blue (MB) treatment (Callaway et al., 2002). Administration of 1 mg/kg MB restored spatial memory retention impaired by systemic administration of sodium azide and was associated with an increase in C.O. activity (Callaway et al., 2002; Callaway et al., 2004).

Systemic C.O. inhibition differentially affects regional brain metabolism; the decreases in C.O. activity ranged from 26–37% (Cada et al., 1995). This is comparable to the 24–39% decrease in C.O. activity found in the PCC in AD brains (Valla et al., 2001). Focal administration of sodium azide in the striatum decreases the concentration of several neurochemicals, including ATP (Brouillet et al., 1994). However, the regional effects of focal administration of sodium azide on brain C.O. activity and behavior have not been examined.

This dissertation addressed the hypothesis that isolated C.O. inhibition in the PCC impairs memory in a spatial task and that this deficit can be reversed by MB administration. We tested spatial memory in rats after bilateral injections of sodium azide in the PCC. The results confirm that inhibition of C.O. activity impairs spatial learning and memory. Specifically, inhibition of PCC metabolism alone is sufficient to cause deficits in memory retention in a spatial holeboard

task. This is not to say that the PCC is the only region responsible for spatial navigation. Rather, these studies confirm that the PCC is an important component in a network that mediates spatial memory. In addition, low dose MB prevented memory impairment caused by sodium azide.

5.1 Summary of Findings

5.1.1 Energy Hypometabolism in the PCC Causes Spatial Memory Impairment Associated with Oxidative Damage and Cell Loss

The first experiment examined if hypometabolism in the PCC is sufficient to cause spatial memory impairment. Rats were trained in a food retrieval task using a holeboard. After they acquired the task, we injected sodium azide directly into the PCC and tested their memory 24 h later. We found that inhibition of C.O. activity in the PCC significantly impaired memory of a previously-learned baited holeboard. These results are consistent with extensive literature documenting PCC's contribution to spatial memory processing (Sutherland et al., 1988; Gabriel, 1993; Whishaw et al., 2001).

After completion of the retraining phase five days after surgery, the brains were quickly removed and analyzed for C.O. activity. Quantitative histochemistry confirmed regional metabolic inhibition and verified that the C.O. inhibition was limited to the PCC. In addition, sodium azide produced significant increases in gliosis and neuronal loss in the PCC. C.O. metabolic changes did not occur in regions that are anatomically connected to the PCC. PCC-interregional correlations in control animals revealed that: 1) C.O. activity in the PCC was positively correlated with secondary visual areas and the hippocampal formation (DGv, CA1v, CA3v, SUB, PRh, Ent); and 2) PCC activity was positively correlated with the caudate putamen, an area that contains head-direction cells

(Taube, 1998). These significant positive correlations were not present in animals with PCC hypometabolism. In the sodium azide-treated group, there was only one negative correlation—between the PCC and CA3d. Therefore, C.O. inhibition resulted in functional dissociation between the PCC and visual and hippocampal areas. Such dissocation may have contributed to the spatial memory deficits observed in this group. To our knowledge, this is the first study in rats to show that memory impairment caused by isolated energy hypometabolism in the PCC is associated with functional uncoupling between the PCC and other brain regions involved in spatial memory.

During retraining, the sodium azide-treated rats performed at the same level as control rats. It is plausible that the young adult rats in our study were using compensatory or competing learning processes during this training phase. In the holeboard task, response/procedural learning could also yield high reference memory (Whishaw et al., 2001). Perhaps if the PCC was damaged, and allocentric processing disturbed, the alternate strategy could dominate. Desgranges et al. (2002) showed that limbic brain areas such as entorhinal and posterior cingulate cortices were associated with episodic memory in healthy controls and less severely-affected AD patients; while neocortical structures were more correlated with better recall in patients with severe AD. These results suggest that although the entorhinal cortex and PCC are impaired early in AD, other brain regions compensate to process memory. In our study, a similar phenomenon may have occurred during retraining in sodium azide-treated rats.

5.1.2 Low Dose MB Enhances Memory and Improves Cellular Respiration

The second study proposed that low dose MB can enhance memory and brain oxygen utilization without nonspecific effects on behavior and motivation.

We determined that rats treated with low dose MB improved memory retention without affecting locomotion, exploration, or motivation. Our lab has previously conducted studies that suggest that low dose MB facilitates memory retention in rats by increasing brain C.O. activity (Callaway et al., 2004; Gonzalez-Lima and Bruchey, 2004; Wrubel et al., 2007).

Our dose-response study determined the proper MB dose that facilitated memory without changing general behavioral activity. Administration of 4 mg/kg MB improved memory in both tasks without changing nonspecific behaviors. Generally, the 1–10 mg/kg MB-treated rats did not differ from saline-treated rats in locomotor activity or motivation. But, rats treated with higher doses of MB (50 and 100 mg/kg) showed locomotor impairment and decreased motivation. The 4 mg/kg MB dose improved behavioral habituation in an open field chamber. The 4 mg/kg and 10 mg/kg MB doses improved object recognition, a task that is believed to test episodic memory in rats (Lebrun et al., 2000). Rats injected with 10 mg/kg MB dose showed increased exploration in the open field and high variance in the object recognition test.

In the second study, we also determined that 1 mg/kg MB increased brain oxygen consumption 24 h after administration. Our study is the first to show a direct increase of brain oxygen consumption following MB administration. Our findings are consistent with the Callaway et al. (2004) study that showed an increase in C.O. activity 24 h after a single 1 mg/kg MB injection. This dose of MB was previously shown to reverse memory impairment caused by chronic sodium azide treatment (Callaway et al., 2002). Together, these studies demonstrate that low dose MB facilitates C.O. activity and increases oxygen

consumption. Therefore, the memory-enhancing effects of MB may be due to increased brain oxygen consumption and C.O. activity.

The dose-response effects of MB on C.O. activity *in vitro* revealed an inverted U-shaped dose-response curve between 0.5 µM and 10 µM, with the most effective concentration being 5 µM (Callaway et al., 2004). Another study showed that 50 mg/kg MB given to mice impaired memory retention (Martinez et al., 1978). The higher variance produced by 10 mg/kg MB in the object recognition test and the dose-response characteristics in the *in vitro* C.O. activity study indicates that MB has nootropic properties (Baxter et al., 1994) and may be beneficial for the treatment of AD.

5.1.3 Low Dose MB Prevents Spatial Memory Impairment Caused by PCC Hypometabolism

The third study tested the hypothesis that low dose MB reverses memory impairment caused by sodium azide administration in the PCC. As determined in the previous study, the effective MB dose (4 mg/kg) was administered to rats with PCC hypometabolism and their spatial memory retention was tested using a holeboard task. MB prevented the impairment in spatial memory that occurred from sodium azide. Histochemistry determined the corresponding C.O. activity changes in the brain one day after injection. As in the second study, the only region showing C.O. inhibition was the PCC. MB did not prevent the metabolic impairment in the PCC caused by sodium azide administration.

Consistent with our second study, sodium azide significantly increased glia and neuronal loss in both dorsal and ventral regions of the PCC. This implies that C.O. inhibition was caused by enzyme loss rather than impaired catalytic activity. Although MB prevented memory loss, it did not prevent cell loss, as determined in Nissl-stained brain tissue. Neuronal and glial cell counts

in the PCC were the same between AZ-treated rats and AZ+MB-treated rats. One implication of these results is that the memory-enhancing effects of systemic MB administration were not mediated by prevention of sodium azide-induced neurotoxicity. Zhang et al (2006) showed that rotenone-induced neurodegeneration in the retinal ganglion cell layer was prevented by the co-administration of MB along with rotenone. It is likely that local co-administration of MB in the PCC would confer neuroprotection in our model of focal PCC hypometabolism.

MB treatment may have improved memory by mediating functional associations between brain regions, as evidenced by the PCC-interregional correlations. Although there were only half as many significant correlations in the AZ+MB-treated group as compared to the control group, most of the correlations found in the AZ+MB group were identical to the correlations in the control group. In contrast, the AZ group only showed one significant correlation that was identical to the control group (between PCC and CA1v). The common associations in the AZ+MB group and the control group included correlations between the PCC and dorsal hippocampus (DGd, CA1d), zona incerta, and secondary visual cortex. In addition, although some of the significant correlations found in the control group were not significant in the AZ+MB group, their correlational value was higher than the same correlations in the AZ group. Horwitz (1987) noted that AD patients have fewer correlations in metabolic activity between cortical regions. The change in PCC-interregional correlations due to focal administration of sodium azide in the PCC mimic some of these observations.

Our studies confirm existing evidence that several structures are involved in spatial memory. After a spatial memory task, metabolic activity in the PCC was significantly correlated with activity in the hippocampal formation, thalamic nuclei, and subicular, entorhinal, and perirhinal cortices. An important novel finding were the significant correlations in metabolic activity in several areas of the Papez circuit, whose function has been proposed to mediate learning and memory (Valenstein et al., 1987; Holdstock et al., 2000; Harker and Whishaw, 2002; van Groen et al., 2004). PCC hypometabolism by focal injections of sodium azide eliminated several significant correlations between the PCC and other brain regions that were found in the control group. The PCC-interregional correlations suggest that decreasing the functional relationships in the Papez network can impair memory.

The PCC may be a vulnerable brain region. It has a high baseline activity in healthy human subjects (Minoshima et al., 1997). The PCC has extensive reciprocal connections with the anterior thalamic nuclei (Shibata, 1998). Approximately 70% of the anterior thalamic projections to the PCC are excitatory synapses (Gonzalo-Ruiz et al., 1997). To fulfill a high energy demand, C.O. expression is upregulated (Wong-Riley et al., 1998), which makes the PCC vulnerable to other metabolic insults such as vascular problems or C.O. inhibition. In rats, systemic administration of an NMDA antagonist produces region-specific neurotoxicity, with the PCC being the most affected region (Li et al., 2002). Likewise, the PCC would be one of the first areas affected by C.O. inhibition that leads to compromised energy metabolism and eventually cell death.

5.2 Alternative Explanations

1. It is possible that the memory impairment observed in sodium azide-treated rats was caused by diaschisis. Diaschisis refers to functional changes in brain areas remote from the site of damage, but that is connected to it by neurons (Thirumala et al., 2002). Diaschisis is one mechanism thought to underlie functional recovery in stroke recovery in humans (Seitz et al., 1999). It is possible that the memory recovery in the sodium azide-treated subjects (study 2) that occurred during retraining was a result of other brain regions compensating for the loss in function due to the lesion.

However, if other brain regions compensated during the memory task, metabolic activity in that region would change to reflect such a situation. Since brain function and metabolism are correlated, C.O. histochemistry would reveal if there were functional changes in other brain regions in the sodium azide-treated animals during retraining. At the time examined, there were no differences in metabolic activity in other brain regions that might account for the memory impairment.

2. One explanation for the effects of MB on memory may be due to some cells in the PCC gaining function while others deteriorated. For example, perhaps the spared neurons within the PCC increased plasticity and strengthened their connections to brain regions mediating spatial navigation. The analysis of C.O. histochemistry did not detail specific layers or cell types within the PCC. Nissl-staining did not determine if there were differential effects between the AZ and AZ+MB groups. However, the covariance analysis of metabolic activity between the PCC and other brain regions suggests a different possibility.

Covariance analysis of the PCC connections in the control group revealed high correlations between the PCC and connecting afferent and efferent regions. However, several of these correlations were greatly decreased in the AZ+MB-treated rats. Although the AZ+MB-treated rats showed significant PCC inhibition, they exhibited the same performance as control rats in the holeboard probe test. One possibility is that these two groups were using different memory strategies to perform the same retention test. In the control group, the strategy was PCC-dependent, but in the AZ+MB group, it was PCC-independent. The idea of multiple memory systems acting in parallel or in an interactive manner is established in the literature (McIntyre et al., 2003). Experimental studies in animals that confirm this theory show that lesioning one brain area facilitates task performance (Bussey et al., 1996). Thus, in an intact animal, two strategies may compete or one may dominate during learning and memory. However, when the tendency to use one of the strategies is removed, as with a lesion, the competing process proceeds.

5.3 Improvements

1. AD is defined by chronic, progressive metabolic and memory impairment. Our C.O. inhibition model did not produce memory impairment during the retraining stage. In our studies, at the time of the probe test, there was a 17% decrease in C.O. activity in the PCC. Chronic treatment with sodium azide results in learning and memory deficits that are associated with a 26–37% decrease in C.O. activity (Cada et al., 1995). In our study, rats with PCC inhibition showed memory deficits one day after treatment but later recovered to the level of control rats. It is possible that greater C.O. inhibition may cause progressive impairment.

2. Because we were cautious not to spread sodium azide beyond the limits of the PCC, the anterior and dorsal regions showed more impairment than the posterior and ventral regions. The dorsal and ventral regions of the PCC are distinct components that provide projections to different parts of the same area (van Groen and Wyss, 1992a; van Groen and Wyss, 2003; Shibata et al., 2004). These different projections may transmit different spatial information. Partial lesions of the PCC produce a less severe impairment in spatial memory performance than complete lesions (Vann et al., 2003). Thus, it is likely that greater impairment in the holeboard task would result from inhibiting these regions as well. Future studies should attempt to inject in such a way as to impair the entire antero-posterior extent of the PCC.

5.4 Future Directions

1. It is unclear if the sparing within the ventral PCC region was due to injection volume or, alternatively, differential C.O. vulnerability in the dorsal region. Distinguishing among different neuronal populations could determine if some are more vulnerable to C.O. inhibition. It is hypothesized that cells with high neuronal demand, and therefore high C.O. density, would show more inhibition from sodium azide treatment. For example, pyramidal cells which receive a lot of glutamatergic innervation from anterior thalamic nuclei should be more affected than GABAergic interneurons.

2. To model the changes seen in Alzheimer's patients, it would be interesting to combine another risk factor such as aging or vascular impairment (de la Torre et al., 2004) with the sodium azide-induced hypometabolism in order to induce greater energy failure. This might better model chronic inhibition in AD patients. For example, Bennett et al (Bennett et al., 1996a) found that

129

simultaneous administration of sodium azide and corticosterone impaired learning and memory in the water maze. However, these doses did not impair learning when administered alone (Bennett et al., 1996b). Corticosterone administration decreased glucose uptake and potentiated the energy impairment due to C.O. inhibition.

5.5 A Novel Therapeutic Strategy

AD is a devastating neurological disorder and the therapeutic options are limited. Drugs that inhibit the breakdown of the neurotransmitter acetylcholine are the foundation of therapy. Four of the five drugs on the market are acetylcholinesterase inhibitors; the fifth is memantine. Although the majority of these drugs do not produce serious side effects, there is only a modest cognitive improvement, at best (Clegg et al., 2001; Delagarza, 2003; Loveman et al., 2006). In addition, the reports of their efficacy on global functioning, behavior, and mood are inconsistent (Clegg et al., 2001; Delagarza, 2003; Loveman et al., 2006; Reisberg et al., 2006).

It is not clear whether C.O. inhibition is the cause or the result of AD. However, it is apparent that C.O. inhibition occurs before the onset of cognitive decline (Blass et al., 2002). Because C.O. activity and neuronal function are tightly coupled, any drug that enhances C.O. activity should lead to an increase in oxygen consumption and ATP synthesis. One mechanism to alleviate the metabolic and possible behavioral consequences of C.O. inhibition is to increase mitochondrial respiration. However, an increase in mitochondrial respiration may lead to increased free radical production. MB is a compound that can both increase metabolism and decrease free radical production through its mechanisms as an electron transporter and as an antioxidant.

5.5.1 Mitochondria as a Therapeutic Target

Mitochondria are a major source of free radicals and are responsible for activating apoptotic cell death. Attempts to protect neurons by using antioxidants have been successful in animal studies of neuronal cell death (Kelso et al., 2001; Szeto, 2006). MB is lipophilic and diffuses readily in the mitochondria with several beneficial mechanisms of action, such as decreasing free radicals, and increasing brain C.O. activity and oxygen consumption (Salaris et al., 1991; Callaway et al., 2004; Riha et al., 2005/chapter 3). *In vivo*, MB increases mitochondrial long-chain fatty acid oxidation (Visarius et al., 1999). Long-chain fatty acids provide structural components for various lipids and proteins, and are a high-energy source for OXPHOS. Low dose MB (1-2 µM) also decreases amyloid aggregation and neurofibrillary tangle assembly *in vitro* (Wischik et al., 1996; Taniguchi et al., 2005). Thus, MB administration to AD patients may be highly beneficial: it would not only increase brain metabolism and decrease free radical production, but would also decrease amyloid plaque formation and neurofibrillary tangles commonly observed in the late stages of AD. Further research is necessary to determine the efficacy of MB on AD.

MB provides neurons more metabolic energy to fuel energy demands that facilitate memory retention. It is possible that MB may improve memory retention in humans with AD and other conditions that are characterized by metabolic energy deficiency, such as individuals with age-related memory impairment, stroke victims, and patients with vascular dementia (Valla et al., 2001; Aliev et al., 2003). Memory impairment in AD is correlated with dysfunctional brain metabolism (de la Torre, 2004; Beal, 2005). The ability to slow the disease

progression in patients with early-stage AD is foreseeable since MCI is recognized as a major risk factor for AD.

Typical pharmacological treatments that improve memory modify specific neurotransmitters. However, metabolic enhancers like MB that target mitochondria may improve overall brain energy production and memory retention without producing the side effects associated with modifying a particular neurotransmitter system. MB is an FDA-approved drug that has been used safely and without significant side effects for many years (Naylor et al., 1986). Studies of low dose MB in humans are needed to examine its effects in AD patients and those with MCI.

5.6 Conclusions

A major problem in AD research continues to be determining which abnormalities are primary and which are secondary. Amyloid plaques, neurofibrillary tangles, oxidative stress, acetylcholine signaling, mtDNA mutations, decreased C.O. activity, brain hypometabolism, and neuronal degeneration are all interrelated. *In vitro*, a defect in one can lead to abnormalities in the others. Despite the difficulty in classifying the abnormalities, it is clear that C.O. inhibition is one of the first markers that appear in AD and in patients with MCI who develop AD. Therapy aimed at improving C.O. activity might slow the decline of MCI to AD. PCC hypometabolism is observed in patients with MCI who later develop AD and in subjects carrying a common AD susceptibility gene. Measuring brain metabolism in the PCC could noninvasively evaluate the efficacy of drugs that target C.O.

Sodium azide administration impairs C.O. activity and results in memory impairment in both aversively and appetitively-motivated tasks. In rats, a primary

reduction in C.O. activity is sufficient to induce other pathological changes in the brain such as impaired LTP, decreased PKC activation, and a decrease in several markers of acetylcholine transmission (Bennett et al., 1992; Bennett et al., 1995; Luques et al., 2007). Sodium azide-treated cells exhibit changes in amyloid processing (Gabuzda et al., 1994; Gasparini et al., 1997) and decreases in the mitochondrial membrane potential (Cassarino et al., 1998). Rats treated with sodium azide reproduce several changes observed in AD patients.

There is no animal model that can mimic all the cognitive, behavioral, biochemical and histopathological abnormalities observed in AD patients. However, an animal model of C.O. hypometabolism in the PCC can provide information to understand the mechanisms that regulate early pathological degeneration, provide information as to the underlying pathology, and possibly reveal new therapeutic strategies aimed at reducing or preventing cognitive decline.

Hopefully, the proposed animal model of PCC hypometabolism can replicate some of the cognitive impairments and neuropathological changes that are observed in the earliest stages of AD. Further investigation of this model may clarify pathological mechanisms and allow assessment of new treatment strategies. MCI is now considered prodromal AD. Therefore, it is crucial to try and target the initial stages of AD before the disease progresses.

References

Adkins DL, Voorhies AC, Jones TA (2004) Behavioral and neuroplastic effects of focal endothelin-1 induced sensorimotor cortex lesions. Neuroscience 128:473-486.

Aleman A (2005) Feelings you can't imagine: Towards a cognitive neuroscience of alexithymia. Trends Cogn Sci 9:553-555.

Bartolini L, Casamenti F, Pepeu G (1996) Aniracetam restores object recognition impaired by age, scopolamine, and nucleus basalis lesions. Pharmacol Biochem Behav 53:277-283.

Baxter MG, Lanthorn TH, Frick KM, Golski S, Wan R-Q, Olton DS (1994) D-cycloserine, a novel cognitive enhancer, improves spatial memory in aged rats. Neurobiol Aging 15:207-213.

Beal MF (2005) Mitochondria take center stage in aging and neurodegeneration. Ann Neurol 58:495-505.

Bennett MC, Diamond DM, Stryker SL, Parks JK, Parker WD, Jr. (1992) Cytochrome oxidase inhibition: A novel animal model of Alzheimer's disease. J Geriatr Psychiatry Neurol 5:93-101.

Bennett MC, Rose GM (1992) Chronic sodium azide treatment impairs learning of the Morris water maze task. Behav Neural Biol 58:72-75.

Bennett MC, Fordyce DE, Rose GM, Wehner JM (1995) Chronic sodium azide treatment decreases membrane-bound protein kinase c activity in the rat hippocampus. Neurobiol Learn Mem 64:187-190.

Bennett MC, Mlady GW, Fleshner M, Rose GM (1996a) Synergy between chronic corticosterone and sodium azide treatments in producing a spatial learning deficit and inhibiting cytochrome oxidase activity. Proc Natl Acad Sci USA 93:1330-1334.

Bennett MC, Mlady GW, Kwon YH, Rose GM (1996b) Chronic *in vivo* sodium azide infusion induces selective and stable inhibition of cytochrome c oxidase. JNeurochem 66:2606-2611.

Benzi G, Moretti A (1995) Age- and peroxidative stress-related modifications of the cerebral enzymatic activities linked to mitochondria and the glutathione system. Free Radic Biol Med 19:77-101.

Berndt JD, Callaway NL, Gonzalez-Lima F (2001) Effects of chronic sodium azide on brain and muscle cytochrome oxidase activity: A potential model to investigate environmental contributions to neurodegenerative diseases. J Toxicol Environ Health A 63:67-77.

Berthoz A (1997) Parietal and hippocampal contribution to topokinetic and topographic memory. Philos Trans R Soc Lond B Biol Sci 352:1437-1448.

Blass JP, Gibson GE, Hoyer S (2002) The role of the metabolic lesion in Alzheimer's disease. J Alzheimers Dis 4:225-232.

Blennow K, de Leon MJ, Zetterberg H (2006) Alzheimer's disease. Lancet 368:387-403.

Borroni B, Anchisi D, Paghera B, Vicini B, Kerrouche N, Garibotto V, Terzi A, Vignolo LA, Di Luca M, Giubbini R, Padovani A, Perani D (2006) Combined 99mTc-ECD SPECT and neuropsychological studies in MCI for the assessment of conversion to AD. Neurobiol Aging 27:24-31.

Brouillet E, Hyman BT, Jenkins BG, Henshaw DR, Schulz JB, Sodhi P, Rosen BR, Beal MF (1994) Systemic or local administration of azide produces striatal lesions by an energy impairment-induced excitotoxic mechanism. Exp Neurol 129:175-182.

Buehring GC, Jensen HM (1983) Lack of toxicity of methylene blue chloride to supravitally stained human mammary tissues. Cancer Res 43:6039-6044.

Bussey TJ, Muir JL, Everitt BJ, Robbins TW (1996) Dissociable effects of anterior and posterior cingulate cortex lesions on the acquisition of a conditional visual discrimination: Facilitation of early learning vs. impairment of late learning. Behav Brain Res 82:45-56.

Bussey TJ, Muir JL, Everitt BJ, Robbins TW (1997) Triple dissociation of anterior cingulate, posterior cingulate, and medial frontal cortices on visual discrimination tasks using a touchscreen testing procedure for the rat. Behav Neurosci 111:920-936.

Cada A, Gonzalez-Lima F, Rose GM, Bennett MC (1995) Regional brain effects of sodium azide treatment on cytochrome oxidase activity: A quantitative histochemical study. Metab Brain Dis 10:303-320.

Callaway NL, Riha PD, Wrubel KM, McCollum D, Gonzalez-Lima F (2002) Methylene blue restores spatial memory retention impaired by an inhibitor of cytochrome oxidase in rats. Neurosci Lett 332:83-86.

Callaway NL, Riha PD, Bruchey AK, Munshi Z, Gonzalez-Lima F (2004) Methylene blue improves brain oxidative metabolism and memory retention in rats. Pharmacol Biochem Behav 77:175-181.

Cammalleri R, Gangitano M, D'Amelio M, Raieli V, Raimondo D, Camarda R (1996) Transient topographical amnesia and cingulate cortex damage: A case report. Neuropsychologia 34:321-326.

Cardoso SM, Proenca MT, Santos S, Santana I, Oliveira CR (2004a) Cytochrome c oxidase is decreased in Alzheimer's disease platelets. Neurobiol Aging 25:105-110.

Cardoso SM, Santana I, Swerdlow RH, Oliveira CR (2004b) Mitochondria dysfunction of Alzheimer's disease cybrids enhances abeta toxicity. J Neurochem 89:1417-1426.

Cassarino DS, Swerdlow RH, Parks JK, Parker WD, Jr., Bennett JP, Jr. (1998) Cyclosporin A increases resting mitochondrial membrane potential in SY5Y cells and reverses the depressed mitochondrial membrane potential of Alzheimer's disease cybrids. Biochem Biophys Res Commun 248:168-173.

Cassarino DS, Bennett JP, Jr. (1999) An evaluation of the role of mitochondria in neurodegenerative diseases: Mitochondrial mutations and oxidative pathology, protective nuclear responses, and cell death in neurodegeneration. Brain Res Brain Res Rev 29:1-25.

Cerbone A, Sadile AG (1994) Behavioral habituation to spatial novelty: Interference and noninterference studies. Neurosci Biobehav Rev 18:497-518.

Chandrasekaran K, Stoll J, Giordano T, Atack JR, Matocha M, Brady DR, Rapoport SI (1992) Differential expression of cytochrome oxidase (COX) genes in different regions of monkey brain. J Neurosci Res 32:415-423.

Chandrasekaran K, Giordano T, Brady DR, Stoll J, Martin LJ, Rapoport SI (1994) Impairment in mitochondrial cytochrome oxidase gene expression in Alzheimer disease. Brain Res Mol Brain Res 24:336-340.

Chandrasekaran K, Hatanpaa K, Rapoport SI, Brady DR (1997) Decreased expression of nuclear and mitochondrial DNA-encoded genes of oxidative phosphorylation in association neocortex in Alzheimer disease. Brain Res Mol Brain Res 44:99-104.

Chase TN, Foster NL, Fedio P, Brooks R, Mansi L, Di Chiro G (1984) Regional cortical dysfunction in Alzheimer's disease as determined by positron emission tomography. Ann Neurol 15 Suppl:S170-S174.

Chen LL, Lin LH, Green EJ, Barnes CA, McNaughton BL (1994) Head-direction cells in the rat posterior cortex. I. Anatomical distribution and behavioral modulation. Exp Brain Res 101:8-23.

Chetelat G, Desgranges B, De la Sayette V, Lalevee C, Landeau B, Dupuy B, Hannequin D, Viader F, Eustache F, Baron JC (2001) Selective metabolic reduction in the posterior cingulate cortex in the pre-dementia stage of Alzheimer's disease (AD). Neuroimage 13:S646.

Cho J, Sharp PE (2001) Head direction, place, and movement correlates for cells in the rat retrosplenial cortex. Behav Neurosci 115:3-25.

Clegg A, Bryant J, Nicholson T, McIntyre L, De Broe S, Gerard K, Waugh N (2001) Clinical and cost-effectiveness of donepezil, rivastigmine and galantamine for Alzheimer's disease: A rapid and systematic review. Health Technol Assess 5:1-137.

Cooke SF, Attwell PJE, Yeo CH (2004) Temporal properties of cerebellar-dependent memory consolidation. J Neurosci 24:2934-2941.

Curti D, Rognoni F, Gasparini L, Cattaneo A, Paolillo M, Racchi M, Zani, Bianchetti A, Trabucchi M, Bergamaschi S, Govoni S (1997) Oxidative metabolism in cultured fibroblasts derived from sporadic Alzheimer's disease (AD) patients. Neurosci Lett 236:13-16.

de la Torre JC (2000) Critically attained threshold of cerebral hypoperfusion: The catch hypothesis of Alzheimer's pathogenesis. Neurobiol Aging 21:331-342.
de la Torre JC (2004) Alzheimer's disease is a vasocognopathy: A new term to describe its nature. Neurol Res 26:517-524.

Delagarza VW (2003) Pharmacologic treatment of Alzheimer's disease: An update. Am Fam Physician 68:1365-1372.

Desgranges B, Baron JC, Eustache F (1998) The functional neuroanatomy of episodic memory: The role of the frontal lobes, the hippocampal formation, and other areas. Neuroimage 8:198-213.

Desgranges B, Baron J-C, Lalevee C, Giffard B, Viader F, de La Sayette V, Eustache F (2002) The neural substrates of episodic memory impairment in Alzheimer's disease as revealed by FDG-PET: Relationship to degree of deterioration. Brain 125:1116-1124.

Doppenberg EMR, Zauner A, Bullock R, Ward JD, Fatouros PP, Young HF (1998) Correlations between brain tissue oxygen tension, carbon dioxide tension, pH, and cerebral blood flow--a better way of monitoring the severely injured brain? Surg Neurol 49:650-654.

Duong TQ, Iadecola C, Kim SG (2001) Effect of hyperoxia, hypercapnia, and hypoxia on cerebral interstitial oxygen tension and cerebral blood flow. Magn Reson Med 45:61-70.

Finch DM, Derian EL, Babb TL (1984) Afferent fibers to rat cingulate cortex. Exp Neurol 83:468-485.

Flood JF, Landry DW, Jarvik ME (1981) Cholinergic receptor interactions and their effects on long-term memory processing. Brain Res 215:177-185.

Floyd RA (1999) Antioxidants, oxidative stress, and degenerative neurological disorders. Proc Soc Exp Biol Med 222:236-245.

Foot NC (1954) Vital staining. Ann N Y Acad Sci 59:259-267.

Franck N, O'Leary DS, Flaum M, Hichwa RD, Andreasen NC (2002) Cerebral blood flow changes associated with schneiderian first-rank symptoms in schizophrenia. J Neuropsychiatry Clin Neurosci 14:277-282.

Gabriel M (1993) Discriminative avoidance learning: A model system. In: Neurobiology of cingulate cortex and limbic thalamus (Vogt BA, Gabriel M, eds), pp 478-523. Boston: Birkhauser.

Gabrielli D, Belisle E, Severino D, Kowaltowski AJ, Baptista MS (2004) Binding, aggregation and photochemical properties of methylene blue in mitochondrial suspensions. Photochem Photobiol 79:227-232.

Gabuzda D, Busciglio J, Chen LB, Matsudaira P, Yankner BA (1994) Inhibition of energy metabolism alters the processing of amyloid precursor protein and induces a potentially amyloidogenic derivative. J Biol Chem 269:13623-13628.

Gasparini L, Racchi M, Benussi L, Curti D, Binetti G, Bianchetti A, Trabucchi M, Govoni S (1997) Effect of energy shortage and oxidative stress on amyloid precursor protein metabolism in cos cells. Neurosci Lett 231:113-117.

Ghosh SS, Swerdlow RH, Miller SW, Sheeman B, Parker WD, Jr., Davis RE (1999) Use of cytoplasmic hybrid cell lines for elucidating the role of mitochondrial dysfunction in Alzheimer's disease and Parkinson's disease. Ann N Y Acad Sci 893:176-191.

Gonzalez-Lima F, Jones D (1994) Quantitative mapping of cytochrome oxidase activity in the central auditory system of the gerbil: A study with calibrated activity standards and metal-intensified histochemistry. Brain Res 660:34-49.

Gonzalez-Lima F, Cada A (1998) Quantitative histochemistry of cytochrome oxidase activity. In: Cytochrome oxidase in neuronal metabolism and Alzheimer's disease (Gonzalez-Lima F, ed), pp 55-90. New York: Plenum Press.

Gonzalez-Lima F, Bruchey AK (2004) Extinction memory improvement by the metabolic enhancer methylene blue. Learn Mem 11:633-640.

Gonzalo-Ruiz A, Sanz JM, Morte L, Lieberman AR (1997) Glutamate and aspartate immunoreactivity in the reciprocal projections between the anterior thalamic nuclei and the retrosplenial granular cortex in the rat. Brain Res Bull 42:309-321.

Harding AJ, Halliday GM, Cullen K (1994) Practical considerations for the use of the optical disector in estimating neuronal number. J Neurosci Methods 51:83-89.

Harker KT, Whishaw IQ (2002) Impaired spatial performance in rats with retrosplenial lesions: Importance of the spatial problem and the rat strain in identifying lesion effects in a swimming pool. J Neurosci 22:1155-1164.

Haznedar MM, Buchsbaum MS, Hazlett EA, Shihabuddin L, New A, Siever LJ (2004) Cingulate gyrus volume and metabolism in the schizophrenia spectrum. Schizophr Res 71:249-262.

Hevner RF, Wong-Riley MT (1989) Brain cytochrome oxidase: Purification, antibody production, and immunohistochemical/histochemical correlations in the CNS. J Neurosci 9:3884-3898.

Hevner RF, Duff RS, Wong-Riley MT (1992) Coordination of ATP production and consumption in brain: Parallel regulation of cytochrome oxidase and Na+, k(+)-ATPase. Neurosci Lett 138:188-192.

Hof PR, Morrison JH (1990) Quantitative analysis of a vulnerable subset of pyramidal neurons in Alzheimer's disease: II. Primary and secondary visual cortex. J Comp Neurol 301:55-64.

Holdstock JS, Mayes AR, Cezayirli E, Isaac CL, Aggleton JP, Roberts N (2000) A comparison of egocentric and allocentric spatial memory in a patient with selective hippocampal damage. Neuropsychologia 38:410-425.

Holroyd S, Shepherd ML (2001) Alzheimer's disease: A review for the ophthalmologist. Surv Ophthalmol 45:516-524.

Horwitz B, Grady CL, Schlageter NL, Duara R, Rapoport SI (1987) Intercorrelations of regional cerebral glucose metabolic rates in Alzheimer's disease. Brain Res 407:294-306.

Johnson SC, Schmitz TW, Moritz CH, Meyerand ME, Rowley HA, Alexander AL, Hansen KW, Gleason CE, Carlsson CM, Ries ML, Asthana S, Chen K, Reiman EM, Alexander GE (2006) Activation of brain regions vulnerable to Alzheimer's disease: The effect of mild cognitive impairment. Neurobiol Aging 27:1604-1612.

Kasischke KA, Vishwasrao HD, Fisher PJ, Zipfel WR, Webb WW (2004) Neural activity triggers neuronal oxidative metabolism followed by astrocytic glycolysis. Science 305:99-103.

Katayama K, Takahashi N, Ogawara K, Hattori T (1999) Pure topographical disorientation due to right posterior cingulate lesion. Cortex 35:279-282.

Kelner MJ, Alexander NM (1985) Methylene blue directly oxidizes glutathione without the intermediate formation of hydrogen peroxide. J Biol Chem 260:15168-15171.

Kelner MJ, Bagnell R, Hale B, Alexander NM (1988) Potential of methylene blue to block oxygen radical generation in reperfusion injury. Basic Life Sci 49:895-898.

Kelso GF, Porteous CM, Coulter CV, Hughes G, Porteous WK, Ledgerwood EC, Smith RAJ, Murphy MP (2001) Selective targeting of a redox-active ubiquinone to mitochondria within cells. Antioxidant and antiapoptotic properties. J Biol Chem 276:4588-4596.

Kish SJ, Bergeron C, Rajput A, Dozic S, Mastrogiacomo F, Chang LJ, Wilson JM, DiStefano LM, Nobrega JN (1992) Brain cytochrome oxidase in Alzheimer's disease. J Neurochem 59:776-779.

Knyihar-Csillik E, Okuno E, Vecsei L (1999) Effects of *in vivo* sodium azide administration on the immunohistochemical localization of kynurenine aminotransferase in the rat brain. Neuroscience 94:269-277.

Kositprapa C, Zhang B, Berger S, Canty JM, Jr., Lee TC (2000) Calpain-mediated proteolytic cleavage of troponin i induced by hypoxia or metabolic inhibition in cultured neonatal cardiomyocytes. Mol Cell Biochem 214:47-55.

Krause BJ, Hautzel H, Schmidt D, Flub MO, Poeppel TD, Muller H-W, Halsband U, Mottaghy FM (2006) Learning related interactions among neuronal systems involved in memory processes. J Physiol Paris 99:318-332.

Kupfer A, Aeschlimann C, Cerny T (1996) Methylene blue and the neurotoxic mechanisms of ifosfamide encephalopathy. Eur J Clin Pharmacol 50:249-252.

Lannert H, Hoyer S (1998) Intracerebroventricular administration of streptozotocin causes long-term diminutions in learning and memory abilities and in cerebral energy metabolism in adult rats. Behav Neurosci 112:1199-1208.

Lebrun C, Pilliere E, Lestage P (2000) Effects of S 18986-1, a novel cognitive enhancer, on memory performances in an object recognition task in rats. Eur J Pharmacol 401:205-212.

Lee I, Kesner RP (2003) Time-dependent relationship between the dorsal hippocampus and the prefrontal cortex in spatial memory. J Neurosci 23:1517-1523.

Lerch S, Kupfer A, Idle JR, Lauterburg BH (2006) Cerebral formation in situ of S-carboxymethylcysteine after ifosfamide administration to mice: A further clue to the mechanism of ifosfamide encephalopathy. Toxicol Lett 161:188-194.

Li Q, Clark S, Lewis DV, Wilson WA (2002) NMDA receptor antagonists disinhibit rat posterior cingulate and retrosplenial cortices: A potential mechanism of neurotoxicity. J Neurosci 22:3070-3080.

Lindahl PE, Oberg KE (1961) The effect of rotenone on respiration and its point of attack. Exp Cell Res 23:228-237.

Loveman E, Green C, Kirby J, Takeda A, Picot J, Payne E, Clegg A (2006) The clinical and cost-effectiveness of donepezil, rivastigmine, galantamine and memantine for Alzheimer's disease. Health Technol Assess 10:iii-iv.

Luques L, Shoham S, Weinstock M (2007) Chronic brain cytochrome oxidase inhibition selectively alters hippocampal cholinergic innervation and impairs memory: Prevention by ladostigil. Exp Neurol 206:209-219.

Maguire EA (1997) Hippocampal involvement in human topographical memory: Evidence from functional imaging. Philos Trans R Soc Lond B Biol Sci 352:1475-1480.

Malhi GS, Lagopoulos J, Owen AM, Ivanovski B, Shnier R, Sachdev P (2007) Reduced activation to implicit affect induction in euthymic bipolar patients: An fMRI study. J Affect Disord 97:109-122.

Markesbery WR (1997) Oxidative stress hypothesis in Alzheimer's disease. Free Radic Biol Med 23:134-147.

Martinez JL, Jr., Jensen RA, Vasquez BJ, McGuinness T, McGaugh JL (1978) Methylene blue alters retention of inhibitory avoidance responses. Physiol Psychol 6:387-390.

May JM, Qu Z, Whitesell RR (2003) Generation of oxidant stress in cultured endothelial cells by methylene blue: Protective effects of glucose and ascorbic acid. Biochem Pharmacol 66:777-784.

Mayer B, Brunner F, Schmidt K (1993) Novel actions of methylene blue. Eur Heart J 14 Suppl I:22-26.

McGaugh JL (2000) Memory--a century of consolidation. Science 287:248-251.
McGeorge AJ, Faull RL (1989) The organization of the projection from the cerebral cortex to the striatum in the rat. Neuroscience 29:503-537.

McIntyre CK, Marriott LK, Gold PE (2003) Patterns of brain acetylcholine release predict individual differences in preferred learning strategies in rats. Neurobiol Learn Mem 79:177-183.

McKhann G, Drachman D, Folstein M, Katzman R, Price D, Stadlan EM (1984) Clinical diagnosis of Alzheimer's disease: Report of the nincds-adrda work group under the auspices of department of health and human services task force on Alzheimer's disease. Neurol 34:939-944.

Mecocci P, MacGarvey U, Beal MF (1994) Oxidative damage to mitochondrial DNA is increased in Alzheimer's disease. Ann Neurol 36:747-751.

Mecocci P, Cherubini A, Beal MF, Cecchetti R, Chionne F, Polidori MC, Romano G, Senin U (1996) Altered mitochondrial membrane fluidity in AD brain. Neurosci Lett 207:129-132.

Mello e Souza T, Roesler R, Madruga M, de-Paris F, Quevedo J, Rodrigues C, Sant'Anna MK, Medina JH, Izquierdo I (1999) Differential effects of post-training muscimol and AP5 infusions into different regions of the cingulate cortex on retention for inhibitory avoidance in rats. Neurobiol Learn Mem 72:118-127.

Merker MP, Bongard RD, Linehan JH, Okamoto Y, Vyprachticky D, Brantmeier BM, Roerig DL, Dawson CA (1997) Pulmonary endothelial thiazine uptake: Separation of cell surface reduction from intracellular reoxidation. Am J Physiol 272:L673-L680.

Mesulam MM, Nobre AC, Kim YH, Parrish TB, Gitelman DR (2001) Heterogeneity of cingulate contributions to spatial attention. Neuroimage 13:1065-1072.

Mielke MM, Lyketsos CG (2006) Lipids and the pathogenesis of Alzheimer's disease: Is there a link? Int Rev Psychiatry 18:173-186.

Minoshima S, Giordani B, Berent S, Frey KA, Foster NL, Kuhl DE (1997) Metabolic reduction in the posterior cingulate cortex in very early Alzheimer's disease. Ann Neurol 42:85-94.

Mizumori SJY, Yeshenko O, Gill KM, Davis DM (2004) Parallel processing across neural systems: Implications for a multiple memory system hypothesis. Neurobiol Learn Mem 82:278-298.

Mosconi L (2005) Brain glucose metabolism in the early and specific diagnosis of Alzheimer's disease. FDG-PET studies in MCI and AD. Eur J Nucl Med Mol Imaging 32:486-510.

Mowry S, Ogren PJ (1999) Kinetics of methylene blue reduction by ascorbic acid. J Chem Educ 76:970-973.

Mutisya EM, Bowling AC, Beal MF (1994) Cortical cytochrome oxidase activity is reduced in Alzheimer's disease. J Neurochem 63:2179-2184.

Nair HP, Gonzalez-Lima F (1999) Extinction of behavior in infant rats: Development of functional coupling between septal, hippocampal, and ventral tegmental regions. J Neurosci 19:8646-8655.

Narsapur SL, Naylor GJ (1983) Methylene blue: A possible treatment for manic depressive psychosis. J Affect Disord 5:155-161.

Naylor GJ, Martin B, Hopwood SE, Watson Y (1986) A two-year double-blind crossover trial of the prophylactic effect of methylene blue in manic-depressive psychosis. Biol Psychiatry 21:915-920.

Naylor GJ, Smith AHW, Connelly P (1987) A controlled trial of methylene blue in severe depressive illness. Biol Psychiatry 22:657-659.

Neave N, Lloyd S, Sahgal A, Aggleton JP (1994) Lack of effect of lesions in the anterior cingulate cortex and retrosplenial cortex on certain tests of spatial memory in the rat. Behav Brain Res 65:89-101.

Nugent AC, Milham MP, Bain EE, Mah L, Cannon DM, Marrett S, Zarate CA, Pine DS, Price JL, Drevets WC (2006) Cortical abnormalities in bipolar disorder investigated with mri and voxel-based morphometry. Neuroimage 30:485-497.

Nunomura A, Perry G, Hirai K, Aliev G, Takeda A, Chiba S, Smith MA (1999) Neuronal rna oxidation in Alzheimer's disease and down's syndrome. Ann N Y Acad Sci 893:362-364.

Nyberg L, McIntosh AR, Cabeza R, Nilsson LG, Houle S, Habib R, Tulving E (1996) Network analysis of positron emission tomography regional cerebral blood flow data: Ensemble inhibition during episodic memory retrieval. J Neurosci 16:3753-3759.

Ohnishi T, Matsuda H, Hirakata M, Ugawa Y (2006) Navigation ability dependent neural activation in the human brain: An fMRI study. Neurosci Res 55:361-369.

Packard MG, Cahill L (2001) Affective modulation of multiple memory systems. Curr Opin Neurobiol 11:752-756.

Papez JW (1937) A proposed mechanism of emotion. Arch Neurol Psychiatry 38:725-743.

Parker WD, Jr., Mahr NJ, Filley CM, Parks JK, Hughes D, Young DA, Cullum CM (1994a) Reduced platelet cytochrome c oxidase activity in Alzheimer's disease. Neurol 44:1086-1090.

Parker WD, Jr., Parks J, Filley CM, Kleinschmidt-DeMasters BK (1994b) Electron transport chain defects in Alzheimer's disease brain. Neurol 44:1090-1096.

Parker WD, Jr., Parks JK (1995) Cytochrome c oxidase in Alzheimer's disease brain: Purification and characterization. Neurol 45:482-486.

Partridge RS, Monroe SM, Parks JK, Johnson K, Parker WD, Jr., Eaton GR, Eaton SS (1994) Spin trapping of azidyl and hydroxyl radicals in azide-inhibited rat brain submitochondrial particles. Arch Biochem Biophys 310:210-217.

Paxinos G, Watson C (1997) The rat brain in stereotaxic coordinates. San Diego: Academic Press.

Perry G, Nunomura A, Hirai K, Takeda A, Aliev G, Smith MA (2000) Oxidative damage in Alzheimer's disease: The metabolic dimension. Int J Dev Neurosci 18:417-421.

Peter C, Hongwan D, Kupfer A, Lauterburg BH (2000) Pharmacokinetics and organ distribution of intravenous and oral methylene blue. Eur J Clin Pharmacol 56:247-250.

Petrozzi L, Ricci G, Giglioli N, Siciliano G, Mancuso M (2007) Mitochondria and neurodegeneration. Biosci Rep 27:87-104.

Pitsikas N, Rigamonti AE, Cella SG, Muller EE (2002) Effects of the nitric oxide donor molsidomine on different memory components as assessed in the object-recognition task in the rat. Psychopharmacologia 162:239-245.

Reddy PH, Beal MF (2005) Are mitochondria critical in the pathogenesis of Alzheimer's disease? Brain Res Brain Res Rev 49:618-632.

Reiman EM, Caselli RJ, Yun LS, Chen K, Bandy D, Minoshima S, Thibodeau SN, Osborne D (1996) Preclinical evidence of Alzheimer's disease in persons homozygous for the epsilon 4 allele for apolipoprotein E. N Engl J Med 334:752-758.

Reisberg B, Doody R, Stoffler A, Schmitt F, Ferris S, Mobius HJ (2006) A 24-week open-label extension study of memantine in moderate to severe Alzheimer disease. Arch Neurol 63:49-54.

Riekkinen P, Jr., Kuitunen J, Riekkinen M (1995) Effects of scopolamine infusions into the anterior and posterior cingulate on passive avoidance and water maze navigation. Brain Res 685:46-54.

Riha PD, Bruchey AK, Echevarria DJ, Gonzalez-Lima F (2005) Memory facilitation by methylene blue: Dose-dependent effect on behavior and brain oxygen consumption. Eur J Pharmacol 511:151-158.

Roth RM, Koven NS, Randolph JJ, Flashman LA, Pixley HS, Ricketts SM, Wishart HA, Saykin AJ (2006) Functional magnetic resonance imaging of executive control in bipolar disorder. Neuroreport 17:1085-1089.

Salaris SC, Babbs CF, Voorhees WD, III (1991) Methylene blue as an inhibitor of superoxide generation by xanthine oxidase : A potential new drug for the attenuation of ischemia/reperfusion injury. Biochem Pharmacol 42:499-506.

Sanderson KJ, Dreher B, Gayer N (1991) Prosencephalic connections of striate and extrastriate areas of rat visual cortex. Exp Brain Res 85:324-334.

Schallert T, Fleming SM, Leasure JL, Tillerson JL, Bland ST (2000) CNS plasticity and assessment of forelimb sensorimotor outcome in unilateral rat models of stroke, cortical ablation, parkinsonism and spinal cord injury. Neuropharmacology 39:777-787.

Scott A, Hunter FE, Jr. (1966) Support of thyroxine-induced swelling of liver mitochondria by generation of high energy intermediates at any one of three sites in electron transport. J Biol Chem 241:1060-1066.

Seitz RJ, Azari NP, Knorr U, Binkofski F, Herzog H, Freund HJ (1999) The role of diaschisis in stroke recovery. Stroke 30:1844-1850.

Shaw A, Li Z, Thomas Z, Stevens C (2002) Assessment of tissue oxygen tension: Comparison of dynamic fluorescence quenching and polarographic electrode technique. Critical Care 6:76-80.

Sheehan JP, Swerdlow RH, Miller SW, Davis RE, Parks JK, Parker WD, Tuttle JB (1997) Calcium homeostasis and reactive oxygen species production in cells transformed by mitochondria from individuals with sporadic Alzheimer's disease. J Neurosci 17:4612-4622.

Shibata H (1994) Terminal distribution of projections from the retrosplenial area to the retrohippocampal region in the rat, as studied by anterograde transport of biotinylated dextran amine. Neurosci Res 20:331-336.

Shibata H (1998) Organization of projections of rat retrosplenial cortex to the anterior thalamic nuclei. Eur J Neurosci 10:3210-3219.

Shibata H (2000) Organization of retrosplenial cortical projections to the laterodorsal thalamic nucleus in the rat. Neurosci Res 38:303-311.

Shibata H, Kondo S, Naito J (2004) Organization of retrosplenial cortical projections to the anterior cingulate, motor, and prefrontal cortices in the rat. Neurosci Res 49:1-11.

Shimizu E, Hashimoto K, Ochi S, Fukami G, Fujisaki M, Koike K, Okamura N, Ohgake S, Koizumi H, Matsuzawa D, Zhang L, Watanabe H, Nakazato M, Shinoda N, Komatsu N, Morita F, Iyo M (2007) Posterior cingulate gyrus metabolic changes in chronic schizophrenia with generalized cognitive deficits. J Psychiatr Res 41:49-56.

Silverman DHS (2004) Brain 18f-FDG PET in the diagnosis of neurodegenerative dementias: Comparison with perfusion SPECT and with clinical evaluations lacking nuclear imaging. J Nucl Med 45:594-607.

Simonian NA, Hyman BT (1994) Functional alterations in Alzheimer's disease: Selective loss of mitochondrial-encoded cytochrome oxidase mrna in the hippocampal formation. J Neuropathol Exp Neurol 53:508-512.

Smith MA, Sayre LM, Monnier VM, Perry G (1995) Radical AGEing in Alzheimer's disease. Trends Neurosci 18:172-176.

Smith MA, Sayre LM, Anderson VE, Harris PL, Beal MF, Kowall N, Perry G (1998) Cytochemical demonstration of oxidative damage in Alzheimer disease by immunochemical enhancement of the carbonyl reaction with 2,4-dinitrophenylhydrazine. J Histochem Cytochem 46:731-735.

Smith TS, Bennett JP, Jr. (1997) Mitochondrial toxins in models of neurodegenerative diseases. I: *In vivo* brain hydroxyl radical production during systemic mptp treatment or following microdialysis infusion of methylpyridinium or azide ions. Brain Res 765:183-188.

Snehalatha T, Rajanna KC, Saiprakash PK (1997) Methylene blue - ascorbic acid: An undergraduate experiment in kinetics. J Chem Educ 74:228-233. Sokoloff L (1989) Circulation and energy metabolism of the brain. In: Basic neurochemistry: Molecular, cellular, and medical aspects, 4th Edition (Siegel GJ, Agranoff BW, Albers RW, Molinoff PB, eds), pp 565-590. New York: Raven Press.

Souza MM, Mello e Souza T, Vinade ER, Rodrigues C, Choi HK, Dedavid e Silva TL, Medina JH, Izquierdo I (2002) Effects of posttraining treatments in the posterior cingulate cortex on short- and long-term memory for inhibitory avoidance in rats. Neurobiol Learn Mem 77:202-210.

Sutherland RJ, Whishaw IQ, Kolb B (1988) Contributions of cingulate cortex to two forms of spatial learning and memory. J Neurosci 8:1863-1872.

Swerdlow RH, Parks JK, Cassarino DS, Maguire DJ, Maguire RS, Bennett JP, Jr., Davis RE, Parker WD, Jr. (1997) Cybrids in Alzheimer's disease: A cellular model of the disease? Neurol 49:918-925.

Szabados T, Dul C, Majtenyi K, Hargitai J, Penzes Z, Urbanics R (2004) A chronic Alzheimer's model evoked by mitochondrial poison sodium azide for pharmacological investigations. Behav Brain Res 154:31-40.

Szeto HH (2006) Mitochondria-targeted peptide antioxidants: Novel neuroprotective agents. AAPS J 8:E521-531.

Taniguchi S, Suzuki N, Masuda M, Hisanaga S-i, Iwatsubo T, Goedert M, Hasegawa M (2005) Inhibition of heparin-induced tau filament formation by phenothiazines, polyphenols, and porphyrins. J Biol Chem 280:7614-7623.

Taube JS (1998) Head direction cells and the neurophysiological basis for a sense of direction. Prog Neurobiol 55:225-256.

Thal DR, Rub U, Schultz C, Sassin I, Ghebremedhin E, Del Tredici K, Braak E, Braak H (2000) Sequence of aβ-protein deposition in the human medial temporal lobe. J Neuropathol Exp Neurol 59:733-748.

Thirumala P, Hier DB, Patel P (2002) Motor recovery after stroke: Lessons from functional brain imaging. Neurol Res 24:453-458.

Treit D, Fundytus M (1988) Thigmotaxis as a test for anxiolytic activity in rats. Pharmacol Biochem Behav 31:959-962.

Valenstein E, Bowers D, Verfaellie M, Heilman KM, Day A, Watson RT (1987) Retrosplenial amnesia. Brain 110:1631-1646.

Valla J, Berndt JD, Gonzalez-Lima F (2001) Energy hypometabolism in posterior cingulate cortex of Alzheimer's patients: Superficial laminar cytochrome oxidase associated with disease duration. J Neurosci 21:4923-4930.

Valla J, Schneider L, Reiman EM (2006a) Age- and transgene-related changes in regional cerebral metabolism in PSAPP mice. Brain Res 1116:194-200.

Valla J, Schneider L, Niedzielko T, Coon KD, Caselli R, Sabbagh MN, Ahern GL, Baxter L, Alexander G, Walker DG, Reiman EM (2006b) Impaired platelet mitochondrial activity in Alzheimer's disease and mild cognitive impairment. Mitochondrion 6:323-330.

van Groen T, Wyss JM (1992a) Connections of the retrosplenial dysgranular cortex in the rat. J Comp Neurol 315:200-216.

van Groen T, Wyss JM (1992b) Projections from the laterodorsal nucleus of the thalamus to the limbic and visual cortices in the rat. J Comp Neurol 324:427-448.

van Groen T, Wyss JM (2003) Connections of the retrosplenial granular b cortex in the rat. J Comp Neurol 463:249-263.

van Groen T, Kadish I, Wyss JM (2004) Retrosplenial cortex lesions of area rgb (but not of area rga) impair spatial learning and memory in the rat. Behav Brain Res 154:483-491.

Vann SD, Brown MW, Aggleton JP (2000) Fos expression in the rostral thalamic nuclei and associated cortical regions in response to different spatial memory tests. Neuroscience 101:983-991.

Vann SD, Aggleton JP (2002) Extensive cytotoxic lesions of the rat retrosplenial cortex reveal consistent deficits on tasks that tax allocentric spatial memory. Behav Neurosci 116:85-94.

Vann SD, Kristina Wilton LA, Muir JL, Aggleton JP (2003) Testing the importance of the caudal retrosplenial cortex for spatial memory in rats. Behav Brain Res 140:107-118.

Vertes RP, Albo Z, Viana Di Prisco G (2001) Theta-rhythmically firing neurons in the anterior thalamus: Implications for mnemonic functions of Papez's circuit. Neuroscience 104:619-625.

Visarius TM, Stucki JW, Lauterburg BH (1997) Stimulation of respiration by methylene blue in rat liver mitochondria. FEBS Lett 412:157-160.

Visarius TM, Stucki JW, Lauterburg BH (1999) Inhibition and stimulation of long-chain fatty acid oxidation by chloroacetaldehyde and methylene blue in rats. J Pharmacol Exp Ther 289:820-824.

Vogt BA, Miller MW (1983) Cortical connections between rat cingulate cortex and visual, motor, and postsubicular cortices. J Comp Neurol 216:192-210. Wainwright M, Crossley KB (2002) Methylene blue--a therapeutic dye for all seasons? J Chemother 14:431-443.

Wallace DC (1999) Mitochondrial diseases in man and mouse. Science 283:1482-1488.

Warburton EC, Aggleton JP, Muir JL (1998) Comparing the effects of selective cingulate cortex lesions and cingulum bundle lesions on water maze performance by rats. Eur J Neurosci 10:622-634.

Whishaw IQ, Maaswinkel H, Gonzalez CLR, Kolb B (2001) Deficits in allothetic and idiothetic spatial behavior in rats with posterior cingulate cortex lesions. Behav Brain Res 118:67-76.

Wischik CM, Edwards PC, Lai RY, Roth M, Harrington CR (1996) Selective inhibition of Alzheimer disease-like tau aggregation by phenothiazines. Proc Natl Acad Sci USA 93:11213-11218.

Wong-Riley MT, Nie F, Hevner RF, Liu S (1998) Brain cytochrome oxidase: Functional significance and bigenomic regulation in the CNS. In: Cytochrome oxidase in neuronal metabolism and Alzheimer's disease (Gonzalez-Lima F, ed), pp 1-53. New York: Plenum Press.

Wright RO, Lewander WJ, Woolf AD (1999) Methemoglobinemia: Etiology, pharmacology, and clinical management. Ann Emerg Med 34:646-656.

Wrubel KM, Riha PD, Maldonado MA, McCollum D, Gonzalez-Lima F (2007) The brain metabolic enhancer methylene blue improves discrimination learning in rats. Pharmacol Biochem Behav 86:712-717.

Zhang X, Rojas JC, Gonzalez-Lima F (2006) Methylene blue prevents neurodegeneration caused by rotenone in the retina. Neurotoxicity Research 9:47-57.

Vita

Penny Riha was born in Schulenburg, Texas on September 19, 1975. Her parents are Frank and Debbie Riha. She has five siblings. Penny attended Schulenburg High School and graduated with honors in May of 1994. She then entered the University of Texas at Austin in the fall of 1994. She received several academic awards, most significantly, a four-year scholarship from the Stanzel Family Foundation. She graduated with a B.A. in Psychology in December of 1998. Penny began doctoral study in Behavioral Neuroscience within the Psychology department in August of 1999. She joined Dr. Francisco Gonzalez-Lima's laboratory to study animal behavior and brain metabolism.

Permanent address: 610 Pressler St.   Austin, TX 78703

This dissertation was typed by Penny D. Riha.